

**T.C.
MARMARA UNIVERSITY
INSTITUTE FOR GRADUATE STUDIES IN
PURE AND APPLIED SCIENCES**

**PROPERTIES OF CHEMICAL SLUDGE FLOCS AND
IMPLICATIONS RELATED TO DEWATERING**

Serdar ŞAM
(Environmental Engineer)
(141100820030292)

**THESIS
FOR THE DEGREE OF MASTER OF SCIENCE
IN
ENVIRONMENTAL ENGINEERING PROGRAMME**

**SUPERVISOR
Prof. Dr. Mehmet Ali YÜKSELEN**

İSTANBUL 2005

ACKNOWLEDGEMENT

I would like to thank my supervisor Prof. Dr. Mehmet Ali Yükselen for his valuable knowledge and encouraging support throughout this study.

August, 2005

Serdar Şam

TABLE OF CONTENTS

	<u>PAGE</u>
ABSTRACT	I
ÖZET	II
ABBREVIATIONS	III
LIST OF FIGURES	IV
LIST OF TABLES	VII
LIST OF APPENDICES	VIII
CHAPTER I INTRODUCTION	1
CHAPTER II GENERAL BACKGROUND	4
II.1. FUNDAMENTALS OF FLOCCULATION.....	4
II.1.1. Colloid Interactions	5
II.1.1.1. Van Der Waals Interaction.....	6
II.1.1.2. Electrical Interaction.....	7
<i>1.a Origins of Surface Charge.....</i>	<i>7</i>
<i>1.b Electrical Double Layers.....</i>	<i>8</i>
II.1.2. Combined Interaction – Colloid Stability.....	10
II.1.2.1. Hydration Effects.....	10
II.1.3. Hydrophobic Interaction.....	11
II.1.4. Steric Interaction.....	11
II.1.5. Polymer Bridging.....	13
II.2. FLOC SIZE AND FORM	15
II.2.1. The Nature of Aggregates	15
II.3. COAGULANT CHEMISTRY.....	17
II.3.1. Hydrolysis of Al(III) and Fe(III).....	18
II.3.1.1. Monomeric Hydrolysis Products.....	18
II.3.1.2. Polynuclear Species.....	21
II.3.1.3. Precipitate Formation.....	23

	<u>PAGE</u>
II.4. MECHANISMS OF COAGULATION.....	25
II.4.1. Charge Neutralisation.....	25
II.4.2. Sweep Flocculation.....	28
II.5. PRE-HYDROLYSED COAGULANTS.....	32
II.6. FLOC STRENGTH AND BREAK-UP.....	34
CHAPTER III MATERIALS AND METHODS	41
III.1. SUSPENSION.....	41
III.2. COAGULANTS.....	42
III.3. APPARATUS	42
III.4. PROCEDURE	46
CHAPTER IV RESULTS & DISCUSSION.....	50
IV.1. OPTIMUM DOSE DETERMINATION.....	50
IV.2. FLOC FORMATION, BREAKAGE, AND RE-FORMATION..	53
IV.3. EFFECT OF BREAKAGE DURATION.....	55
IV.4. EFFECT OF RAPID MIXING DURATION	66
CHAPTER V CONCLUSION.....	79
REFERENCES	81
APPENDICES	85
BIOGRAPHY	95

ABSTRACT

PROPERTIES OF CHEMICAL SLUDGE FLOCS AND IMPLICATIONS RELATED TO DEWATERING

The effects of breakage duration and rapid mixing duration on the formation, breakage and re-formation of synthetic flocs (generated using kaolin clay suspensions) formed with aluminium sulfate (alum) and polyaluminium chloride (PACl) were investigated together with implications related to dewatering via capillary suction time (CST) test and sludge content analysis.

Using the experimentally determined optimum dosage of aluminium sulfate and an equivalent Al amount of PACl, flocculation of high turbidity (1000 NTU) kaolin suspensions was achieved using the conventional jar test procedure and floc formation was observed by continuous optical monitoring (PDA-Photometric Dispersion Analyser). Flocs were formed after 400 rpm (a mean shear rate of $G = 518 \text{ s}^{-1}$) rapid mixing for 10 s and 40 rpm ($G = 16 \text{ s}^{-1}$) slow mixing for 10 min. The “effect of breakage duration” was investigated exposing these flocs to higher shear rate ($G = 518 \text{ s}^{-1}$) for different durations (10-300 s). In the “effect of rapid mixing duration” experiments, different rapid mixing times (0-300 s) were carried out.

Results showed that in each case breakage of flocs is irreversible for hydrolysing metal salts. Residual turbidity increased and CST decreased as floc size decreased. Larger flocs were formed with shorter rapid mixing durations, which yielded better residual turbidity and but worse dewaterability in terms of CST.

August, 2005

Serdar Şam

ÖZET

KİMYASAL ÇAMUR FLOKLARININ ÖZELLİKLERİ VE BUNLARIN SUSUZLAŞTIRMAYA ETKİSİ

Kırılma süresinin ve hızlı karıştırma süresinin, kaolin kili süspansiyonlarının alüminyum sülfat (alum) ve polialüminyum klorür (PACl) ile flokülasyonundan elde edilen sentetik flokların oluşumuna, kırılımına ve yeniden oluşumuna etkisi ve oluşan çamurların susuzlaştırılmasıyla ilişkisi CST (Capillary Suction Time) testi çamur analizi ile incelenmiştir.

Alüminyum sülfatın deneysel olarak belirlenen optimum dozu ve PACl'nin buna denk miktarda Al içeren dozu kullanılarak yüksek bulanıklıktaki (1000 NTU) kaolin süspansiyonlarının flokülasyonu kavanoz testi ile gerçekleştirilmiş ve flok oluşumu devingen optik bir alet (PDA-Photometric Dispersion Analyser) ile izlenmiştir. Floklar 10 sn. boyunca 400 dev./dk hızda (ortalama $G = 518s^{-1}$) hızlı karıştırma ve 10 dk. boyunca 40 dev./dk hızda (ortalama $G = 16s^{-1}$) yavaş karıştırma ile oluşturulmuştur. “Kırma süresinin etkisi” bu flokları farklı süreler boyunca (10-300 sn.) yüksek hızda karıştırmaya maruz bırakarak incelenmiştir. “Hızlı karıştırmanın etkisi” incelenirken ise koagülasyonda farklı hızlı karıştırma süreleri (0-300 sn) uygulanmıştır.

Sonuçlar göstermiştir ki metal tuzlarıyla flokülasyon sonucu oluşan floklar kırıldıktan sonra eski boyutlarına dönememektedir. Flok boyutu küçüldükçe bakiye bulanıklık artmakta, CST ise azalma eğilimi göstermektedir. Kısa süreli hızlı karıştırma ile daha büyük boyutlu floklar elde edilmiş; bunların bakiye bulanıklık değerlerinin daha az, susuzlaştırılmalarının ise ölçülen yüksek CST değerleri ile daha kötü olduğu gözlenmiştir.

August, 2005

Serdar Şam

ABBREVIATIONS

CST	: Capillary Suction Time
FI	: Flocculation Index
HA	: Humic Acid
NTU	: Nephelometric Turbidity Units
PACl	: Polyaluminium Chloride
PDA	: Photometric Dispersion Analyser
RPM	: Revolutions Per Minute
SV	: Sludge Volume

LIST OF FIGURES

	<u>PAGE</u>
Figure-II.1 The electrical double layer model.....	9
Figure-II.2 Concentrations of monomeric hydrolysis products of Fe(III) and Al(III) in equilibrium with the amorphous hydroxides, at zero ionic strength and 25 °C	20
Figure-II.3 Proportions (mole fractions) of dissolved hydrolysis products in equilibrium with amorphous hydroxides	21
Figure-II.4 Titration curves for neutralisation of aluminium salt solutions, showing variation of pH with added base $B (=OH/Al)$	22
Figure-II.5 Schematic illustration of the concept of the Precipitation Charge Neutralisation (PCN) model	27
Figure-II.6 Deposition of metal hydroxide species on oppositely charged particles, showing charge neutralisation and charge reversal	27
Figure-II.7 Electrophoretic Mobility (EM) and residual turbidity for kaolin suspensions (50 mg/L) with low dosages of aluminum sulfate (alum) at pH 6	28
Figure-II.8 As Fig.II.7, but over a wider range of alum dosages and at pH 7	30
Figure-II.9 Dynamic monitoring of kaolin suspensions at two dosages of alum, under the same conditions as for Fig. II.8	31
Figure-II.10 Schematic diagram showing the interaction of aluminium species with initially negatively charged particles in water. The particles on the right hand side are initially stable and then become destabilised by charge neutralisation. At higher coagulant dosages they can become restabilised by charge reversal and incorporated in a flocculent hydroxide precipitate (sweep flocculation)	32
Figure-II.11 Dynamic monitoring of kaolin suspensions, showing formation, breakage and partial re-formation of flocs. In all cases suspensions were dosed with alum (130 mM Al) and stirred at 50 rpm for 10 min. A higher stirring speed (400 rpm) was then applied for times of 10–300 s (as indicated on curves), followed by further stirring at 50 rpm....	37
Figure-III.1 Turbidimeter (WTW Turb 550).....	42
Figure-III.2 Photometric Dispersion Analyser (PDA 2000, Rank Brothers Ltd., Cambridge, UK).....	43
Figure-III.3 Peristaltic pump (Watson Marlow 505Di).....	44
Figure-III.4 Sludge settling and CST measurement; a) Imhoff cones, b) Capillary Suction Timer, Type 304M, Triton Electronics Ltd.....	45
Figure-III.5 Experimental setup for dynamic monitoring of floc formation in jar-test procedure.....	46

Figure-III.6	Schematics of the experimental setup for dynamic monitoring of floc formation in jar-test procedure.....	47
Figure-III.7	Schematics of the experimental setup for dynamic monitoring of floc formation in jar-test procedure	49
Figure-IV.1	Residual turbidity after 30min and 2hrs settling vs. dosage.....	51
Figure-IV.2	The change of capillary suction time with alum dosage.....	52
Figure IV.3	Amount of sludge vs. alum dosage.....	52
Figure IV.4	Floc formation, breakage and re-formation with optimum alum dose (6.8 mg/L as Al). Rapid mixing at 400rpm for 10s, followed by 10min of slow stirring at 40rpm, then floc breakage at 400rpm for 10s and re-formation at 40rpm	54
Figure IV.5	Residual turbidity at formation, breakage and re-formation (conditions are same with those in Fig.-IV.4).....	55
Figure IV.6	Breakage and re-formation of flocs with alum at 400 rpm for different durations and at 40 rpm for 10 min, respectively.....	56
Figure IV.7	Strength, Recovery and Breakage Factors; investigation of the effect of breakage time with alum	57
Figure IV.8	Residual turbidity for different durations of breakage after 30min settling with alum.....	58
Figure IV.9	Residual turbidity for different durations of breakage after 2 hr settling with alum	58
Figure IV.10	CST test results for different durations of breakage after 2hr settling with alum	59
Figure IV.11	Sludge volume for different durations of breakage after 30min and 2hr settling with alum	60
Figure IV.12	Alum sludge content; % solids (w/w)	60
Figure IV.13	Breakage and re-formation of flocs with PACl at 400 rpm for different durations and at 40 rpm for 10 min, respectively	61
Figure IV.14	Strength, Recovery and Breakage Factors; investigation of the effect of breakage time with PACl	62
Figure IV.15	Residual turbidity for different durations of breakage after 30 min settling with PACl	62
Figure IV.16	Residual turbidity for different durations of breakage after 2 hr settling with PACl	63
Figure IV.17	CST test results for different durations of breakage after 30 min and 2 hr settling with PACl.....	63
Figure IV.18	Sludge volume for different durations of breakage after 30 min and 2 hr settling with PACl	64
Figure.IV.19	PACl sludge content; % solids (w/w)	65
Figure.IV.20	Floc formation, breakage and re-formation for different rapid mixing durations with alum.....	66
Figure.IV.21	Strength, Recovery and Breakage Factors; investigation of the effect of breakage time with alum.....	67
Figure.IV.22	Residual turbidity at formation, breakage and re-formation after 30min settling with alum.....	68

Figure.IV.23 Residual turbidity at formation, breakage and re-formation after 2hr settling with alum.....	68
Figure.IV.24 CST at formation, breakage and re-formation after 2 hr settling with alum.....	69
Figure.IV.25 Sludge volume for different durations of rapid mixing after 30 min settling with alum.....	70
Figure.IV.26 Sludge volume for different durations of rapid mixing after 2 hr settling with alum.....	71
Figure.IV.27 Alum sludge content; % solids (w/w).....	71
Figure.IV.28 Floc formation, breakage and re-formation for different rapid mixing durations with PACl.....	72
Figure.IV.29 Strength, Recovery and Breakage Factors; investigation of the effect of breakage time with PACl.....	73
Figure.IV.30 Residual turbidity at formation, breakage and re-formation after 30 min settling with PACl.....	73
Figure.IV.31 Residual turbidity at formation, breakage and re-formation after 2hr settling with PACl.....	74
Figure.IV.32 CST at formation, breakage and re-formation after 2 hr settling with PACl.....	75
Figure.IV.33 Sludge volume for different durations of rapid mixing after 30 min settling with PACl.....	76
Figure.IV.34 Sludge volume for different durations of rapid mixing after 2 hr settling with PACl.....	76
Figure.IV.35 PACl sludge content; % solids (w/w).....	77

LIST OF TABLES

	<u>PAGE</u>
Table II.1 Hydrolysis and solubility constants for Al^{3+} and Fe^{3+} for zero ionic strength and 25 °C	20
Table IV.1 Residual turbidity and sludge volume values after 30 min and 2 hr settling for 10 s breakage case with alum.....	53

APPENDICES

	<u>PAGE</u>
APPENDIX A	85
Figure-A.1: Microphotographs of (a) full grown, (b) re-formed and (c) broken flocs with alum for 10 s breakage condition.....	85
Figure-A.2: Microphotographs of (a) full grown, (b) re-formed and (c) broken flocs with alum for 30 s breakage condition.....	85
Figure-A.3: Microphotographs of (a) full grown, (b) re-formed and (c) broken flocs with alum for 60 s breakage condition.....	86
Figure-A.4: Microphotographs of (a) full grown, (b) re-formed and (c) broken flocs with alum for 300 s breakage condition.....	86
Figure-A.5: Microphotographs of (a) full grown, (b) re-formed and (c) broken flocs with PACl for 10 s breakage condition.	86
Figure-A.6: Microphotographs of (a) full grown, (b) re-formed and (c) broken flocs with PACl for 30 s breakage condition.....	87
Figure-A.7: Microphotographs of (a) full grown, (b) re-formed and (c) broken flocs with PACl for 60 s breakage condition	87
Figure-A.8: Microphotographs of (a) full grown, (b) re-formed and (c) broken flocs with PACl for 300 s breakage condition.....	87
APPENDIX B	88
Figure-B.1: Microphotographs of (a) full grown, (b) re-formed and (c) broken flocs with alum for “no rapid mixing” condition.....	88
Figure-B.2: Microphotographs of (a) full grown, (b) re-formed and (c) broken flocs with alum for 5 s rapid mixing condition.....	88
Figure-B.3: Microphotographs of (a) full grown, (b) re-formed and (c) broken flocs with alum for 10 s rapid mixing condition.....	89
Figure-B.4: Microphotographs of (a) full grown, (b) re-formed and (c) broken flocs with alum for 30 s rapid mixing condition.....	89
Figure-B.5: Microphotographs of (a) full grown, (b) re-formed and (c) broken flocs with alum for 60 s rapid mixing condition.....	89
Figure-B.6: Microphotographs of (a) full grown, (b) re-formed and (c) broken flocs with alum for 120 s rapid mixing condition.....	90
Figure-B.7: Microphotographs of (a) full grown, (b) re-formed and (c) broken flocs with alum for 180 s rapid mixing condition.....	90
Figure-B.8: Microphotographs of (a) full grown, (b) re-formed and (c) broken flocs with alum for 240 s rapid mixing condition.....	90

Figure-B.9: Microphotographs of (a) full grown, (b) re-formed and (c) broken flocs with alum for 300 s rapid mixing condition.....	91
Figure-B.10: Microphotographs of (a) full grown, (b) re-formed and (c) broken flocs with PACl for “no rapid mixing” condition.	91
Figure-B.11: Microphotographs of (a) full grown, (b) re-formed and (c) broken flocs with PACl for 5 s rapid mixing condition.....	91
Figure-B.12: Microphotographs of (a) full grown, (b) re-formed and (c) broken flocs with PACl for 10 s rapid mixing condition.....	92
Figure-B.13: Microphotographs of (a) full grown, (b) re-formed and (c) broken flocs with PACl for 30 s rapid mixing condition.....	92
Figure-B.14: Microphotographs of (a) full grown, (b) re-formed and (c) broken flocs with PACl for 60 s rapid mixing condition.....	92
Figure-B.15: Microphotographs of (a) full grown, (b) re-formed and (c) broken flocs with PACl for 120 s rapid mixing condition.....	93
Figure-B.16: Microphotographs of (a) full grown, (b) re-formed and (c) broken flocs with PACl for 180 s rapid mixing condition.....	93
Figure-B.17: Microphotographs of (a) full grown, (b) re-formed and (c) broken flocs with PACl for 240 s rapid mixing condition.....	93
Figure-B.18: Microphotographs of (a) full grown, (b) re-formed and (c) broken flocs with PACl for 300 s rapid mixing condition.....	94

CHAPTER I

INTRODUCTION

Coagulation/flocculation processes are very important elements of particle separation practice and are widely used to enhance the effectiveness of subsequent solid-liquid separation units (sedimentation, flotation and filtration) by giving large aggregates or flocs which are more easily removable than the original colloidal particles.

Some form of agitation or shear (orthokinetic flocculation) is applied in almost all flocculation processes by means of either mixing of the fluid or motion of fluid in special hydraulic structures. In such units, flocs initially grow at a rate which is determined by the applied shear, the particle concentration, and the collision efficiency (and hence, on the degree of particle destabilisation caused by the added coagulants). As flocs become larger, further growth is restricted by the applied shear for essentially two reasons; existing flocs may be broken as a result of disruptive forces (Matsuo and Unno, 1981) and collision efficiency of particles in a shear field becomes lower as particle size increases (Brakalov, 1987). Steady-state conditions are established after a while during floc formation, where a dynamic balance between floc growth and breakage prevails. This can lead to a steady-state floc size distribution, the limiting size is dependent on the applied shear rate (Mühle, 1993).

The application of fluid shear to increase the collision rate in orthokinetic flocculation may also cause floc breakage. Floc growth occurs only to a limiting size under given shear conditions, and beyond that, breakage of flocs to smaller subunits takes place (Tambo and Hozumi, 1979). The maximum floc size is reduced as the shear rate is increased, giving the most widely accepted empirical indication of floc

strength – the larger the flocs formed under given shear conditions, the stronger they are (Gregory, 1989). The nature of breakage process depends on the size of flocs relative to the turbulence microscale, which is of the order of 100 μm in many cases. For flocs larger than the microscale, deformation and rupture may occur as a result of fluctuating dynamic pressure. For smaller flocs, viscous forces predominate and may cause either erosion of primary particles or small aggregates from large parent flocs, or fragmentation to form smaller flocs of size comparable to each other (Gregory, 1989).

Coagulants based on hydrolysing metal salts are widely used in water treatment applications. These rapidly hydrolyse in water, giving various cationic products. Those cationic species adsorb on negatively charged stabilised particles present in water, and hence reduce or neutralise their surface charge. This type of destabilisation mechanism (charge neutralisation) is likely to occur at low coagulant dosages, however further increase of dose can lead to charge reversal and restabilisation of particles. At much higher dosages, precipitation of amorphous metal hydroxide can predominate. Here, particles become enmeshed in the precipitate and swept out, which is why the mechanism is called ‘sweep flocculation’. In flocculation with hydrolysing metal salts, hydrolysis products are formed very rapidly and very complex and competing processes such as adsorption and precipitation could depend on mixing conditions. The initial rapid mixing can be of great importance; if enough dispersion of coagulant is not satisfied (poor mixing), local charge reversal and restabilisation of particles may take place. It has been suggested that initial mixing conditions are not that important in the case of sweep flocculation (Amirtharajah and Mills, 1982). However, many previous studies on floc formation and breakage with hydrolysing metal salts (Francois, 1987; Spicer *et al.*, 1998; Yukselen and Gregory, 2004b) have shown that mixing conditions affect floc growth significantly. In some cases it was observed that at early minutes of flocculation, flocs increase and then decrease in size (Gregory *et al.*, 2000; Gregory and Rossi, 2001; Yukselen and Gregory, 2002a), even under same stirring conditions. It is generally found that flocs become more compact as a result of applied shear (Serra *et al.*, 1997). Flocs undergo breakage when higher shear rate is applied, however, they can grow back when the previous low shear regime is established. This regrowth can be restricted, as shown with hydrolysing metal salts (Francois, 1987; Francois and Van Haute, 1984; Clark and Flora, 1991; Yukselen

and Gregory, 2002a; Yukselen and Gregory, 2002b; Yukselen and Gregory, 2004a; Yukselen and Gregory, 2004b).

These and similar studies lead to the idea of multilevel floc structures, however, this has been largely replaced by the idea of fractal aggregates (Gorczyca and Ganczarczyk, 1999). Nevertheless, thinking of ‘flocculi’ rather than primary particles as building structures of flocs may still be useful (Francois and Van Haute, 1984). The idea is that; small flocculi are formed during rapid mixing and then they aggregate to form larger flocs during slow stirring. Studies on floc breakage has shown that flocs are not ruptured to primary particles in high shear regimes, possibly this may stem to the idea of flocculi.

Structural properties like floc size, density, and strength together with effectiveness of different coagulants are very important issues in particle separation processes. Such properties of flocs are also major concern for dewatering sludges since flocs are the building structures of sludges. Different techniques for determination of sludge dewaterability are applied, some of which are laboratory scale models of real dewatering units (filter press, centrifuge, vacuum filtration, etc.). Among all, capillary suction time (CST) is the simplest test giving comparative data on water release properties of sludges. The results of the test can be interpreted in conjunction with the properties of flocs mentioned above and conditions under which flocs are formed.

The aim of the present work is to investigate the effect of rapid mixing duration and breakage duration on growth and dewaterability of flocs produced from the flocculation of high turbidity (1000 NTU) clay suspensions by using aluminium sulfate (alum) and polyaluminium chloride (PACl). A convenient optical monitoring technique for floc formation in conventional jar-test procedure was applied. Residual turbidity measurements and CST tests were performed to determine and compare removal efficiencies and dewaterability in each condition, respectively, in conjunction with a representative of floc size (FI – Flocculation Index).

CHAPTER II

GENERAL BACKGROUND

II.1. PRINCIPALS OF FLOCCULATION

Flocculation is a fundamental step in many particle separation processes which are widely used in water and wastewater treatment. The efficiency of solid-liquid separation processes such as sedimentation, flotation and filtration increases significantly as the size of impurity particles is increased. For this, substantial aggregation of particles is to be achieved. These initially very small particles may fall in the colloidal size range which is conventionally assumed to cover sizes between 1nm and 1 μm . Colloidal particles are subject to significant diffusion (Brownian motion) due to their small size, and may settle very slowly, if at all, under ordinary gravity. In addition to this, interparticle forces can become very significant for colloidal sizes and play a large part in the stability of colloids. In colloidal size range, interparticle forces become significant over and overcome the gravitational force. When compared, it can be seen that weight of a colloid with a size of μm order is much smaller than the interaction force (say, electrostatic force) with another colloid of similar size. Colloidal particles are said to be stable if they are resistant to aggregation and unstable if aggregation occurs readily. For particles considerably larger than 1 μm , external forces, such as gravity, become more significant and may outweigh colloidal interactions. Nevertheless, many of the principles discussed below apply to larger particles and, in practice, particles up to around 1 mm in size may be involved in flocculation processes.

Two types of colloids must be distinguished from each other, which are known as hydrophilic and hydrophobic colloids. Hydrophilic colloids essentially consist of water-soluble macromolecules such as starches, proteins, and many others. Although these may be in true solution (dissolved), the size of the molecules gives them some of the properties of dispersed particles. They are thermodynamically stable in water because of their solubility and can be induced to aggregate (or precipitate) only by changing the solvency conditions, for instance by changing the temperature or by adding quite large quantities of inorganic salts (“salting out”).

On the other hand, hydrophobic colloids consist of materials with low solubility, which happen to exist in a finely divided state. In this case, the particles are not stable in a thermodynamic sense, but may be kinetically stable due to interparticle repulsion which is electrical in nature due to the surface charge of the aqueous colloids, so that colliding particles are prevented from forming permanent aggregates (or flocs).

Flocculation occurs only if particles (1) collide with each other and (2) can adhere when brought together by collision (i.e., the particles have low colloid stability). The flocculation process is applied to increase the rate or kinetics of particle aggregation and floc formation in water treatment. The objective is to make a stable suspension, i.e. one that is resistant to aggregation (or attachment to a filter grain), into an unstable one. To achieve this, the mechanisms of colloid stability should be understood well.

II.1.1. Colloid Interactions

When two particles in a suspension approach each other, or a particle in a flowing fluid approaches a stationary surface such as a filter grain, several types of interaction can come into play which may tend to keep the surfaces apart and have a major effect on the flocculation process. There are two different but related ways in which colloid interactions influence flocculation. First, they have a direct effect on the collision efficiency, which is the probability that a pair of colliding particles will form a permanent aggregate. Obviously, if there is strong repulsion between the particles, then the chance of aggregate formation will be very low and flocculation will occur only very slowly, if at all. One of the primary objectives in practical flocculation processes is to ensure, by suitable chemical control, that any interparticle repulsion is reduced or eliminated, so that the collision efficiency is as high as possible. The other aspect of colloid

interactions is their effect on the strength of aggregates, which is much less well understood but of great practical importance.

The two most familiar kinds of colloidal interaction are *van der Waals attraction* and *electrical repulsion* which form the basis of the well-known DLVO theory of colloid stability, developed independently by Deryagin and Landau and Verwey and Overbeek. While these enable a large amount of experimental flocculation data to be explained, at least in a semiquantitative manner, there are many cases where other types of interaction have to be invoked. Initially, these were lumped together under some general heading, such as “structural forces”, but recent advances have given considerable insight into these “extra” or “non-DLVO” forces and it is now possible to give a more detailed classification. In aqueous systems, various kinds of hydration effects can be important, especially at close approach of particles. These are often associated with the hydration of ions at the particle surfaces and usually give an extra repulsion. It is now known that hydrophobic effects can also be important, mostly giving an extra attraction between particles. Other important effects arise from the presence of adsorbed polymers, giving either a repulsion (“steric” interaction) or an attraction (“polymer bridging”).

It is important to mention that practically all colloidal interactions are of quite a short range, almost never extending over distances greater than the size of the particles. This means that they have little influence over the transport of particles, although they are crucial in determining the collision efficiency. To a large extent, this justifies the treatment of transport and attachment as separate steps.

II.1.1.1. Van Der Waals Interaction

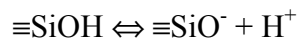
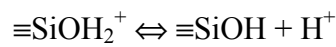
The universal attractive forces between atoms and molecules are known as van der Waals forces. Van der Waals attraction arises from spontaneous electrical and magnetic polarizations that create a fluctuating electromagnetic field within the particles and in the space between them. It also operates between macroscopic objects and plays a very important part in the interaction of colloidal particles. Aggregation of particles would usually be prevented by the hydrodynamic interaction without these forces. As particles approach one another on a collision course, the fluid between them must move out of the way. The repulsive force caused by this displacement of fluid is called hydrodynamic retardation.

II.1.1.2. Electrical Interaction

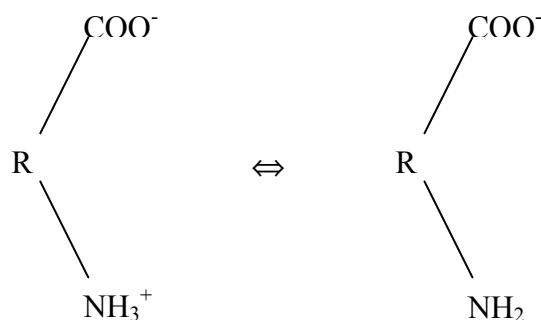
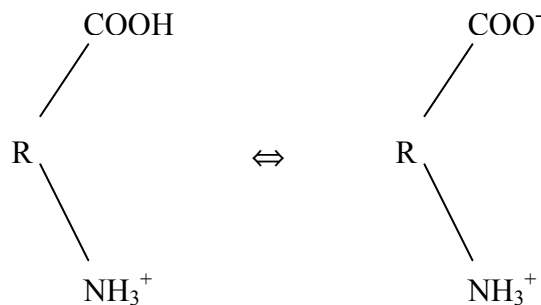
1.a Origins of Surface Charge

Most particles in water, mineral and organic, have electrically charged surfaces, and the sign of the charge is usually negative. Three important processes for producing this charge are considered as follows;

First, surface groups on the solid may react with water and accept or donate protons. For an oxide surface such as silica, the surface site might be indicated by the symbol $\equiv\text{SiOH}$ and the surface site ionization reactions by



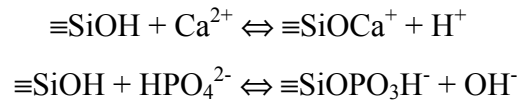
An organic surface can contain carboxyl (COO^-) and amino (NH_3^+) groups that become charged through ionization reactions as follows:



In these reactions, the surface charge on a solid particle depends upon the concentration of protons ($[\text{H}^+]$) or the pH ($= -\log[\text{H}^+]$) in the solution. As the pH increases (i.e., $[\text{H}^+]$ decreases), the four reactions above shift to the right and the surface charge becomes increasingly negative. Silica is negatively charged in water with a pH above 2; proteins contain a mixture of carboxyl and amino groups and

usually have a negative charge at a pH above about 4. The adsorption of NOM onto particles can be responsible for site behaviour like that shown previously.

Second, surface groups can react in water with solutes other than protons. Again, using the $\equiv\text{SiOH}$ surface groups of silica,



These surface complex formation reactions involve specific chemical reactions between chemical groups on the solid surface (e.g., silanol groups) and adsorbable solutes (e.g., calcium and phosphate ions). Surface charge is again related to solution chemistry.

Third, a surface charge may arise because of imperfections within the structure of the particle; this is called isomorphic replacement, or substitution. It is responsible for a substantial part of the charge on many clay minerals. Clays are layered structures and in these structures sheets of silica tetrahedra are typically cross-linked with sheets of alumina octahedra. The silica tetrahedra have an average composition of SiO_2 . If an Al atom is substituted for a Si atom during the formation of this lattice, a negatively charged framework results.

Similarly, a divalent cation such as Mg(II) or Fe(II) may substitute for an Al(III) atom in the aluminium oxide octahedral network, also producing a negative charge. The sign and magnitude of the charge produced by such isomorphic replacements are independent of the characteristics of the aqueous phase after the crystal is formed (Letterman *et al.*, 1999).

1.b Electrical Double Layers

As mentioned above most particles in aqueous media are charged for various reasons, such as the ionization of surface groups, specific adsorption of ions, and several others. In an electrolyte solution, the distribution of ions around a charged particle is not uniform and gives rise to an *electrical double layer*. The essential point is that the charge on a particle surface is balanced by an equivalent number of oppositely charged *counterions* in solution. These counterions are subject to two opposing influences. Electrostatic attraction tending to localize the counterions close to the particles and the tendency of ions to diffuse randomly throughout the solution due to their thermal energy. The surface charge on a particle and the associated

counterion charge together constitute the electrical double layer. A widely accepted model for the double layer is that due to Stern, later modified by Graham, in which part of the counterion charge is located close to the particle surface (the so-called Stern layer) and the remainder is distributed more broadly in the diffuse layer as shown in Figure-II.1.

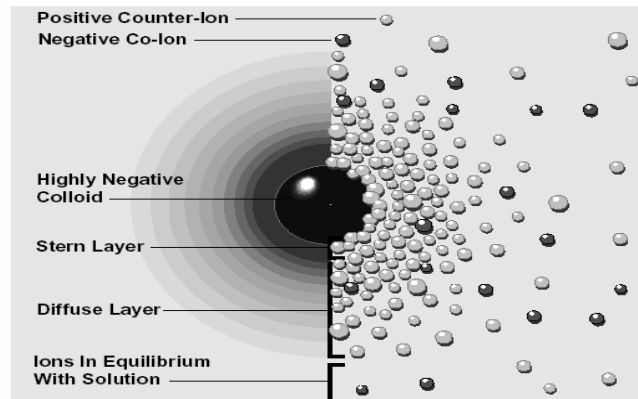


Figure-II.1: The electrical double layer model.

The interaction between charged particles is governed predominantly by the overlap of diffuse layers, so the potential most relevant to the interaction is that at the boundary between the Stern and diffuse layers (the *Stern potential*, ψ_δ), rather than the potential at the particle surface. This boundary (the *Stern plane*) is generally considered to be at a distance of about 0.3 to 0.5 nm from the particle surface, corresponding to the diameter of a hydrated counterion. There is no direct experimental method for determining the Stern potential, but there is good reason to believe that the electrokinetic or *zeta potential*, ζ , is an adequate substitute, although there is still some doubt on this point. The electrokinetic potential is that at the plane of shear, between a particle and a fluid, when there is relative motion between them. The well-known technique of particle electrophoresis is the most common method of determining zeta potentials and is widely used in fundamental studies of colloid stability. The two major influences on electrical interaction between particles are the magnitude of the effective “surface potential” and the extent of the diffuse layer since the latter governs the range of the interaction. Surface potentials can be modified in two distinct ways. If the ionic strength is raised, then a greater proportion of the potential drop occurs across the Stern layer, giving a smaller Stern potential. This effect can be produced by adding any salt, and those which act only

in this way are known as indifferent electrolytes. A more dramatic effect can be produced by the addition of salts with specifically adsorbing counterions. These adsorb on the particles because of some specific, nonelectrostatic affinity and can be regarded as lying in the Stern layer. In many cases, such ions can adsorb to such an extent that they reverse the sign of the Stern potential, which indicates clearly that specific interaction is involved.

Multiple-charged counterions can be adsorbed very strongly and, in the extreme case of polyelectrolytes, adsorption may be quantitative. Many oxides have a surface charge which arises from the ionization of acidic and basic surface groups, so that H^+ and OH^- ions are the important species and the surface charge is pH dependent as mentioned before.

II.1.2. Combined Interaction – Colloid Stability

II.1.2.1. Hydration Effects

The nature of water close to a particle surface can be very different from bulk water for a variety of reasons. As we have seen, colloidal particles can be stabilized by a surface charge, which implies ionic groups at the surface, or adsorbed ions, together with some closely associated counterions (in the Stern layer). Since ions in aqueous solution tend to be hydrated, it is reasonable to suppose that surface ions are also associated with a certain amount of “bound water”. It has been postulated that the “structuring” effect of a surface on adjacent water can extend to quite large distances, but significant effects on colloid stability can arise when only a few molecular layers are involved. The major consequence of hydration at a particle surface is an increased repulsion between approaching particles, because of the need for ions to lose their water of hydration if “contact” between particles is to be achieved. This involves work and hence an increase in free energy of the system.

It seems likely that ionic hydration forces are important in many systems of practical changes within the Stern layer may be of only secondary significance.

II.1.3. Hydrophobic Interaction

It is quite possible (and very likely) that a “hydrophobic” particle will have a hydrophilic surface in the sense that it is readily wetted by water. Insoluble oxides, for instance, become hydrated by hydrogen-bonded water molecules. Surfaces with

bound ionic groups or adsorbed ions can be hydrated leading to short-range repulsion.

In some cases, surfaces may have significant areas with hydrophobic (nonwetable) character, such as polymer latex particles with a low density of surface ionic groups, or negative particles with adsorbed cationic surfactant. This time another type of interaction which can give appreciable attraction – the so-called *hydrophobic interaction* arises. This is because of the extensive hydrogen bonding present in ordinary water, which is responsible for a considerable degree of association between water molecules and a significant “structuring” effect. A hydrophobic surface offers no possibility of hydrogen bonding or ion hydration, so there is no inherent affinity for water. However, the presence of such a surface tends to limit the “structuring” tendency of water molecules simply by reducing the possibility of hydrogen bond formation in certain directions. Consequently, water avoids contact with such surfaces as far as possible. In aqueous solutions, molecules with hydrophobic segments can associate with each other in such a way that contact between water and the hydrophobic regions is minimized. This is known as hydrophobic bonding and the best known examples are in surfactant solutions and proteins (Gregory, 1989).

It was found that the same type of interaction occurs between macroscopic objects with hydrophobic surfaces and that the resulting attractive force can be surprisingly large, of quite long range and stronger than the van der Waals force.

II.1.4. Steric Interaction

In colloid stability adsorbed layers, especially of polymers, can play a very large part in the sense of attraction or repulsion. In some cases, small amounts of adsorbed polymer can promote flocculation by a “bridging” mechanism. With higher adsorbed amounts, polymers can give greatly enhanced stability by an effect which is usually known as *steric stabilization*. The most effective polymers for steric stabilization are those which have some affinity for the particle surface (otherwise no adsorption would occur), but adsorb in such a way that segments of polymer chains extend some way into the aqueous phase. The clearest example is the adsorption of *block copolymers*, which have some segments which adsorb strongly on the particles (perhaps by hydrophobic bonding) and others which are hydrophilic and hence tend to project into the aqueous phase. Such polymers are

often referred to as *terminally anchored chains*. In practice, polyethylene oxide chains, anchored by hydrocarbon “tails”, are often used as steric stabilizers.

The stabilizing action of such materials can be understood in fairly simple terms. As particles approach sufficiently close, the adsorbed layers come into contact and closer approach would involve some overlap of the hydrophilic chains. Under normal conditions, these chains are hydrated, and overlap would cause some dehydration and hence an increase in free energy so that the process would not occur spontaneously. In other words, the stabilizing layers repel each other for much the same reason that hydrophilic polymers are soluble in water – they interact more favorably with water than with their own kind. The adsorbed layer gives hydrophobic particles some of the important properties of hydrophilic colloids.

Although quantitative theories of steric stabilization are becoming available, it is often acceptable to treat the interaction as being infinite as soon as overlap of the adsorbed layers occurs and zero at greater separations. It is clear that the thickness of the adsorbed layer will play a large part in determining the stabilizing effect. If the layer is quite thin, particles will be able to approach close enough so that van der Waals attraction between them is sufficient to give strong attachment. With thicker adsorbed layers, steric repulsion begins when the core particles are separated by a larger distance so that van der Waals attraction may be too weak to cause adhesion. The adsorbed layer thickness controls the depth of the minimum in the potential energy curve, which is reminiscent of the “secondary minimum”. However, with steric repulsion, the depth of the minimum, and hence the strength of attachment, can be adjusted simply by choosing stabilizing layers of different thicknesses. The depth of the secondary minimum in charge-stabilized colloids is much more difficult to control.

Particle size plays an important part in steric stabilization since the van der Waals attraction depends on size, as well as on separation distance. Larger particles attract each other more strongly for a given separation distance and so thicker stabilizing layers would be needed to prevent attachment.

Sterically stabilized dispersions can be destabilized by changing the solvency of the medium for the stabilizing chains. With polyethylene oxide chains, adding certain salts (especially sulfates) and increasing the temperature can cause flocculation.

Polymers in general do not adsorb in the simple manner, but are attached to the particles at many points along the chain. The effective thickness of the adsorbed layer is then more difficult to determine. Nevertheless, the broad principles outlined above still apply – effective stabilization is achieved by fairly thick adsorbed layers, which are well solvated, so that overlap or interpenetration of the layers does not readily occur.

Most particles in the aquatic environment have adsorbed layers of natural organic material, such as humic substances, which can have a dominant effect on their colloidal behavior. Many microorganisms produce extracellular polymers which may adsorb and have a great influence on particle interaction in biological systems. These natural polymers and organics are often weak acids and are anionic at neutral pH values. It is thought that the rather low negative zeta potential found for most natural aquatic colloids is due to the adsorption of this weakly anionic material. The stability of such colloids is usually higher than expected on the basis of zeta potential and ionic strength, using a simple DLVO approach, and it is likely that steric stabilization plays a part in many cases. Humic substances are known to enhance the stability of inorganic colloids and can cause greatly increased flocculant dosages (Gregory, 1989).

II.1.5. Polymer Bridging

Polymers with long molecular chains may adsorb on particles at many points along the chain, and a single polymer molecule becomes attached to more than one particle. In that case, the particles may be said to be “bridged” by adsorbed polymer and this mechanism is of great practical importance in a number of applications. Polymer bridging was postulated by Ruehrwein and Ward in 1952 to account for the aggregation of clay particles by polyelectrolytes, and the concept has been widely accepted since then.

The polymer needs to be of quite high molecular weight (values up to several million are common) for polymer bridging to occur, and to adsorb in such a way that a significant fraction of segments is not in contact with the particle surface, but extend some distance into the aqueous phase. Also, the adsorbed amount should not be too great, so that a significant fraction of the surface remains free of adsorbed polymer. In this way, contacts can occur between unoccupied areas of a particle surface and extended segments of chains adsorbed on other particles. When excess polymer is adsorbed, bridging is prevented because there is insufficient free particle

surface for bridging contacts to occur and the adsorbed layers may also cause steric repulsion. For these reasons, there is an “optimum dosage” of polymer to give good bridging flocculation, and this is usually found to depend on the particle concentration.

When compared, bridging flocculation is found to give much stronger aggregates (flocs) than when particles are destabilized by simply reducing the repulsion between them (usually by adding salt), and the resulting flocs are larger. This was recently shown by Gregory and Yukselen.

Interpretation of flocculation by polymers is often complicated by the fact that many of the polymeric flocculants used in practice are charged (i.e., they are polyelectrolytes). When particles and polymer are of opposite sign (as in the common case of negative particles and cationic polyelectrolytes), charge effects cannot be ruled out. In fact, in many such instances, the action of the polyelectrolyte can be explained simply by the fact that it adsorbs very strongly and neutralizes the particle charge. This could be regarded as an extreme case of a specifically adsorbing counterion. However, here are many cases where the polymeric nature of the flocculant is important and bridging effects may still predominate, especially for high molecular weight materials.

Another mechanism of flocculation with polyelectrolytes is “the electrostatic patch effect”, whereby the polyelectrolyte adsorbs on an oppositely charged particle in such a way that there are “patches” of excess charge because of local charge reversal and areas of unoccupied surface still bearing the original particle charge. This type of adsorption will occur when the charge density of the polyelectrolyte is much greater than that of the particle surface. Particles with polymer adsorbed in this “patchwise” manner can interact in such a way that positive and negative areas of different particles are adjacent, giving strong electrical attraction. More detailed information on adsorption of polymeric flocculants were presented by Gregory (1996).

Recently, another concept of flocculation with polymers has been introduced in which flocculation is achieved in two stages, each with another type of polymer, which is so called ‘dual polymer conditioning’ (Lee and Liu, 2000 and 2001).

II.2. FLOC SIZE AND FORM

II.2.1. The Nature of Aggregates

Various shapes of aggregates are possible in the earliest stages of aggregation. Aggregates containing hundreds or thousands of primary particles are formed in practical flocculation processes and the number of possibilities is virtually limitless. It is obvious that efforts to describe the shape of an aggregate completely is impossible and impractical. Some other shape description is necessary to eliminate the complexity due to these limitless possibilities.

Aggregates are now recognized as fractal objects (Meakin, 1988), which means that they have non-integer dimension. A solid three dimensional body has a mass which depends on the third power of some characteristic length (such as the diameter of a sphere), so that a log-log plot of mass against size would give a straight line with a slope of three. However, lower slopes are found with noninteger values when such plots are made for aggregates (usually of the number of primary particles against the aggregate diameter). The slope of the line is known as the fractal dimension, d_F . In three dimensional space, d_F may take values between 1 and 3, the lower value representing a linear aggregate and the upper one an aggregate of uniform density (or porosity). Generally, intermediate values are found, and the lower the fractal dimension, the more open or “stringy” the aggregate structure. If a constant value of d_F is found over a wide range of aggregate size, then the aggregates are said to have a self-similar structure since the relative arrangement of units within the structure is independent of the scale of observation (or the degree of magnification).

There are important practical implications of the fractal nature of aggregates. One consequence is that flocs have an effective density which decreases with size.

The density of a floc, ρ_F , is simply the mass of particles and included water divided by the “envelope” volume. The “effective” density is just this value minus the density of water, i.e., $\rho_E = \rho_F - \rho_W$. The size and effective density of a floc determine its sedimentation rate. When the effective density of flocs is measured as a function of floc size and the results are plotted in log-log form, a straight line is often obtained, with a characteristic, negative slope. There is a straightforward relationship between this slope and the fractal dimension (the slope of the log mass vs. log size line). The linearity of the log density – log size plot implies an equation

of the form: $\rho_E = Ba^{-y}$, where B and y are constants. Very simple reasoning leads to the following relationship:

$$d_F = 3 - y$$

Measurements of floc densities for many systems of practical interest give values of y in the range 1 to 1.4, corresponding to fractal dimensions of 2 to 1.6, which is typical of the values found in simulations of cluster-cluster aggregation and studies of model colloids. It is worth noting that the values of y quoted here imply a very significant decrease in floc density with increasing floc size. With $y = 1.2$, a 10-fold increase in size gives a 16-fold decrease in effective density. A common reason for producing large flocs is to give more rapid sedimentation, but the large decrease in density acts in the opposite direction (although not enough to outweigh the size effect). For a floc of a given mass (i.e., containing a fixed number of primary particles) the sedimentation rate will be increased as the floc becomes more compact (higher d_F).

Other solid-liquid separation processes are also affected by the density of flocs. Dewatering by cake filtration proceeds more rapidly when flocs are compact since, effectively, there is less solid surface in contact with water and hence less drag. Also, more open floc structures are more liable to restructuring under pressure, and the resulting compression can lead to considerable blocking of pores and a reduced filtration rate. It is significant that, in practice, recirculation of sludge solids in a flocculation process can give a very large improvement in filterability. Such recirculation is known to yield increased floc density. This is thought to be due to the fact that preformed flocs are brought into contact with newly introduced primary particles or microflocs, thus reducing the extent of cluster-cluster aggregation. It was mentioned earlier that aggregation by single particle addition gives higher d_F values than the cluster-cluster process and so this gives the observed higher floc density in units with recirculation has at least some theoretical basis.

In other cases such as flotation, flocs of low density may be required. Also, the flocculation process itself proceeds more rapidly if the flocs formed have low density since the collision radius will be larger for a given degree of aggregation. For a similar reason, the capture of flocs by collectors (as in deep bed filtration) is more efficient for lower density flocs (although filter clogging may occur more rapidly).

II.3. COAGULANT CHEMISTRY

In water treatment, hydrolysing metal salts, based on aluminium or iron, are very widely used as coagulants. Hydrolysing coagulants have been applied routinely since early in the 20th century and play a vital role in the removal of many impurities such as from polluted waters. These impurities include inorganic particles, such as clays, pathogenic microbes and dissolved natural organic matter. Aluminum sulfate (alum), ferric chloride, and ferric sulfate are the most common coagulant types. Other products based on pre-hydrolysed metals are also now widely used, including a range of materials referred to as polyaluminium chloride and polyiron chloride.

As mentioned before, nearly all colloidal impurities in water are negatively charged and, hence, may be stable as a result of electrical repulsion. Destabilisation of these colloids along DLVO lines is necessary in order to separate these particles effectively. This could be achieved either by adding relatively large amounts of salts or smaller quantities of cations that interact specifically with negative colloids and neutralise their charge. Highly charged cations such as Al^{3+} and Fe^{3+} should be effective in this respect. However, over the normal range of pH values in natural waters (say, 5–8), these simple cations are not found in significant concentrations, as a result of hydrolysis, which can give a range of products. Many hydrolysis products are cationic and these can interact strongly with negative colloids, giving destabilisation and coagulation, under the correct conditions of dosage and pH. Excess dosage can give charge reversal and restabilisation of colloids.

Al(III) and Fe(III) both have limited solubility at around neutral pH, because of the precipitation of an amorphous hydroxide, which can play a very important role in practical coagulation and flocculation processes. A very detailed investigation on the role of hydroxides was given by Bache and Papavasiliopoulos (2003). Deposition of positively charged precipitate particles on impurity particles (heterocoagulation) may give the possibility of charge neutralization and destabilization. A further possibility is that surface precipitation of hydroxide could occur, with similar consequences. A practically more important flocculation mechanism is the precipitation of excessive hydroxide, the *sweep flocculation*, in which impurity particles become enmeshed in the growing precipitate and thus effectively removed.

These additives can also remove dissolved natural organic matter (NOM), either by charge neutralisation to give insoluble forms, or by adsorption on precipitated metal hydroxide.

A range of commercial pre-hydrolysed coagulants is available as well as simple hydrolysing salts. These contain cationic hydrolysis products and are often more effective than aluminium or iron salts.

II.3.1. Hydrolysis of Al(III) and Fe(III)

II.3.1.1. Monomeric hydrolysis products

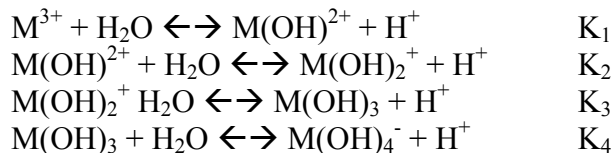
In water all metal cations are hydrated to some extent. It is reasonable to think in terms of a *primary hydration shell*, where water molecules are in direct contact with the central metal ion, and more loosely held water in a secondary hydration shell. In the cases of Al^{3+} and Fe^{3+} , it is known that the primary hydration shell consists of six water molecules in octahedral co-ordination. Owing to the high charge on the metal ion, water molecules in the primary hydration shell are polarised and this can lead to a loss of one or more protons, depending on the solution pH. Effectively, this means that the water molecules in the hydration shell are progressively replaced by hydroxyl ions, giving a lower positive charge, according to the following sequence (omitting co-ordinated water molecules for convenience):



This is an oversimplified scheme, since it is known that dimeric, trimeric and polynuclear hydrolysis products of Al and Fe can form. However, these can often be ignored, especially in dilute solutions, and may not greatly affect the overall metal speciation.

As the pH is increased the hydrolysis scheme above will proceed from left to right, giving first the doubly- and singly-charged cationic species and then the uncharged metal hydroxide, $\text{Me}(\text{OH})_3$. The hydroxide is of very low solubility in the case of both aluminium and iron and an amorphous precipitate can form at intermediate pH values. In practice, this has enormous significance in the action of these materials as coagulants. The soluble anionic form $\text{Me}(\text{OH})_4^-$ becomes dominant with further increase in pH.

The determination of hydrolysis constants can be difficult because of the formation of insoluble hydroxides (and also polynuclear species) and there are significant differences in some published values. Hydrolysis constants can be defined for successive deprotonations in terms of the following equations:



A solubility constant for the metal hydroxide is also needed:



The most stable solids are crystalline forms of metal hydroxides, such as gibbsite and goethite in the case of Al and Fe, respectively, but these are usually formed very slowly (typically weeks or months). The solubility of the amorphous precipitates that form initially is more relevant to be considered in the context of coagulation mechanisms. However, solubility constants for the amorphous forms, K_{sam} are not known precisely and only estimated values can be quoted. Table II.1 gives values for hydrolysis and solubility constants (in pK form), taken from Wesolowski and Palmer (1994) for Al and from (Flynn, 1984) for Fe. The values are for conditions of zero ionic strength and 25 °C. Wesolowski and Palmer (1994) gives extensive data for Al at other temperatures and ionic strengths.

Table II.1: Hydrolysis and solubility constants for Al^{3+} and Fe^{3+} for zero ionic strength and 25 °C. (Values taken from Wesolowski and Palmer (1994) and Flynn (1984))

	pK_1	pK_2	pK_3	pK_4	pK_{sam}
Al^{3+}	4.95	5.6	6.7	5.6	31.5
Fe^{3+}	2.2	3.5	6	10	38

It is possible to plot, as a function of pH, the concentrations of the various species in equilibrium with the amorphous hydroxide precipitate using the values in Table II.1, as shown in Figure-II.2 for Al and Fe. The total amount of soluble species in equilibrium with the amorphous solid is effectively the solubility of the metal and it can be seen that in each case there is a minimum solubility at a certain pH value. For Al this is approximately pH 6, at which the solubility is of the order of 1 μM . Measurements of Al solubility as a function of pH give reasonable agreement with such calculations, even though only monomeric species are included. For Fe, the minimum solubility is much lower—less than 0.01 μM , and the corresponding region is broader than for Al. This gives an operational flexibility

to the coagulation with iron salts since the solubility of the metal is less effected by solution of pH than that of aluminum.

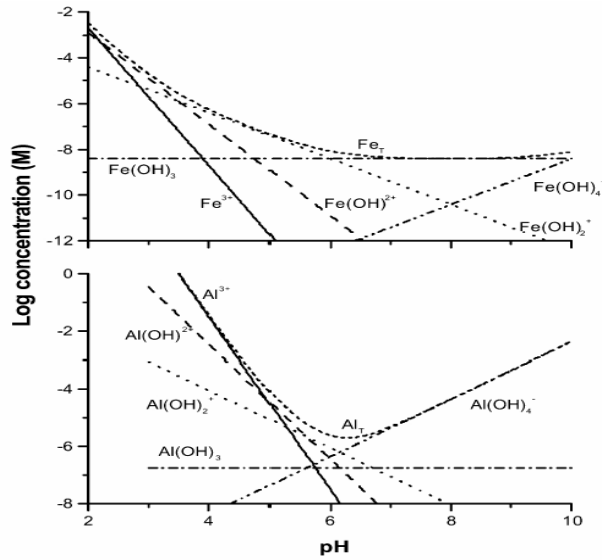


Figure-II.2: Concentrations of monomeric hydrolysis products of Fe(III) and Al(III) in equilibrium with the amorphous hydroxides, at zero ionic strength and 25 °C (Duan and Gregory, 2003).

Martin (1991) has pointed out a significant difference in the hydrolysis behaviour of Al and Fe, which is apparent from the values in Table II.1 and the computed results in Figure-II.2. The hydrolysis constants for Al cover a much narrower range than those for Fe. The latter are spaced over approximately 8 pH units, whereas all of the Al deprotonations are ‘squeezed’ into an interval of less than 1 unit. Martin (1991) explained this feature by the transition from the octahedral hexahydrate $\text{Al}^{3+} \cdot 6\text{H}_2\text{O}$ to the tetrahedral $\text{Al}(\text{OH})_4^-$. This makes the successive hydrolysis steps co-operative in nature. All of the hydrolysed species for Fe^{3+} retain the octahedral co-ordination and the stepwise deprotonations show the expected spread of pK values. This difference is clearly seen in the plots of species distributions in Figure-II.3, which show the mole fraction of the various soluble hydrolysis products in equilibrium with the amorphous precipitate. The ferric species each attain significant relative concentrations in solution at appropriate pH values, whereas for Al, apart from a narrow pH region approximately 5–6, the dominant soluble species are Al^{3+} and $\text{Al}(\text{OH})_4^-$ at low and high pH, respectively (Duan and Gregory, 2003).

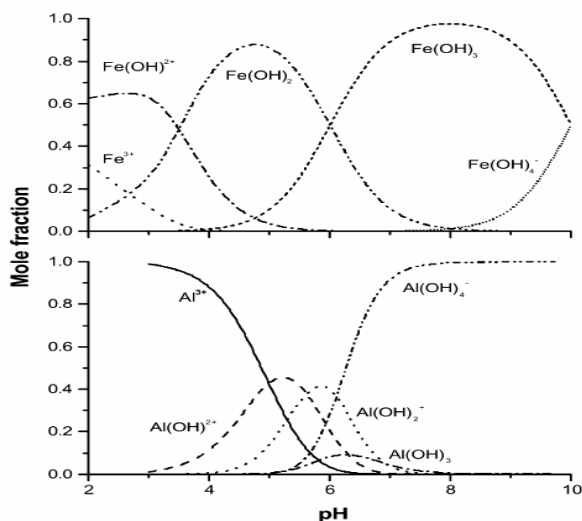


Figure-II.3: Proportions (mole fractions) of dissolved hydrolysis products in equilibrium with amorphous hydroxides (Duan and Gregory, 2003).

II.3.1.2. Polynuclear species

As well as the simple monomeric hydrolysis products discussed above, there are many possible polynuclear forms. Such as $Al_2(OH)_2^{4+}$ and $Al_3(OH)_3^{5+}$ for Al and equivalent species for Fe. Formation constants for the dimers and trimers are known, but, for practical purposes, they do not significantly affect the speciation shown in Figs. 1 and 2. Martin, 1991 showed that the Fe dimer, $Fe_2(OH)_2^{4+}$, could become significant in acid solutions ($pH < 3$), but the corresponding Al dimer does not occur to any significant extent in saturated solutions of $Al(OH)_3$. From the standpoint of coagulation with simple Al and Fe salts, only monomeric hydrolysis products and the amorphous hydroxide precipitate need be considered.

Polynuclear hydrolysis products can be prepared in significant amounts under certain conditions. The best known of these is $Al_{13}O_4(OH)_{24}^{7+}$ or 'Al₁₃', which can be formed by controlled neutralisation of aluminium salt solutions or by several other methods. This tridecamer has the so-called 'keggin' structure, consisting of a central tetrahedral AlO_4^{5-} unit surrounded by 12 Al octahedra with shared edges. Under appropriate conditions, Al₁₃ forms fairly rapidly and essentially irreversibly, remaining stable in aqueous solutions for long periods.

Based on coagulation data some other polynuclear species, such as the octamer, $Al_8(OH)_{20}^{4+}$, have been proposed by Matijevic et al., 1961. However, there is no direct evidence for the octamer and it is probably not found in significant concentrations in practice.

A typical curve like that in Fig.3 is obtained from the titration of an aluminium salt solution with base. Four regions can be distinguished in this plot,

based on the amount of added base B ($= \text{OH} / \text{Al}$). In Region 1 the base neutralises free acid produced by spontaneous hydrolysis, giving a rapid increase of pH. Above approximately pH 4, hydrolysed species are formed and there is an extended phase (Region 2) where pH increases only slowly, since added base is consumed by hydrolysis. In this region, large quantities of polymeric species can be formed and become the predominant soluble species at high B values. During titration, depending on mixing conditions, added base can give local supersaturation and precipitation of the amorphous hydroxide, or excess formation of the $\text{Al}(\text{OH})_4^-$ ion. These conditions may favour the formation of the Al_{13} polymer, although the details are not clear.

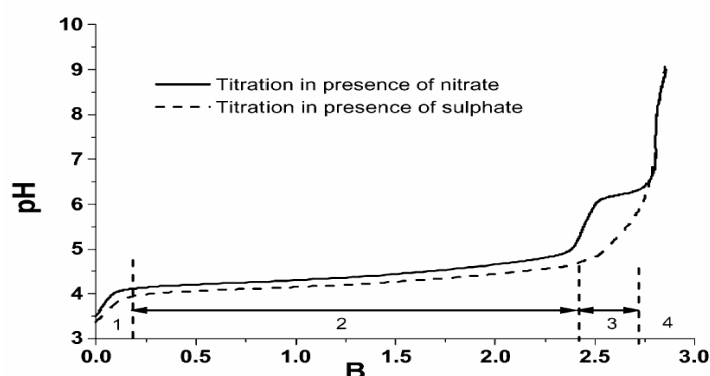


Figure-II.4 : Titration curves for neutralisation of aluminium salt solutions, showing variation of pH with added base B ($=\text{OH}/\text{Al}$) (Duan and Gregory, 2003).

Further increase of B , to the range 2.4–2.8, gives Region 3, in which a small shoulder appears in the curve, following a sharp rise in pH. In this region, supersaturation of the solution with respect to amorphous $\text{Al}(\text{OH})_3$ and rapid precipitation occurs. The presence of highly charged anions, such as sulfate, cause this shoulder to disappear and smoother increase of pH. Such anions can promote hydroxide precipitation (De Hek et al., 1978). In Region 4, the added base reduces the positive surface charge of the colloidal hydroxide particles and visible precipitates are formed. Further addition of base gives a rapid increase in pH.

Smith studied the speciation of Al solutions by a timed colorimetric reaction with ferron reagent (8-hydroxy-7-iodo-5-quinoline sulfonic acid). The method was based on the observation that different forms of Al react at varying rates with ferron. Mononuclear Al species (Al_a) react almost instantaneously and polynuclear species (Al_b) much more slowly. Colloidal or precipitated Al (Al_c) shows practically no reaction with ferron. Typically, the proportion of the various species is determined as a function of the degree of neutralisation, B . For 0.1 M AlCl_3 solution, titrated with 0.5 M NaOH (Smith, 1971), the proportion of Al_b increased from approximately 33% to 83% as B was raised from 1.0 to 2.5. For values of B above

2.5, the amount of precipitate (Al_c) increased significantly. In the same study, it was shown that the Al_b fraction was quite stable to dilution and to changes in pH, and only slowly converted to other forms. This is in marked contrast to monomeric hydrolysis products, which respond very rapidly to changes in chemical conditions.

It is doubtful whether Al_{13} forms under conditions where aluminium salts are added to water at around neutral pH, to give low Al concentrations (typical of water treatment conditions). In this case, it is thought that monomeric hydrolysed species predominate in solution and that amorphous precipitates form without the involvement of Al_{13} species.

II.3.1.3. Precipitate Formation

The formation of precipitated metal hydroxides can be in various ways, such as by neutralisation of the metal salt to $B(OH / M)$ ratios of approximately 3, as mentioned above. However, the precise mechanisms and structure of the precipitate have been the subject of much debate and there is a rather extensive and confusing literature on the topic. The attention shall be restricted mainly to aluminium here because aluminium based coagulants were used in this study. In the case of iron, there are redox as well as hydrolytic reactions to consider (Deng, 1997) and the subject becomes quite complex.

Clark et al. investigated the effect of mixing conditions on aluminium precipitation in some detail. They studied the neutralisation of $AlCl_3$ solutions in a stirred tank reactor and considered the kinetics of hydrolysis reactions in relation to characteristic mixing time scales. They showed that there is a competition between the formation of polynuclear hydrolysis products and precipitated solid. The results indicated that precipitation would be favoured with more intense mixing .

Neutralisation of fairly concentrated metal solutions by added base is not directly relevant to the use of hydrolysing metal coagulants in practice, where the metal salt is added to water, usually containing excess alkalinity, to give a final concentration of approximately $0.1 \mu M$ or less. In this case, neutralisation would occur rapidly and it is very likely that precipitation would occur without the formation of significant polynuclear species such as Al_{13} (Van Benschoten and Edzwald, 1990). It has been shown that precipitates formed by addition of aluminium sulfate and polyaluminium chloride (a prehydrolysed solution containing Al_{13}) give different solid phases. In the latter case, the polymeric structure is maintained in the precipitate and after re-dissolution in acid (Van Benschoten and

Edzwald, 1990). Similar behaviour has been found for ferric sulfate and a pre-hydrolysed form (polyferric sulfate) (Jiang and Graham, 1998).

In coagulation the surface charge characteristics of precipitated metal hydroxides are very important. In common with oxides and other minerals they show an isoelectric point (i.e.p.) at which the apparent (electrokinetic) surface charge is zero. At pH values below the i.e.p. the precipitate is positively charged and at higher pH values it has a negative charge. The value of the i.e.p. depends on the preparation details and on the solution composition, so that there are significant differences in values reported in the literature.

Precipitation from aluminium chloride solutions gives a solid with an i.e.p. in the region of 9 (Ohman and Wagberg, 1997), whereas from aluminium sulfate the value is closer to 8 (Van Benschoten and Edzwald, 1990). For amorphous ferric hydroxide the i.e.p. is somewhat lower. For both aluminium and ferric salts, pre-hydrolysed forms give precipitates with i.e.p. values shifted upwards by one or more pH units.

The precipitation process can be greatly affected by the varying charge with pH. The initially formed colloidal precipitate is positively charged at around neutral pH for aluminium and, hence, is colloidally stable. As the pH is increased towards the i.e.p., the stability decreases and the particles can aggregate into large, settleable flocs. It was shown by precipitation from an aluminium nitrate solution (1 μM) that at low pH the solution appeared clear, but showed a Tyndall beam, indicating the presence of very small, colloidal particles. As the pH increased, the particle size increased, giving higher turbidity. Above approximately pH 7 much larger particles were formed, which settled rapidly to give a reduced turbidity. The i.e.p. in this case was approximately 8, in the middle of the pH range where settleable flocs were produced. The results of precipitation from AlCl_3 solutions are consistent with these findings, although they showed a rather higher i.e.p. value. It is worth noting that the i.e.p. for $\text{Al}(\text{OH})_3$ occurs at a pH value well above that of minimum solubility (Figure-II.2), so that the largest flocs do not correspond with the maximum amount of precipitate (Duan and Gregory, 2003).

Highly charged anions, such as sulfate, are known to have a large effect on hydroxide precipitation. Sulfate can reduce the positive charge of the precipitate in the acid region, so that large flocs are formed over a wider pH range. This was clearly shown by Hayden and Rubin (1974) and others. The sulfate effect is very

important in practice since aluminium and ferric sulfates are commonly used as coagulants and natural waters can contain significant amounts of sulfate.

II.4. MECHANISMS OF COAGULATION

II.4.1. Charge Neutralisation

At very low concentrations of metal, only soluble species are present—the hydrated metal ion and various hydrolysed species, which, assuming only monomeric forms will depend on solution pH, as shown in Figure-II.2. Hydrolysed cationic species such as Al(OH)^{2+} are generally thought to be more strongly adsorbed on negative surfaces than the free, hydrated metal ion (Matijevic, 1973).

Charge neutralisation with aluminium salts generally occurs at quite low metal concentrations—typically a few μM at around neutral pH. It can be seen by the inspection of Figure-II.2 that, the solubility limit of the hydroxide may be exceeded even at very low concentrations. Also, at neutral pH, cationic hydrolysis products should represent only a tiny fraction of the total soluble Al (Figure-II.2), the dominant form being the aluminate ion. This suggests that the effective charge-neutralising species may be colloidal hydroxide particles, which should be positively charged up to approximately pH 8. Even when the bulk hydroxide solubility is not exceeded, a form of *surface precipitation* may take place. James and Healy (1972) among others have suggested that adsorption of soluble hydroxide can lead to a layer of amorphous hydroxide precipitate, by surface nucleation and precipitation.

Dentel (1991) introduced Precipitation Charge Neutralisation (PCN) to explain coagulation by hydrolysing metal salts in water treatment. A schematic illustration of the processes involved is given in Figure-II.5.

According to the PCN model, coagulation with aluminium or iron salts involves three steps:

1. Destabilisation begins after addition of a dose of coagulant that exceeds the *operational solubility limit* of aluminium (or iron) hydroxide.
2. Aluminium or iron hydroxide species are then deposited onto colloidal surfaces, as shown in Figure-II.5. This figure shows that metal hydroxide could end up on particle surfaces by several possible pathways.

3. Under typical conditions, metal hydroxide is positively charged, while the original colloidal particles are negatively charged. So the deposition process can result in charge neutralisation or charge reversal of the colloidal particles at certain doses, as shown in a simplified manner in Figure-II. 6.

At the correct dosage, charge neutralisation by adsorbed hydrolysis products and/or hydroxide precipitate can cause negatively charged particles to become destabilised and hence to coagulate. Electrophoretic mobility (EM) measurements show that the optimum coagulation dosage corresponds with the condition where the zeta potential of the particles is close to zero. Some results for kaolin suspensions (50 mg/l) coagulated with aluminium sulfate ('alum') at pH 6, are shown in Figure-II.7 (Duan, 1997). This shows the *residual turbidity* of the suspensions after standard stirring and settling conditions (*jar test*) as well as the electrophoretic mobility of the particles, soon after coagulant addition. Since the minimum residual turbidity occurs at approximately 8 μM Al, this is the 'optimum dosage' for particle separation. The EM value is very close to zero at this point, indicating that charge neutralisation is responsible for the destabilisation of the clay particles. At slightly higher alum dosages, the EM becomes positive and the residual turbidity increases, indicating that charge reversal causes restabilisation of the particles. According to Figure-II.2, 8 μM Al at pH 6 is slightly above the solubility limit of amorphous $\text{Al}(\text{OH})_3$.

At higher pH values the optimum alum dosage increases because of the decreased positive charge of the adsorbed species. In such systems it appears that the electrokinetic properties of the particles are very like those of the amorphous hydroxide precipitate (Letterman et al., 1982), with an isoelectric point in the pH region 8–9, depending on the anions present in solution. At around the i.e.p. the particles do not become positively charged, even at high Al dosages and so no restabilisation is observed.

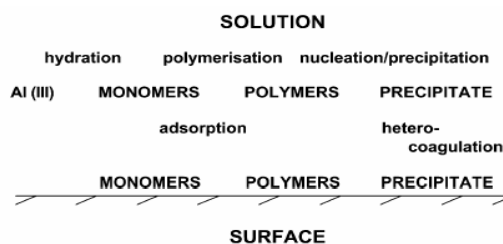


Figure-II.5 : Schematic illustration of the concept of the Precipitation Charge Neutralisation (PCN) model (Dentel, 1991)

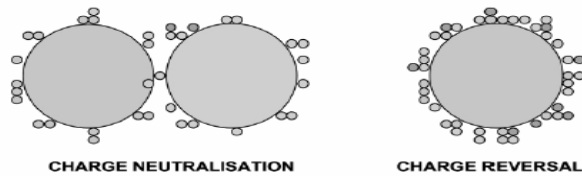


Figure-II.6 : Deposition of metal hydroxide species on oppositely charged particles, showing charge neutralisation and charge reversal (Dentel, 1991)

There should be a stoichiometric relationship between the particle concentration and the optimum coagulant dosage if charge neutralisation is the predominant destabilisation mechanism. Low coagulant dosages should be required at low particle concentrations. Under these conditions coagulation rates can be very low, which causes problems in water treatment. Another practical difficulty is that the

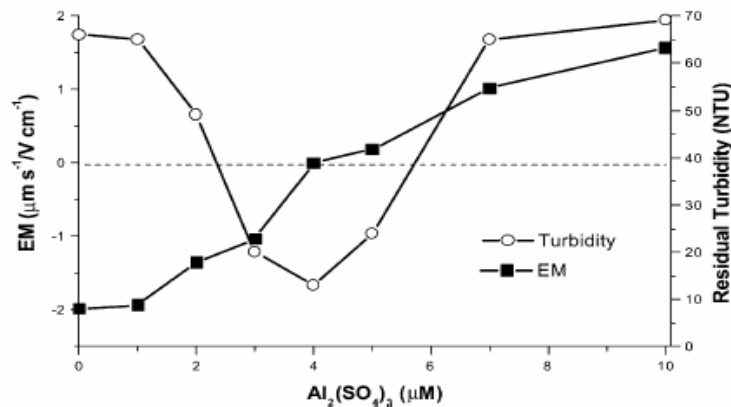


Figure-II.7 : Electrophoretic Mobility (EM) and residual turbidity for kaolin suspensions (50 mg/L) with low dosages of aluminum sulfate (alum) at pH 6 (Duan, 1997)

optimum coagulant dosage range can be quite narrow and sensitive to many factors such as temperature, pH, water composition etc., which requires that rather precise dosing control. Both of these difficulties can be overcome by using higher coagulant dosages, where extensive hydroxide precipitation occurs, giving *sweep flocculation*.

II.4.2. Sweep Flocculation

In many cases, optimal removal of particles from water is achieved under conditions of rapid and extensive hydroxide precipitation. In the case of aluminium coagulants, optimum pH values are approximately 7, close to the minimum solubility (Figure-II.2) but close enough to the i.e.p. to give fairly rapid aggregation of the colloidal precipitate particles. Although details are not fully understood, it seems clear that impurity particles are enmeshed in a growing hydroxide precipitate and are effectively removed from suspension. This process has become known as ‘sweep flocculation’ since particles are ‘swept out’ of water by an amorphous

hydroxide precipitate. Sweep flocculation generally gives considerably improved particle removal than when particles are destabilised just by charge neutralisation. At least part of the reason is the greatly improved rate of aggregation, because of the increased solids concentration. Hydroxide precipitates tend to have a rather open structure, so that even a small mass can give a large effective volume concentration and, hence, a high probability of capturing other particles. It is also possible that binding ('bridging') of particles by precipitated hydroxide may give stronger aggregates. Increasing the coagulant dosage in the sweep region gives progressively larger volumes of sediment (Gregory and Dupont, 2001) but, beyond the operational optimum dosage, there is little further improvement in particle removal.

The different mechanisms outlined above have led to the definition of four *zones* of coagulant dosage, with the following consequences for negatively charged particles:

Zone 1: Very low coagulant dosage; particles still negative and hence stable.

Zone 2: Dosage sufficient to give charge neutralisation and hence coagulation.

Zone 3: Higher dosage giving charge neutralisation and restabilisation.

Zone 4: Still higher dosage giving hydroxide precipitate and sweep flocculation.

In Figure-II.8 an example of the four zones in flocculation is presented by (Duan, 1997) for kaolin suspensions with alum at pH 7. Below approximately 8 μM Al there is essentially no reduction in turbidity, since the particles are negatively charged and colloidally stable (Zone 1). There is a narrow range of lowered turbidity in the region of 15 μM Al, which is close to the dosage where the EM is reduced to zero (Zone 2). By 20 μM Al, the particles are positively charged and completely restabilised, since the residual turbidity is no lower than that for the original clay suspension (Zone 3). Beyond approximately 60 μM Al the turbidity falls again as a result of sweep flocculation (Zone 4). It is very significant that a substantial change in residual turbidity occurs in a region of alum dosage where the EM of the particles is still positive and shows no appreciable reduction. Although there is a gradual reduction in EM as the alum dosage is increased, this is not obviously related to the degree of turbidity removal. Note that the residual turbidity in Zone 4 is significantly lower than in Zone 2, which indicates another advantage of sweep flocculation over flocculation by charge neutralisation; much greater degree of clarification.

Another advantage of sweep flocculation over flocculation by charge neutralisation is the enhanced floc sizes, which contributes to the improved clarification. Figure-II.9 shows the change in Flocculation Index (FI) with time for two different alum dosages at pH 7.0. FI is a semi-empirical index indicating the state of aggregation. It is strongly correlated with floc size. This dynamic measurement of floc growth using a simple optical monitoring technique was introduced by [43] and is based on the principle of turbidity fluctuations. The lower dosage in Figure-II.9 is well within Zone 2 (charge neutralisation) and the higher is in Zone 4 (sweep flocculation).

There are very significant differences between the two curves in Figure-II.9. For 10 μM Al, the FI value begins to increase very soon after dosing (the first minute corresponds to the ‘rapid mixing’ phase of the jar test, where little floc growth occurs). Flocs then grow quite slowly and the FI reaches a plateau, corresponding to a limiting floc size, which depends on the stirring rate. This is consistent with the fairly rapid adsorption of charge-neutralising species on the kaolin particles, followed by quite slow coagulation. The aggregates (flocs) formed are quite weak and grow only to a rather small size. The rapid charge neutralisation is also indicated by the fact that all of the EM reduction occurs during the initial rapid mix phase.

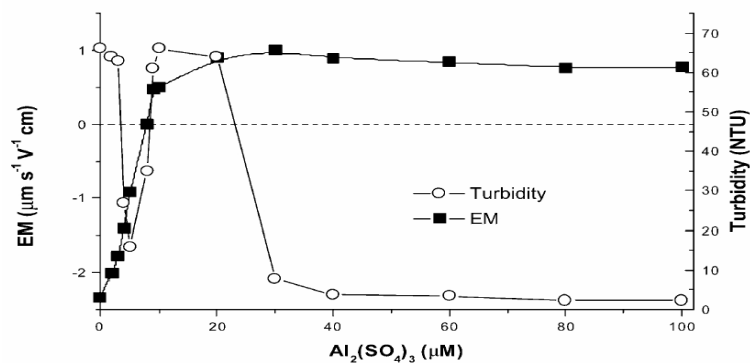


Figure-II.8 : As Fig. 7, but over a wider range of alum dosages and at pH 7. (Replotted from data of Duan, 1997)

There are very significant differences between the two curves in Figure-II.9. For 10 μM Al, the FI value begins to increase very soon after dosing (the first minute corresponds to the ‘rapid mixing’ phase of the jar test, where little floc growth occurs). Flocs then grow quite slowly and the FI reaches a plateau, corresponding to a limiting floc size, which depends on the stirring rate. This is

consistent with the fairly rapid adsorption of charge-neutralising species on the kaolin particles, followed by quite slow coagulation. The aggregates (flocs) formed are quite weak and grow only to a rather small size. The rapid charge neutralisation is also indicated by the fact that all of the EM reduction occurs during the initial rapid mix phase.

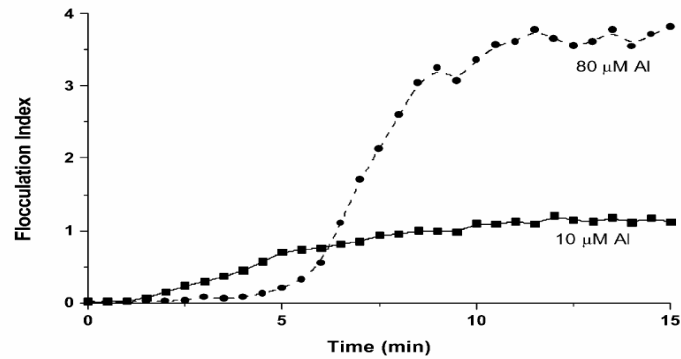


Figure-II.9 : Dynamic monitoring of kaolin suspensions at two dosages of alum, under the same conditions as for Fig. II.8. (Replotted from data of Duan, 1997)

For the dosage of 80 µM Al, the onset of floc formation is considerably delayed—significant rise in the FI value does not begin until approximately 5 min after dosing. However, a very rapid rise then occurs and the FI reaches a value nearly four times that in the other case, indicating much larger flocs. The lag time observed is related to the time required to form relatively large amorphous hydroxide precipitate particles. In the same study (Duan, 1997) it was shown that particles of aluminium hydroxide in the same solution at pH 7, but without kaolin, took several minutes to grow to a detectable size and the delay was of the same order as that observed for the onset of flocculation in Figure-II.9. The delay can be considerably reduced by increasing the alum dosage or by increasing the pH to approximately 8, which is the i.e.p. of the hydroxide precipitate in this system. However, even with a more rapid onset of flocculation, the rate of growth is not significantly greater and the final FI value is about the same (Duan and Gregory, 2003).

These results confirm that there are very important differences between destabilisation by charge neutralisation and sweep flocculation. In particular, flocs form more rapidly (perhaps after an initial delay) and can become much larger in the case of sweep flocculation, so that a greater degree of separation can be achieved. It seems that these effects are closely connected with the formation of a bulk hydroxide precipitate, initially in the form of very small colloidal particles (a few

nm in size), which are positively charged at around neutral pH. It is likely that some of these particles form a coating on the impurity particles, reversing their charge. Subsequently, aggregation of the colloidal hydroxide particles occurs, either on the particle surfaces (a form of *heterocoagulation*) or in bulk solution. Details of this process are still not clear, but microscopic observation of flocs produced under ‘sweep’ conditions show the original impurity particles embedded in an amorphous precipitate. A schematic diagram showing a possible sequence of events in sweep flocculation with aluminium salts is given in Figure-II.10. The Smoluchowski theory for particle aggregation in shear fields (orthokinetic flocculation) leads to the conclusion that flocculation rate is directly proportional to the effective particle volume (Elimelech et al., 1995). Growing hydroxide precipitate consists of very small primary particles in a rather open, fractal structure and it is easy to show that the effective floc volume can become quite large, even for low coagulant doses. It is found that the settled floc volume increases in proportion to the dosage of hydrolysing coagulants under sweep conditions (Gregory and Dupont, 2001). This probably accounts for the enhanced aggregation rate in sweep flocculation. Simply neutralising the particle charge with a rather thin layer of adsorbed species would not give a significantly increased collision radius.

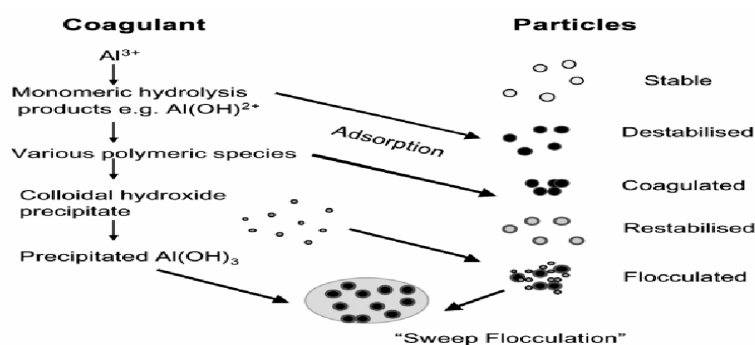


Figure-II.10 : Schematic diagram showing the interaction of aluminium species with initially negatively charged particles in water. The particles on the right hand side are initially stable and then become destabilised by charge neutralisation. At higher coagulant dosages they can become restabilised by charge reversal and incorporated in a flocculent hydroxide precipitate (‘sweep flocculation’). (Duan and Gregory, 2003)

II.5. PRE-HYDROLYSED COAGULANTS

There are now many commercial products that contain pre-hydrolysed forms of the metals, mostly in the form of polynuclear species. In the case of Al, most materials are formed by the controlled neutralisation of aluminium chloride solutions and are generally known as polyaluminium chloride (PACl). It is believed

that many of these products contain substantial proportions of the tridecamer Al_{13} . Although some information on the preparation of such materials and those based on iron is available, some important details are commercially sensitive and not easily found. In the case of aluminium sulfate, it is difficult to prepare pre-hydrolysed forms with high B values, because sulfate encourages hydroxide precipitation. The presence of small amounts of dissolved silica can substantially improve the stability up to B values of approximately 1.5. The resulting product is known as polyaluminosilicate sulfate (PASS).

These pre-hydrolysed materials are often found to be considerably more effective than the traditional coagulants. PACl products seem to give better coagulation than 'alum' at low temperatures and are also claimed to produce lower volumes of residual solids (sludge). Because they are already partially neutralised, they have a smaller effect on the pH of water and so reduce the need for pH correction. However, the mechanisms of action of PACl and similar products are still not well understood.

Explanations are mostly attributed to the high charge associated with species such as Al_{13} and the consequent effectiveness in neutralising the negative charge of colloids in water. The relatively high stability of Al_{13} means that it should be more readily available for adsorption and charge neutralisation at around neutral pH, whereas conventional 'alum' undergoes rapid hydrolysis and precipitation. However, charge neutralisation cannot be the only mechanism of destabilisation, otherwise only 'Zone 2' coagulation would occur, which is less effective than sweep flocculation. It is still not clear what role hydroxide precipitation plays in the action of pre-hydrolysed coagulants. Sulfate also plays an important role in precipitation with PACl (Wang et al., 2002).

Gregory and Dupont (2001) have recently shown that the volume of sediment produced in coagulation of clay suspensions by commercial PACl products is proportional to the coagulant dosage. This implies that some form of sweep flocculation is operating, since the volume of hydroxide precipitate would be expected to depend on the amount of coagulant added.

In the same study they have shown from dynamic studies with a range of hydrolysing coagulants that PACl products give more rapid flocculation and stronger flocs than for 'alum' at equivalent dosages. However, in all cases, floc breakage was irreversible to some extent, as found previously for alum. This is further evidence that the pre-hydrolysed products do not act simply by charge neutralisation and that some form of sweep flocculation is involved. It is very likely

that the nature of the precipitate differs in the case of PACl materials, as has been shown for precipitation from solutions of Al_{13} .

II.6. FLOC STRENGTH AND BREAK-UP

Ultimately, the strength of an aggregate must depend on the interparticle forces and on the number of particle-particle contacts. For weak interaction, as in the secondary minimum, flocculation may be easily reversible. In such cases, equilibrium concepts can be applied and the degree of aggregation depends on the particle concentration below a certain critical concentration, only single particles are found, but at higher concentrations, aggregates and single particles are in equilibrium. Since the depth of the secondary minimum depends on particle size, the critical particle concentration should also be size dependent, a point which was confirmed experimentally by Long et al. for a series of latex samples. In principle, the depth of the secondary minimum can be derived from such experiments.

Another form of reversibility is that which can be achieved simply by lowering the concentration of salt as evidence for a layer of hydrated counterions between aggregated particles. For a related reason, the flocculation of sterically stabilized particles can be reversed by changing the solution conditions.

In orthokinetic flocculation which is the flocculation mechanism employed in this study, the application of fluid shear to increase the collision rate also gives the possibility of floc breakage. Under given shear conditions; it is generally found that flocs grow only to a certain limiting size beyond which breakage to smaller units occurs. As the shear rate is increased the maximum floc size decreases and this remains one of the most effective empirical indications of floc strength. The larger the flocs formed under given shear conditions, the stronger they are. In stirred vessels, limiting floc diameters may range from several millimeters for low shear down to around 50 μm for higher shear levels (or weaker flocs).

A complication with flocculation in stirred vessels is that the local energy dissipation (and hence the effective shear rate) can show very large deviations from the mean value (determined by the total energy dissipation or the stirrer rotation speed). Near the tips of rotating blades, the shear rate can be ten times the mean value for the whole vessel. The limiting floc size depends on the maximum shear

rate encountered by flocs, whereas the rate of floc growth is governed more by the mean shear rate.

The nature of the breakage process depends on the size of flocs relative to the turbulence microscale (of the order of $100\mu\text{m}$ in many cases). For larger flocs, deformation and rupture may occur as a result of fluctuating dynamic pressure. For flocs smaller than the microscale viscous forces predominate and may cause either *erosion* of primary particles or small aggregates from large parent flocs, or *fragmentation* to form smaller flocs of comparable size. In most cases, collisions between flocs appear to have little influence on the breakage process.

The fractal nature of flocs raises some interesting questions on floc strength and break-up. The number of particle-particle contacts in an aggregate will be greater for more compact (higher d_F) structures and hence such aggregates should be stronger than those with lower fractal dimension. However, in an empirical floc strength determination the size of flocs under given shear conditions may be taken as a measure of floc strength. The size of an aggregate, for a certain mass of particles, depends on the fractal dimension and so the interpretation of such measurements is not entirely straightforward. Also, one of the factors leading to more compact flocs is a low collision efficiency, which may imply a lower interparticle attraction and hence a lower floc strength. Studies which incorporate particle-particle interaction and the fractal character of aggregates in a self-consistent manner would be valuable.

Intuitively, flocs formed by cluster-cluster aggregation might be expected on breakage to the original cluster. There is not much information on this point, but it is reminiscent of older ideas on the “hierarchical” nature of flocculation in which small flocs, composed of primary particles, were distinguished from “aggregates” of these flocs. Only “aggregates” were considered to break under shear, giving “flocs” which were resistant to break-up.

Nearly all practical applications of hydrolysing coagulants are nearly always under conditions of turbulent fluid motion. Mixing of coagulant involves quite intense agitation (‘rapid mix’) for a short time and this is usually followed by a longer period of gentler mixing (slow mix), either in a stirred tank or some form of hydraulic flocculator. The purpose of the second phase is to promote orthokinetic collisions of particles and hence floc growth. Flocs grow initially at a rate that depends on the energy dissipation (or applied shear), as well as on the particle

concentration and collision efficiency. As flocs become larger, further growth is restricted by the applied shear for essentially two reasons. Existing flocs may be broken as a result of disruptive forces (Matsuo and Unno, 1981) and the collision efficiency of particles in a shear field becomes lower as particle size increases (Brakalov, 1987). A dynamic balance between floc growth and breakage often leads to a steady-state floc size distribution, where the limiting size depends on the applied shear rate (Muhle and Dobias, 1993).

Pre-formed flocs can be broken if the effective shear rate is increased, in a manner, which depends on the floc size relative to the turbulence microscale (Muhle and Dobias, 1993). When flocs are subjected to an increased shear rate, floc break-up may occur. This may be by rupture of flocs into roughly equal-sized fragments or erosion of small particles from the surface of flocs. The mode of breakage in turbulent flow depends on the floc size relative to turbulence microscale (Mühle, 1993; Serra et al., 1997).

Bache et al. (1999) suggested an electrostatic bridge model in which the positive charge of the precipitate is shared by the negative charges of the primary particles. They claimed that the durability of this bridge mainly depends on the negative charges of the primary colloids. In order to prove this, they used four different suspensions, the particle surface charges (zeta potentials) of which were different, and they showed that flocs of primary particles with the lowest zeta potential are the strongest and vice versa.

Flocs formed by hydrolysing coagulants tend to be rather weak, so that breakage occurs readily. In the case of sweep flocculation, this breakage is not fully reversible, so that flocs do not completely re-form when the original shear conditions are restored. This effect is well known in practice, but has received rather little systematic attention (Francois and Van Haute, 1984; Francois, 1987; Spicer et al., 1998). Recent work (Yukselen and Gregory, 2002; Yukselen and Gregory, 2004) has given more detailed information on the subject, although the underlying mechanisms are still not well understood.

Yukselen and Gregory (2002, 2004) showed using the same dynamic monitoring method mentioned earlier that flocs formed with kaolin suspensions and aluminium sulfate, ferric sulfate, polyaluminium chloride and polyiron chloride were broken irreversibly at high stirring speeds and that the degree of irreversibility depended on the time of breakage. An example of their results is shown in Figure-II.11. In this case a kaolin suspension (50 mg/l) was flocculated by alum at a dosage

of 130 μM Al at around neutral pH (i.e. well within the sweep floc regime). Flocs were formed by stirring for 10 min at 50 rpm (slow mix) and then the stirring rate was increased to 400 rpm (breakage). These stirring rates correspond to mean shear rates (G values) of approximately 25 and 520 s^{-1} , respectively. The high stirring speed was maintained for between 10 and 300 s and was then reduced to the original 50 rpm. From the change in Flocculation Index with time, it is clear that, under slow stirring conditions, flocs grew fairly rapidly to a limiting size. When the stirring speed was increased, there was an immediate and rapid drop in the FI value, by a factor of nearly 10, showing very substantial breakage of flocs. Most of the breakage was achieved after approximately 10 s. When the stirring rate was returned to 50 rpm, some re-growth of flocs occurred, but not back to the previous FI value. Furthermore, the degree of recovery decreased for longer breakage times. This is especially apparent for the 300 s breakage case.

Many types of model suspensions, jars, agitators and shear field devices have been used to investigate floc strength. The studies agree on certain point, however, there are still many points of debate, which is due to the different techniques and equipment employed to determine floc strength (Jarvis et al., 2005).

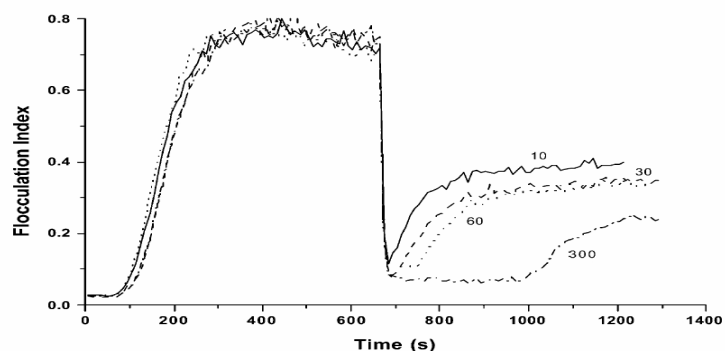


Figure-II.11 : Dynamic monitoring of kaolin suspensions, showing formation, breakage and partial re-formation of flocs. In all cases suspensions were dosed with alum (130 mM Al) and stirred at 50 rpm for 10 min. A higher stirring speed (400 rpm) was then applied for times of 10–300 s (as indicated on curves), followed by further stirring at 50 rpm. (From Yukselen and Gregory (2002))

As yet, there is no adequate model to explain these findings. The effect seems to be specific to the sweep flocculation case, since flocs formed using cationic polyelectrolytes, which destabilise the clay particles by charge neutralisation and electrostatic patch effects, showed almost complete re-formation after breakage (Yukselen and Gregory, 2002). It is likely that breakage of metal hydroxide flocs involves rupture of chemical bonds, which are unable to re-form.

Rapid mixing conditions have been shown to influence floc growth and structure. A necessary condition is that raw water solids receive a positively charged coating. When the coating arises from the nucleation of positively charged monomers, these only exist for a very short time (~ 1 s) before transforming to the amorphous precipitate (Amirtharajah and Tambo, 1991). During this time, they must be dispersed throughout the suspension in order to avoid arriving as neutrally charged $\text{Al}(\text{OH})_3$. So it is a race between the time to disperse the coagulant and the time scale of the chemistry.

Amirtharajah and Mills (1982) suggested that initial mixing conditions are not so important in the case of sweep flocculation, but this is not well established. On the contrary, recent studies have shown that rapid mixing is crucial to floc growth for sweep flocculation (Bache et al., 1999; Yukselen and Gregory, 2004b)

Bache et al. (1999) claimed that the conclusion of Amirtharajah and Mills (1982) was a misconception, stemming from a focus on the quality of the settled water rather than on the nature of the floc (e.g. floc strength). They investigated the effect of rapid mixing on floc strength. To do this, they added the colloids 5 min after coagulation (simulating an extreme case of poor mixing). They showed that the floc strength is significantly reduced compared with addition of the coagulant into the suspension with good rapid mixing. In the case of good mixing, the zeta potential of the coated particle was +22 mV whereas in the case of poor mixing, the corresponding zeta potential was about -5 mV. From this data, they concluded that due to fairly low zeta potential (as in the case of poor mixing) the electrostatic bridging forces will also be low and are the likely cause of the reduced strength.

Yukselen and Gregory (2004b) studied the effect of rapid mixing time on floc growth. They used kaolin suspensions, turbidity of which was initially adjusted to 100 NTU. They found that floc size decreased as rapid mixing time increased. Residual turbidity measurements pointed to an optimum rapid mixing time of 10 s both with alum and PACl. They concluded that there was less chance of compact aggregates being formed with only brief periods of rapid mixing and more open, larger flocs can grow, and although the smaller flocs resulting from extended rapid mix periods should give a higher density; they were less readily removed by sedimentation. This could be due to the fact that density effects cannot overcome size effects (Gregory, 1997).

Francois and Van Haute (1984) showed that the diameter of ruptured and regrown flocs decreases as the duration of rapid mixing increases. They observed a

maximum diameters around 30 s and 60 s rapid mixing for both ruptured and regrown flocs and the floc diameters did not change significantly for prolonged rapid mixing times (150 s and longer).

Francois (1988) reported that a rapid mixing time longer than the critical mixing time lead to a longer floc build-up time because of temporary decrease in floc growth. A rapid mixing time shorter than the minimum time required to build up flocculi (i.e., so called building units of flocs) also resulted in the same way.

There are also some other studies (Rossini et al., 1998; Kan et al., 2002) which conclude the same way that as the rapid mixing duration increases floc size decreases.

Since floc strength and mixing parameters are closely related to floc structure, they are also related to sludge dewatering.

CST has been widely used as a measure of ease for sludge dewatering. However, its application field is generally found in sludge conditioning with polymers, and especially determination of optimum polymer dose. General practice is that conditioning of metal hydroxide sludges with polymers enhance dewaterability, mainly due to loss of intrafloc water (Knocke et al., 1993). A dose giving the lowest CST is taken as the optimum dose, and generally further polymer dosing is found to give no significant improvement or worsening in dewatering (Lee and Liu, 2000, 2001; Wu et al., 2003).

Wu et al. Studied polymer conditioning of a waste activated sludge from a fiber plant. They found that floc strength was significantly increased with polymer dose until the optimum dose. Further dosing slightly increased floc strength. Breakage tests showed that average floc size of optimum and under dose sludges decreased with increasing mixing intensity (G.t). However, the reverse is observed with over dose sludge flocs. They claimed that this was due to the need for much intense mixing of over dosed sludge.

CST was shown to increase with floc size reduction for under dosed sludge. A slight increase in CST with increasing breakage mixing intensity was observed for optimum dosed sludges is logical; floc size and density is significantly increased after polymer conditioning, and when these flocs are ruptured floc size and CST may show worsening depending on the strength of conditioned sludge flocs. The lower the floc strength of polymer conditioned sludge flocs is, the greater the increase in CST with breakage mixing intensity is. However, the situation might be

different with metal hydroxide flocs due to the chemical nature of flocs and difference in flocculation mechanisms compared to polymer conditioning.

In some cases it appears that flocs with more open structure are more readily dewatered (Waite, 1999). Lower density, porous flocs may be permeable to water for flocs of given mass, and significant flow could occur through floc as well as around floc. This suggests that better dewaterability may be observed as floc size increases (which was observed by Yukselen and Gregory, 2002b). On the other hand, this ignores the possibility that higher density structures may give faster dewaterability because of smaller floc size and reduced drag. This study presents relevant data to the latter suggestion; CST values were generally observed to decrease with decreasing floc size. Similar findings were also reported by Turchiuli and Fargues (2004). It is thought that larger size flocs consist of a package of solid particles and some water entrapped in the solid structure (intrafloc water). However, this water component may disappear or be significantly reduced when the size of flocs are smaller, which may give lower CST values as a sign of better dewatering.

There are many studies on polymer conditioning of sludges. However, very few studies on the dewaterability of sludges formed with only hydrolysing coagulants. Nevertheless, it may be very useful to keep in mind that sludges conditioned with polymer are priorly formed with hydrolysing coagulants. Thus, dewaterability of polymer conditioned sludges may be significantly affected by the properties of flocs formed with hydrolysing coagulants. This study aims to investigate the effects of floc breakage duration and rapid mixing duration on alumino-hydroxide sludges of highly turbid kaolin suspensions flocculated with alum and a PACl coagulant.

CHAPTER III

MATERIALS & METHODS

III.1. SUSPENSION

Kaolin clay (Aldrich) was used as a model suspension. The suspension was prepared as described in (Yukselen and Gregory, 2002a) which is as follows:

Two hundred grams of kaolin was dispersed in 500 mL of deionized water in a high-speed blender. The pH of the suspension was raised to about 7.5 to obtain full dispersion of kaolin, which was done by necessary amount of N/10 NaOH addition. The clay suspension was blended at 4000 rpm for 10 min and then was diluted to 1L with deionized water. The prepared suspension was left in a measuring cylinder overnight. Next day, the top 800 mL was withdrawn, and its solids content was measured gravimetrically to be 132 g/L. Finally, this was diluted with deionized water to give a solids content of 50 g/L.

For the flocculation tests, the stock suspension was added into 1-L jars filled with 800 mL tap water. The calcium content in the tap water causes destabilization and slow coagulation of the kaolin particles. This would cause problems in interpreting the results with hydrolyzing coagulants. A small amount of commercial humic acid (Aldrich, Milwaukee, WI) was added to the stock kaolin suspension to avoid this difficulty. Adsorbance of humic acid on the clay particles gives enhanced stability against divalent metal ions such as Ca^{2+} . Necessary amount of the prepared humic acid solution was added into the stock solution of kaolin (50 g/L) to give a HA concentration of 0.5 g/L. The turbidity of suspensions used in all of the flocculation experiments was adjusted to give about 1000 NTU (about 740 mg/L

kaolin, 7.4 mg/L HA), which was determined by WTW Turb 550 turbidimeter (Figure-III.1).



Figure-III.1: Turbidimeter (WTW Turb 550).

III.2. COAGULANTS

Aluminium sulfate octadeca hydrate ($\text{Al}_2(\text{SO}_4)_3 \cdot 18\text{H}_2\text{O}$; Merck) ‘alum’ was used. The salt was dried in oven at 103-105°C and dissolved in deionized water at a concentration of M/10. This alum stock solution was kept in refrigerator at 4-5°C.

A commercial polyaluminium chloride (PACl) product (Kemira Kemi AB, Helsingborg, Sweden) was used. This PACl coagulant, which was named as PAX-216 had a density of 1.35 g/cm³, was supplied as an 8.1 wt % Al solution. This solution was used without any dilution.

III.3. APPARATUS

The procedure of floc formation experiments was similar to those described before in a number of works (Gregory and Duan, 1998; Yukselen and Gregory, 2002a; Yukselen and Gregory, 2002b; Yukselen and Gregory, 2004a; Yukselen and Gregory, 2004b; Yukselen and Gregory, 2004c) employing an on-line optical

flocculation monitoring device (Photometric Dispersion Analyser - PDA 2000, Rank Brothers Ltd., Cambridge, UK; Figure-III.2) in modified jar-tests.



Figure-III.2: Photometric Dispersion Analyser (PDA 2000, Rank Brothers Ltd., Cambridge, UK).

800 mL of synthetic suspensions were included in 1-L jars, each stirred with mixing units connected to a Flocculator 90 semiautomatic jar-test device (Kemira Kemwater, Helsingborg, Sweden; Figure-III.3). The rapid and slow mixing times and speeds can be set either on the menu of this device or by a software through computer connection. Sample from one beaker was circulated for dynamic monitoring of floc growth through transparent plastic tubing (3 mm i.d.) via a peristaltic pump (Watson Marlow 505Di; Figure-III.4). This pump was located after

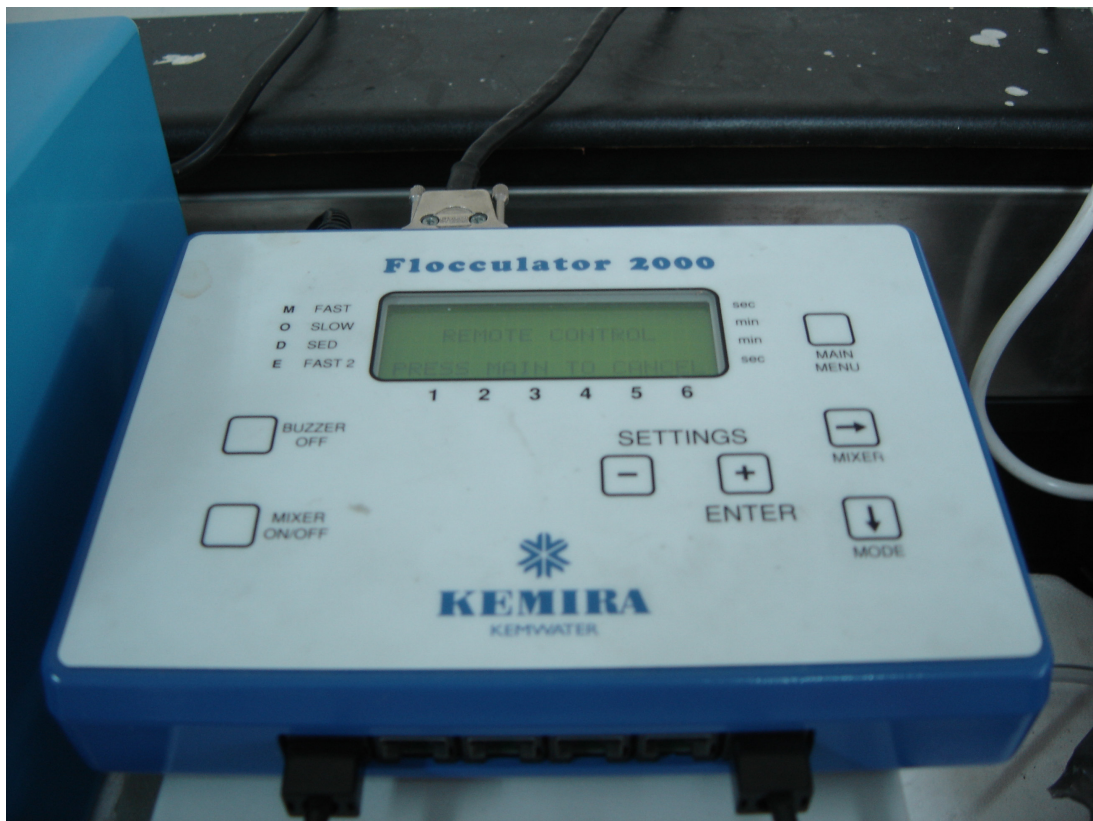


Figure-III.3: Flocculator 90 semiautomatic jar-test device (Kemira Kemwater, Helsingborg, Sweden).

the PDA instrument to prevent floc breakage since flocs are likely to be broken in the pinch portion of pump. The tubing was clamped in the PDA instrument so that the flowing sample was illuminated by a narrow light beam (850 nm wavelength). The PDA 2000 measures the average transmitted light intensity (dc value) and the root mean square (rms) value of the fluctuating component. The ratio of the latter to the former (rms/dc), which is the Flocculation Index (FI), gives a sensitive index of particle aggregation (Gregory and Nelson, 1986).



Figure-III.4: Peristaltic pump (Watson Marlow 505Di).

The FI value is not an exact measure of the floc sizes, it can only be used as comparative information on floc properties under different coagulation kinetics conditions such as different mixing intensities and times, different coagulant types and doses, etc. However, the FI value was shown to be in good correlation with mean floc size and residual turbidity after sedimentation (Gregory and Hiller, 1995; McCurdy *et al.*, 2004). As flocs in the sheared grow, a corresponding increase in the FI value is observed, and the rate of increase is a good indication of flocculation rate. By the same way, floc breakage is apparent by a reduction in the FI value, and so is re-growth of flocs by a following increase. Considering the difficulties in determining the absolute floc sizes under dynamic conditions using currently available methods, this ‘turbidity fluctuation technique’ used by PDA is very practical in many circumstances. The experimental setup for dynamic monitoring of floc growth is presented in Figure-III.6 illustrated in Figure-III.7.

Imhoff cones (Figure-III.5a) were used for the settlement of sludges and sludge volume index (SVI) measurements. CST tests were applied to settled sludge samples. For this, a capillary suction timer device (Capillary Suction Timer, Type 304M, Triton Electronics Ltd.; Figure-III.5b) was employed.

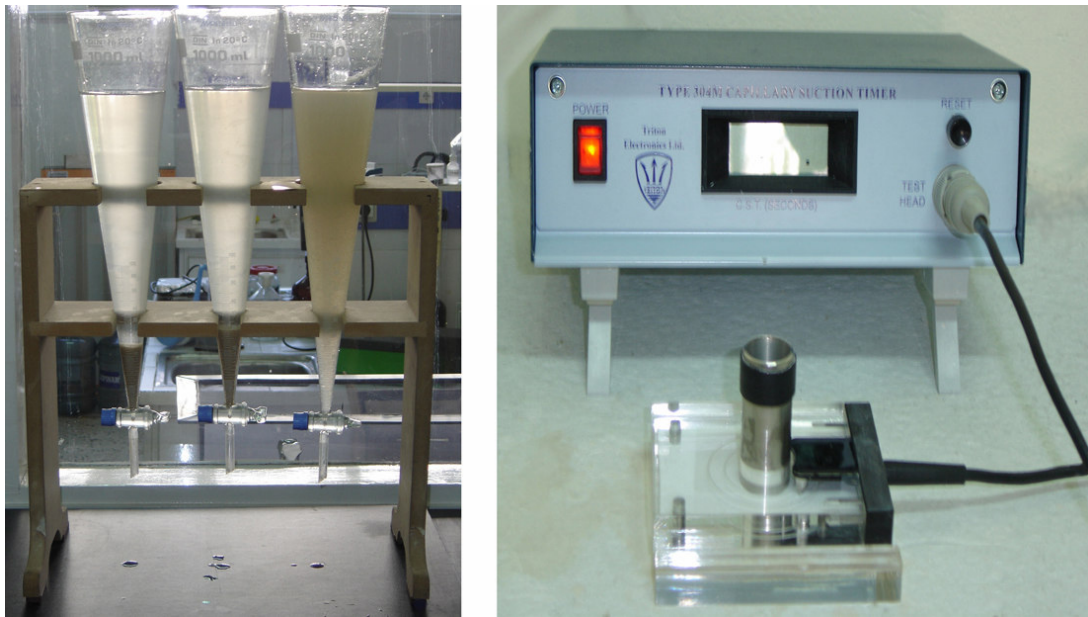


Figure-III.5: Sludge settling and CST measurement; a) Imhoff cones, b) Capillary Suction Timer, Type 304M, Triton Electronics Ltd.

Microphotographs of floc was taken by a light microscope (Leica DM LB2) which was equipped with a high resolution Leica camera.

III.4. PROCEDURE

For standard jar test, 800 mL of synthetic kaolin suspension (turbidity = 1000 NTU) was placed in a 1-L jar. The sample was circulated from the stirred jar at a flow rate about 25 mL/min through a plastic transparent tubing which was attached to the PDA instrument. After allowing 2 minutes for steady-state readings to be established, coagulant was dosed and immediately after dosing the sample was stirred at 400 rpm ($G = 518 \text{ s}^{-1}$) for required durations to provide complete mixing of the coagulant. After rapid mixing the stirring speed was reduced to 40 rpm ($G = 16 \text{ s}^{-1}$) and kept at this value for 10min to allow growth of flocs. In order to achieve floc breakage the stirring speed was increased to 400 rpm for required durations. After floc breakage the stirring speed was reduced back to the previous slow mixing condition (e.g. 40 rpm for another 10 min). The G values given above were calculated according to Mejia and Cisneros (2000), who used a similar jar test device.

At the end of each jar test, a small sample was withdrawn with an automatic pipette, plastic tip of which was cut to enlarge the opening in order to prevent breakage of flocs while transferring for microphotography. The flocculated suspension was then transferred into an Imhoff cone to settle. Volume of the settled sludge and residual turbidity of the supernatant were measured after 30 min and 2 hr settling period. At the end of 2 hr settling, 5mL sludge sample was taken from the bottom of the Imhoff cone and the CST test was applied. Another 5 mL sludge sample was also taken for sludge solids content analysis. This sludge sample was weighed, filtered through a filter paper (weight of which was measured). The filtered cake was dried in an oven at 103-105°C and then weighed. The final dried weight gives the weight of the sludge solids whereas the difference of two weights gives the weight of the water content of the sludge. Sludge solids content and moisture content calculations were done according to those weight data.



Figure-III.6: Experimental setup for dynamic monitoring of floc formation in jar-test procedure.

For *optimisation* studies, the rapid mixing and slow mixing were conducted at 400 rpm for a duration of 10 sec and at 40 rpm for a duration of 10 min, respectively. Alum was dosed at 0.68 – 33.75 mg/L concentrations in order to determine the optimum dosage with respect to minimum residual turbidity and capillary suction time (CST).

Four different breakage times (10 – 300 sec) at 400 rpm for the investigation of *the effect of breakage duration* were applied following the ‘rapid mixing at 400

rpm for 10 sec and slow mixing at 40 rpm for 10 min' procedure. The results were compared by means of flocculation index (FI) values, residual turbidity and capillary suction time (CST) data.

For the effect of rapid mixing duration analysis, nine different rapid mixing times (0 – 300 sec) were studied followed by slow stirring at 40 rpm for 10 min, breakage at 400 rpm for 10 sec and slow stirring for re-formation of flocs at 40 rpm for 10 min. Again, the results were compared by means of flocculation index (FI) values, residual turbidity and capillary suction time (CST) data.

All experiments were carried out two or three times for reproducibility of data.

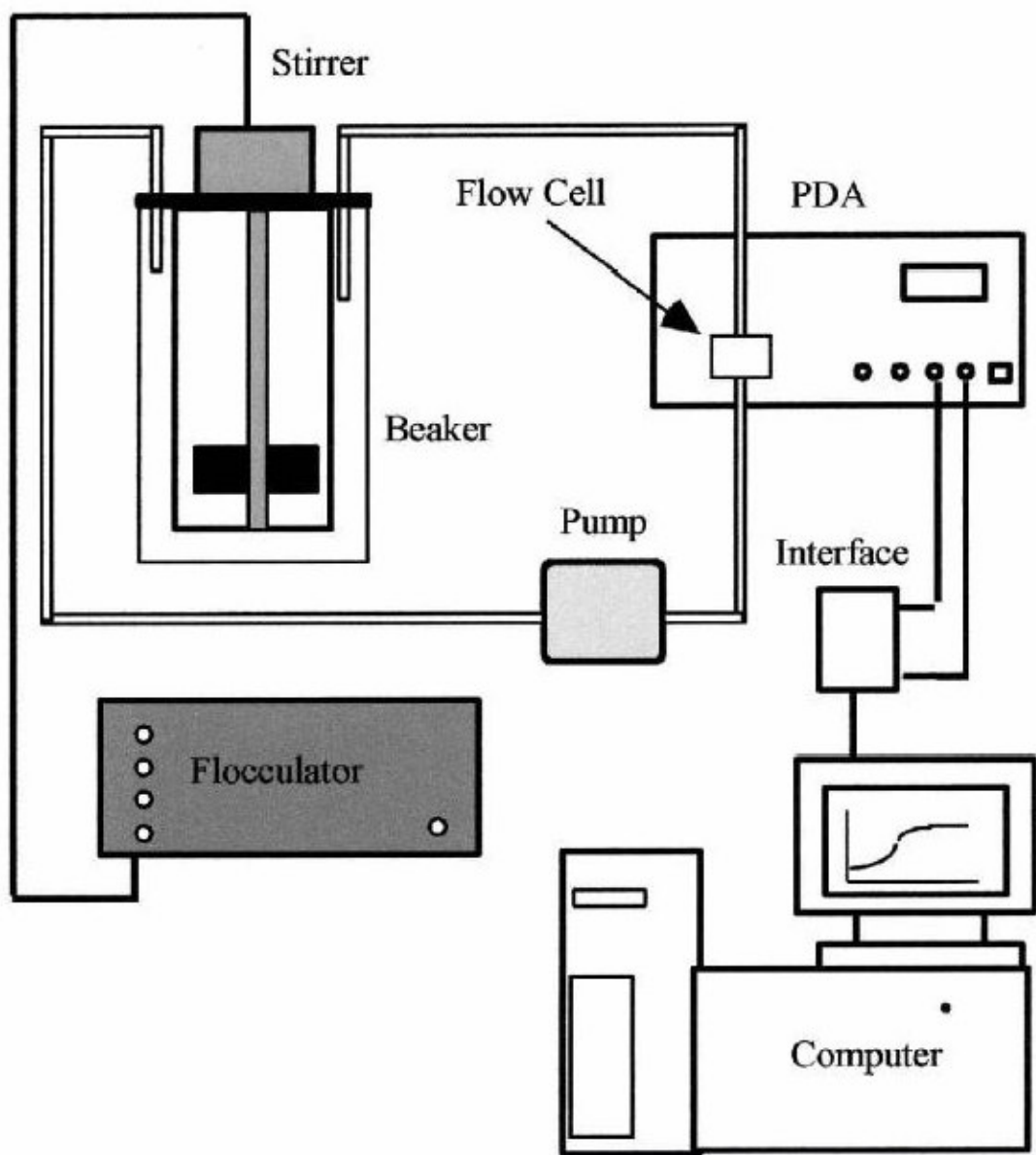


Figure-III.7: Schematics of the experimental setup for dynamic monitoring of floc formation in jar-test procedure (Yukselen and Gregory, 2002a).

CHAPTER IV

RESULTS & DISCUSSION

Different rapid mixing and breakage durations were applied during the jar test experiments to investigate how these factors affect floc formation (in terms of relative size), residual turbidity and water release properties of the formed sludges (in terms of capillary suction time-CST). Two different aluminium based hydrolysing coagulants, aluminium sulfate (alum) and polyaluminium chloride (PACl – PAX 216) were used and their results were compared. The FI curves from the PDA instrument allow to make comparisons between different coagulants and different shear regimes. Breakage and recovery factors can be calculated from these curves and be used as indicatives for floc strength and reversibility of floc breakage. Residual turbidity data measured correlate well with the findings of relative floc sizes. Finally, these and the CST results (as a measure of dewaterability) were linked to each other.

IV.1. OPTIMUM DOSE DETERMINATION

Different doses between (0.68 – 33.75 mg/L as Al) were added to the kaolin suspension (turbidity = 1000 NTU) to determine the optimum dose for alum. The jar tests were carried out under a rapid mixing at 400 rpm ($G = 518 \text{ s}^{-1}$) for 10 s and a slow mixing at 40 rpm ($G = 16 \text{ s}^{-1}$) for 10 min. The response of residual turbidity to dosage is presented in Figure-IV.1, measured after 30 minutes and 2 hours settling.

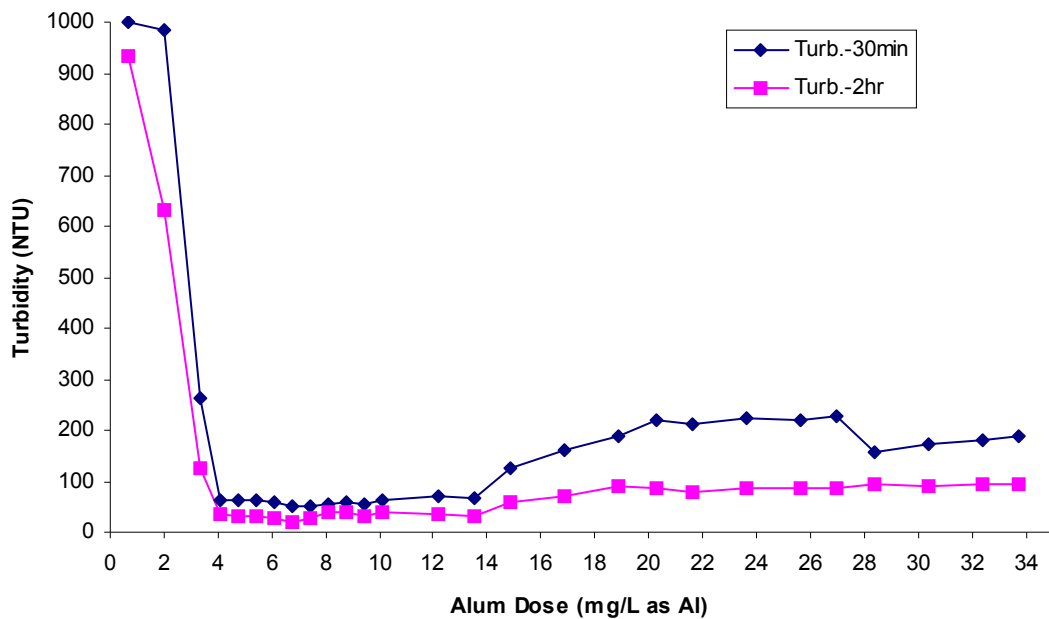


Figure-IV.1: Residual turbidity after 30 min and 2 hrs settling vs. dosage.

There is a rapid decrease in residual turbidity up to a dosage of about 4 mg/L as Al, and then the residual turbidity makes a minimum at the dosage of 6.75 mg/L as Al, both after 30 min (51.2 NTU) and 2 hrs settling (20.7 NTU). The residual turbidity does not change significantly with further dosing.

This correlates well with the CST data, presented in Figure-IV.2. There seems a minimum CST value (79.4 s) at the dosage of 7.48 mg/L as Al. The CST value for 6.75 mg/L as Al dose is 82.6 s, which is a little bit higher than the CST of 7.48 mg/L as Al dose. However, 6.75 mg/L as Al dose gave lower residual turbidity values, thus this dosage was chosen as the optimum dosage. After that dosage the CST increases slightly and stays almost around the same value of 85 s. The CST value of the first two dosages is not given in Figure-IV.2 because sufficient amount of sludge for the CST test (~5 mL) was not formed with those dosages, as seen in Figure-IV.3.

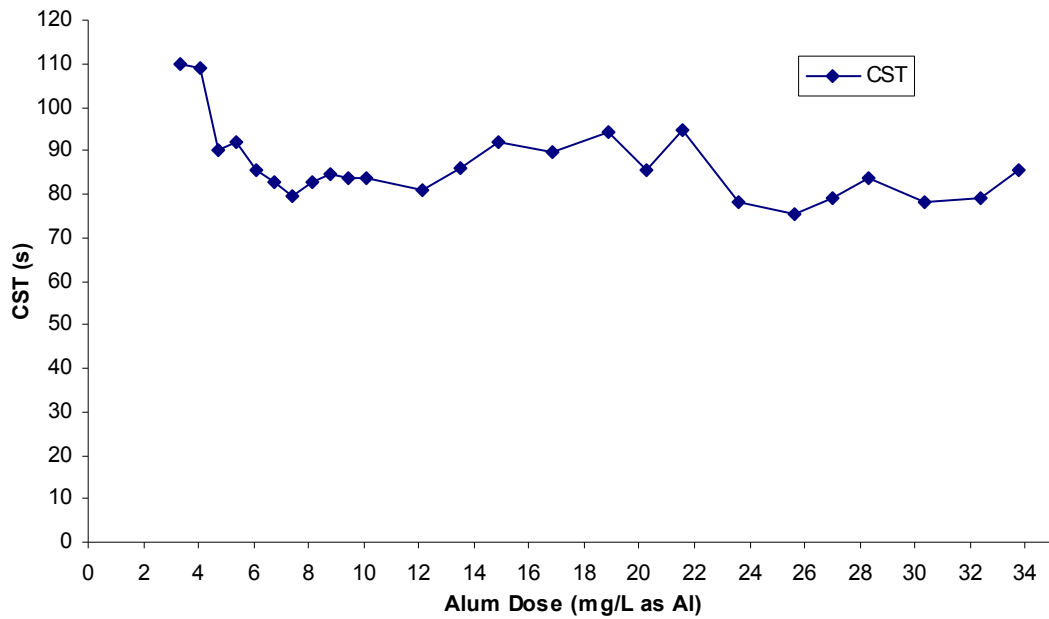


Figure-IV.2: The change of capillary suction time with alum dosage.

The summary of what is seen in Figure-IV.3 is that the amount of settled sludge increases as alum dose increases. Similar observations were given in literature (e.g. Bache and Papavasiliopoulos, 2003).

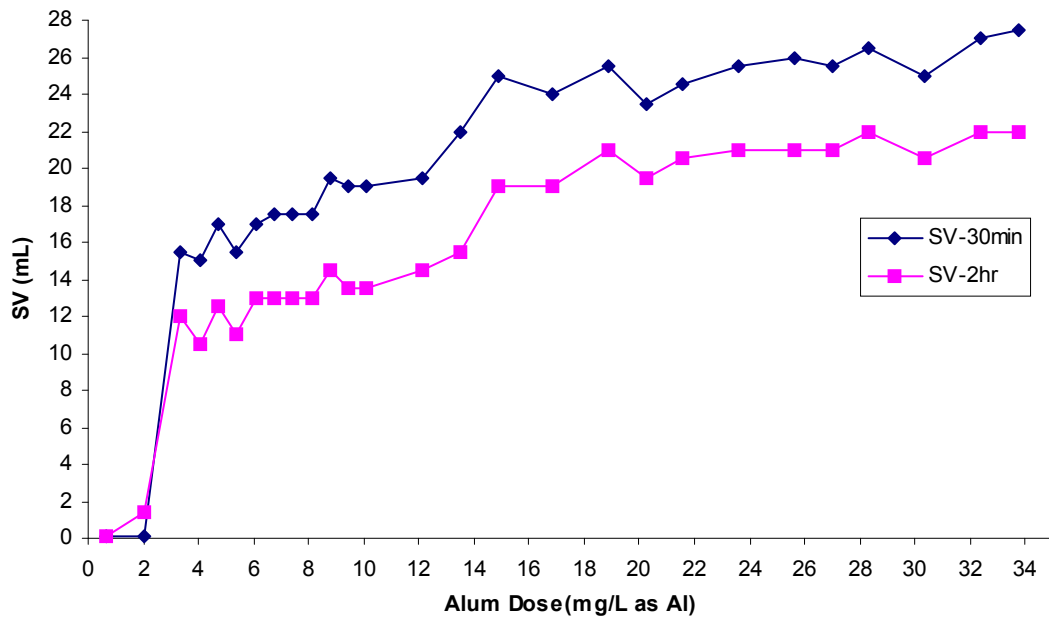


Figure-IV.3: Amount of sludge vs. alum dosage.

According to these findings the optimum dose was chosen to be 6.75 mg/L. This dosage is well within the ‘sweep flocculation’ regime. An equivalent dosage (in terms of mg/L as Al) was used for PACl for comparison purposes.

IV.2. FLOC FORMATION, BREAKAGE, AND RE-FORMATION

Analysis of floc formation, breakage and re-formation was carried out at the optimum alum dose. The flocs were formed under 400 rpm ($G = 518 \text{ s}^{-1}$) rapid mixing for 10 s and 40 rpm ($G = 16 \text{ s}^{-1}$) slow stirring for 10 min. After formation these flocs were exposed to a high shear rate of 518 s^{-1} for a duration of 10 s for breakage and then the shear rate was reduced to its original low value ($G = 16 \text{ s}^{-1}$). At the end of the jar tests the flocculated suspensions were taken into Imhoff cones for sludge settling. After 30 minutes and 2 hours settling volumes of settled sludges were measured and water samples were withdrawn from the supernatant for residual turbidity measurement. 5 mL of the settled sludge samples were taken after 2 hours settling for CST analysis.

For these analysis, different jar tests were carried out; in the first set the flocs were formed, in the second set the flocs were broken after formation, and in the third set the broken flocs were re-formed. These sets are referred to as “1st peak”, “Breakage” and “2nd peak”. The results are given in Table-IV.1.

Table-IV.1: Residual turbidity and sludge volume values after 30 min and 2 hr settling for 10 s breakage case with alum.

	10sec-1st peak	10sec-breakage	10sec-2nd peak
Turbidity-30min	50.7	79.0	64.5
Turbidity-2hr	27.5	42.6	32.4
SV-30min	17.0	18.3	18.7
SV-2hr	12.2	12.8	13.8

The results indicate that the residual turbidity increases as floc size decreases. This correlates well with the relative floc size curve (FI curve) of the PDA shown in Figure-IV.4.

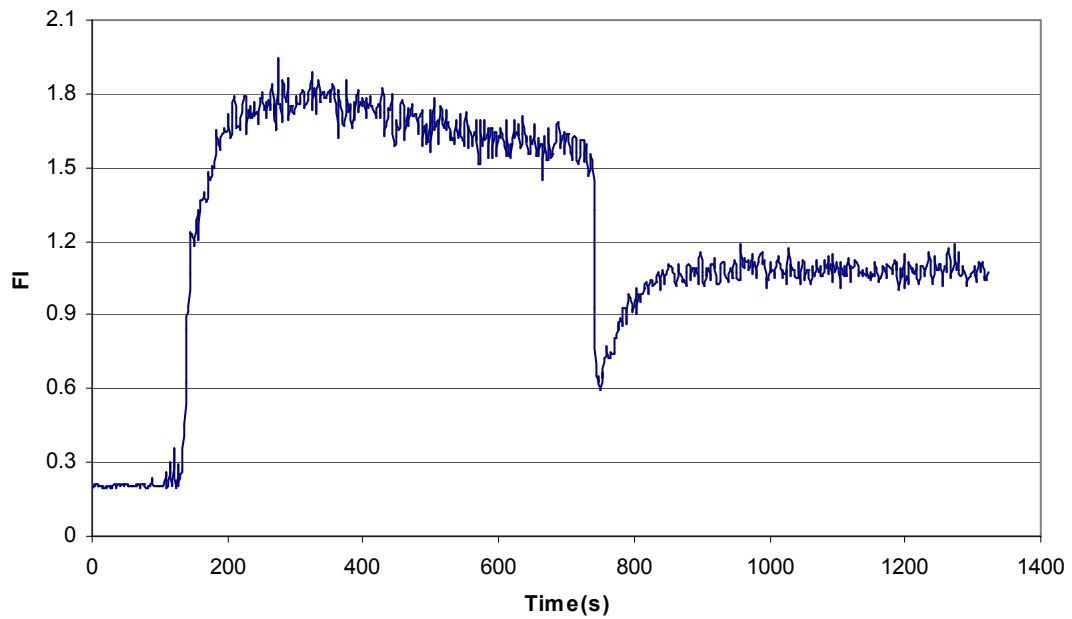


Figure-IV.4: Floc formation, breakage and re-formation with optimum alum dose (6.75 mg/L as Al). Rapid mixing at 400 rpm for 10 s, followed by 10 min of slow stirring at 40 rpm, then floc breakage at 400 rpm for 10 s and re-formation at 40 rpm.

As seen in Figure-IV.4, the FI value is the highest at the 1st peak (floc formation), which means the largest flocs under the given conditions were formed. After 10 min slow stirring, these flocs were ruptured due to increased shear rate applied for 10 s. When the shear rate was returned back to its original low value, the broken flocs regrow to some extent, but not to their previous size before breakage, showing the irreversible nature of floc breakage with hydrolysing coagulants. These relative floc sizes are closely related to the residual turbidity values given in Table-IV.1; the larger the flocs are, the better they settle and the lower the residual turbidity they give is. This is shown in Figure-IV.5.

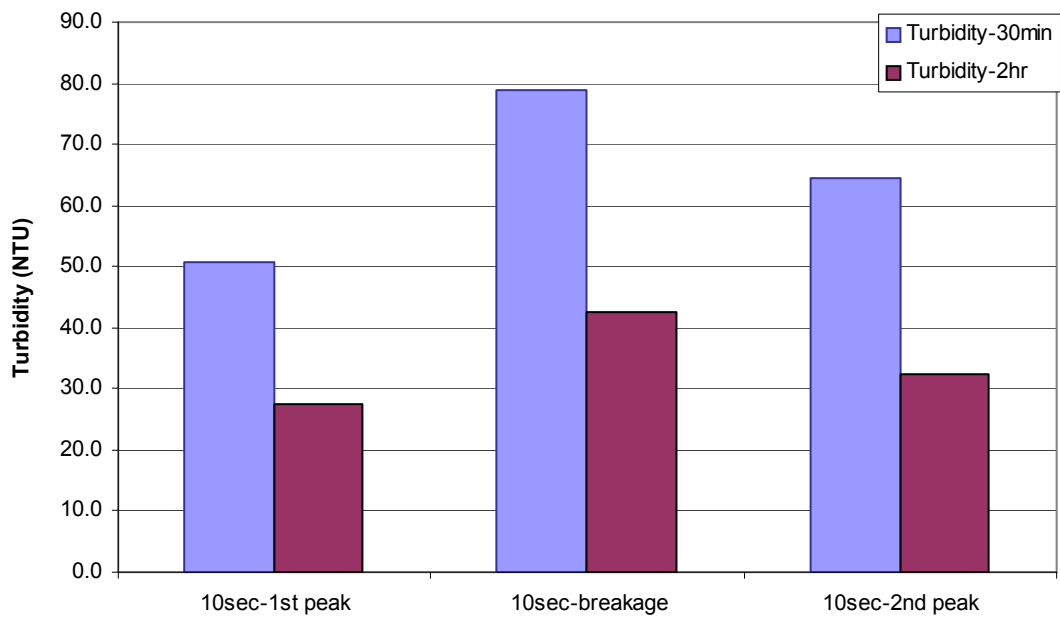


Figure-IV.5: Residual turbidity at formation, breakage and re-formation (conditions are same with those in Fig.-IV.4).

IV.3. EFFECT OF BREAKAGE DURATION

To investigate the effect of breakage time on floc formation, four different breakage durations (10, 30, 60, and 300 s) was applied to the flocculated suspension. The procedure is as follows:

After allowing 2 minutes for steady-state readings to be established, the optimum coagulant dose (6.75 mg/L as Al) was added while mixing at 400 rpm. After 10 s, the stirring speed was reduced to 40 rpm for 10 min, and then increased to 400 rpm for the different durations. At the end of breakage period the stirring speed decreased to 40 rpm for 10 min to allow regrowth of flocs. The results of these four flocculation experiments are presented in Figure-IV.6.

The region of constant FI (or floc size) is generally thought to reflect a balance between floc growth and breakage at a given shear rate. The similarity of the FI curves during the first minutes of flocculation (until breakage) reflects the reproducibility of the test. It is apparent that, at the higher alum dosages, there is some reduction in the FI value after a few minutes of stirring at 40 rpm. This thought to be due to some restructuring of flocs. It does not result from partial settling of flocs during the slow stirring period, because the effect becomes more noticeable at higher stirring speeds where floc settling should be less significant. This was also observed by Gregory *et al.* (2000) and Yukselen and Gregory (2002a).

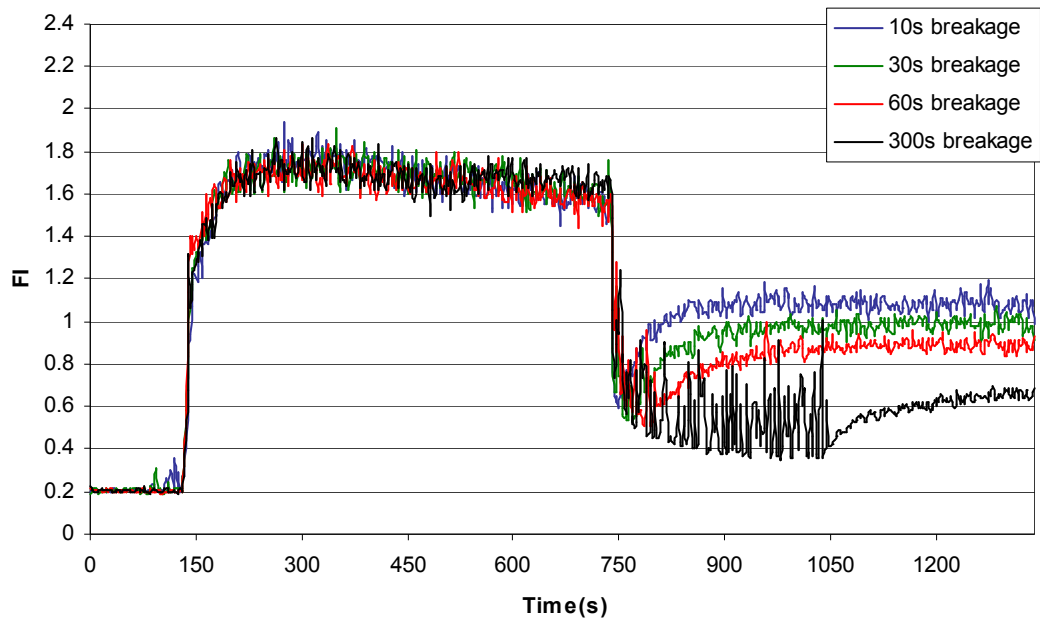


Figure-IV.6: Breakage and re-formation of flocs with alum at 400 rpm for different durations and at 40 rpm for 10 min, respectively.

Following Francois (1987), the breakage and regrowth of flocs under cycled shear conditions can be quantified by a “breakage factor” and a “recovery factor.” In terms of Flocculation Index for fully grown (FI_1), broken flocs (FI_2) and regrown (FI_3), these can be written as:

$$\text{Strength factor} = (FI_2 / FI_1) * 100$$

$$\text{Recovery factor} = [(FI_3 - FI_2) / (FI_1 - FI_2)] * 100$$

$$\text{Breakage factor} = (FI_1 - FI_2) / FI_1 * 100$$

where FI_1 is the flocculation index for fully grown flocs, FI_2 is the value after breakage, and FI_3 is the value after regrowth.

It is clear that initial floc breakage is rather rapid, almost a 4-fold reduction occurs in FI value with 10 s breakage and the 30 s and 60 s breakage periods give nearly the same decrease in FI as seen in Figure-IV.7. The floc strength and the degree of recovery after the stirring speed is reduced to 40 rpm gradually decreases with increased breakage time. It is likely that the ability of flocs to regrow and reestablish bonds is diminished. With only 10 s at 400 rpm the FI value shows a smaller decrease, probably because there is insufficient time to complete the initial rapid breakage. For 10 s breakage, there is a greater degree of recovery at 40 rpm, and the rise in FI is much more rapid than for the longer breakage periods. Also, it seem like time to reach the maximum regrown floc size in the recovery zone is

increased with breakage duration. For 5 min breakage at 400 rpm, decrease in FI is much more gradual with a more limited recovery at 40 rpm.

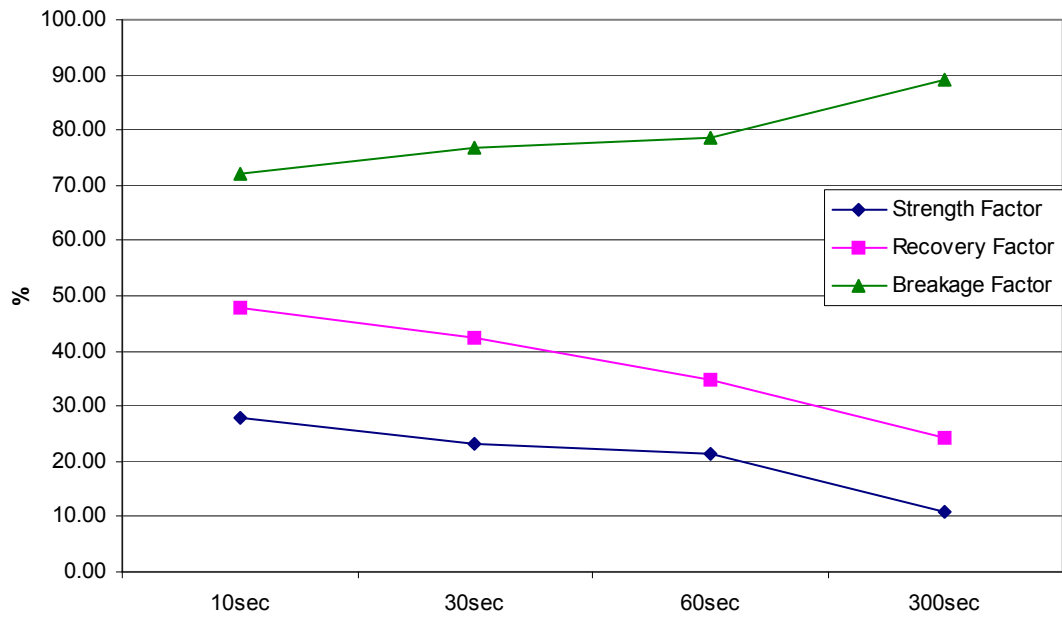


Figure-IV.7: Strength, Recovery and Breakage Factors; investigation of the effect of breakage time with alum.

Again, it is apparent in Figure-IV.8 and Figure-IV.9 that the residual turbidity increases as floc size decreases.

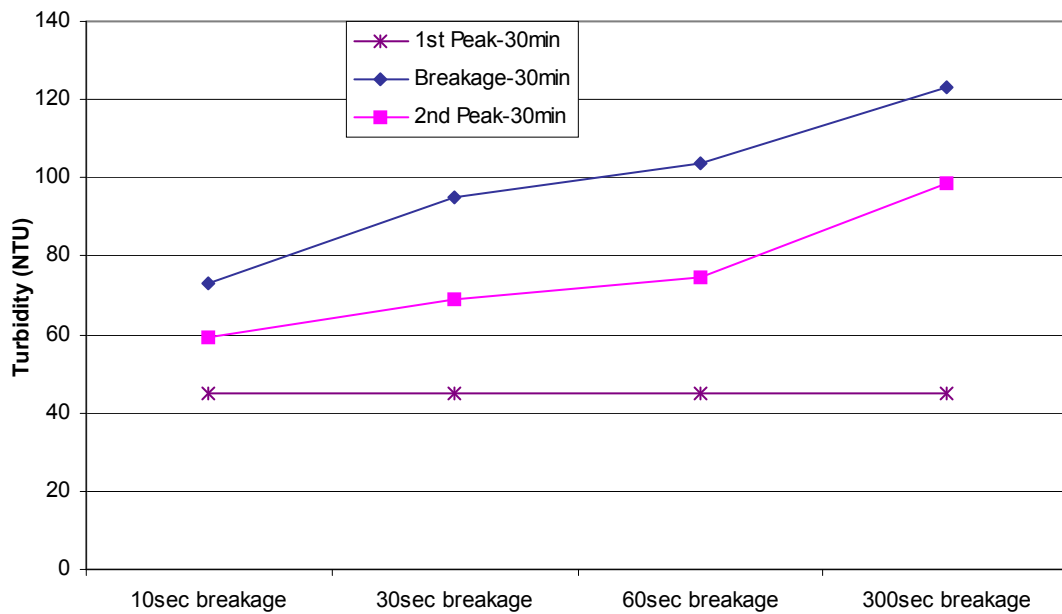


Figure-IV.8: Residual turbidity for different durations of breakage after 30 min settling with alum.

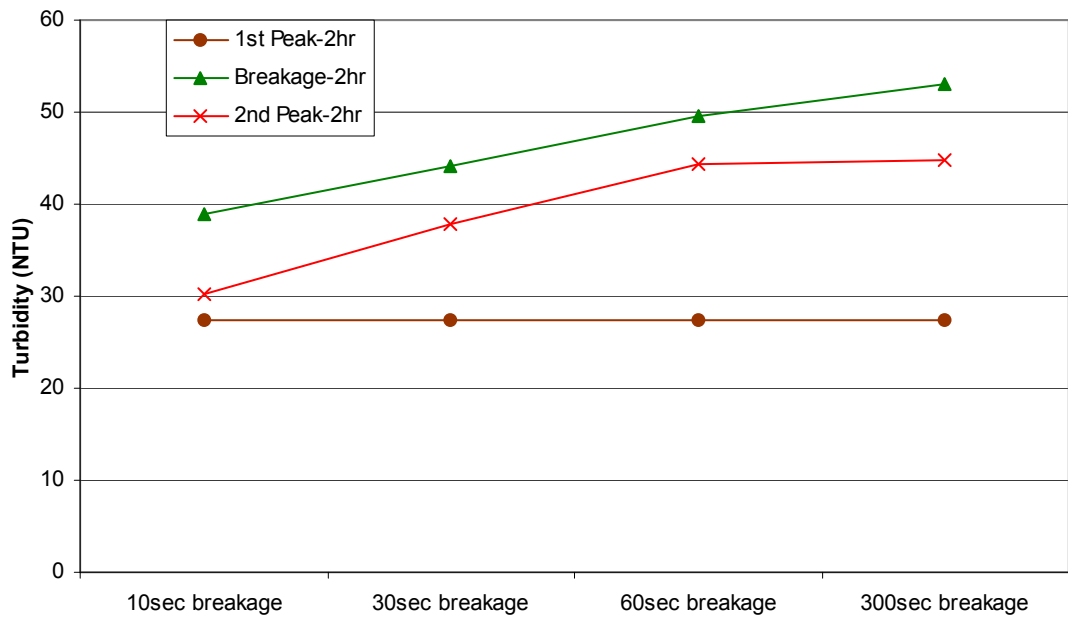


Figure-IV.9: Residual turbidity for different durations of breakage after 2 hr settling with alum.

When the CST test results in Figure-IV.10 are examined it is seen that there is a minimum after 30 s breakage and for longer breakage durations a trend of increasing CST with decreasing floc size is observed.

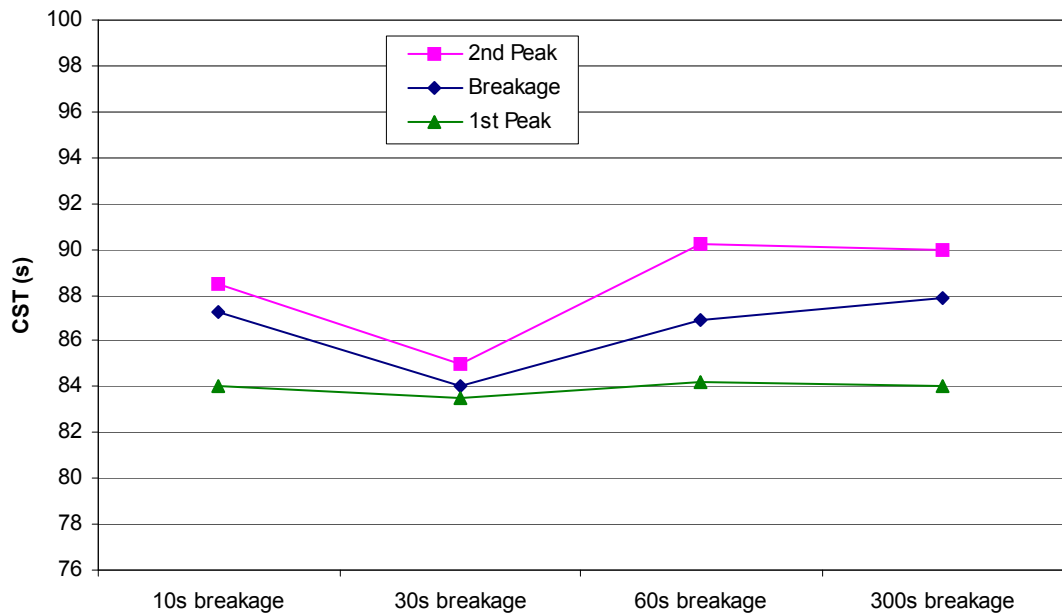
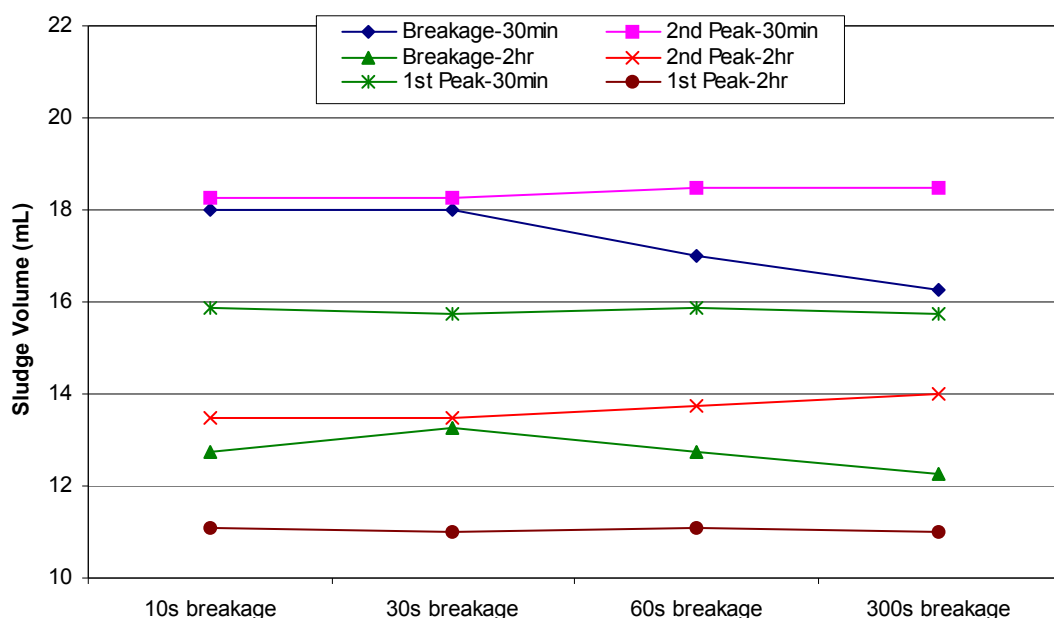


Figure-IV.10: CST test results for different durations of breakage after 2 hr settling with alum.

Figure-IV.11 shows sludge volumes after 30 min and 2 hrs settling. The general trend for each breakage time case is that the 1st peak sludge shows the least volume whereas the 2nd peak sludge gives the highest volume. This must be linked to the floc size. The 1st peak flocs have the greatest size (probably looser in structure) as presented in Figure-IV.6. These flocs may be compressed and compacted and the sludge consolidates to give the least volume (the highest sludge volume reduction between 30 min and 2 hr settling is observed with these flocs). On the other hand, broken flocs have the smallest size in each case. These broken flocs show worst settling (as seen by the residual turbidity values in Figures IV.8 and IV.9) together with the fact that these small flocs occupy less volume when settled. The 2nd peak flocs are somewhere between; they show better settling than broken flocs thus more amount of sludge is expected but they are smaller than 1st peak flocs thus weaker compaction and consolidation is observed when compared to 1st peak flocs and sludges. The 2nd peak flocs are thought to have highest amount of intrafloc water because they have the least amount of solids content (Figure-IV.12) and highest CST values (Figure-IV.11) in each breakage case. As the breakage time increases, the settlability decreases, thus solids content increases and because of



cake blinding due to decreasing floc size, CST also increases.

Figure-IV.11: Sludge volume for different durations of breakage after 30min and 2hr settling with alum.

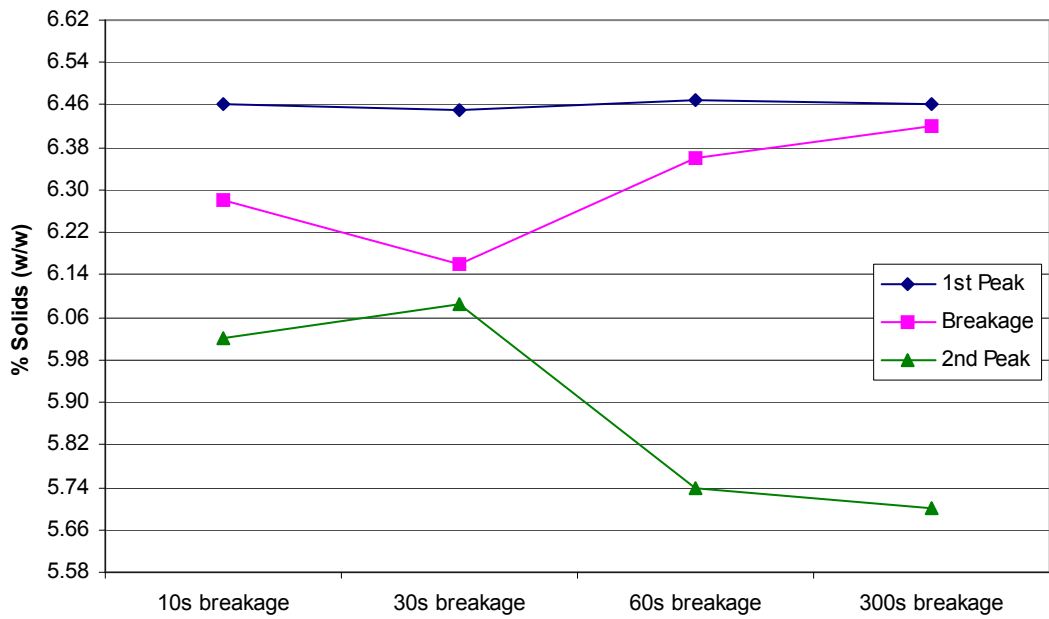


Figure-IV.12: Alum sludge content; % solids (w/w).

The same set of experiments was repeated, only PACl (PAX 216) was used as coagulant this time. FI curves of the PDA are given in Figure-IV.13.

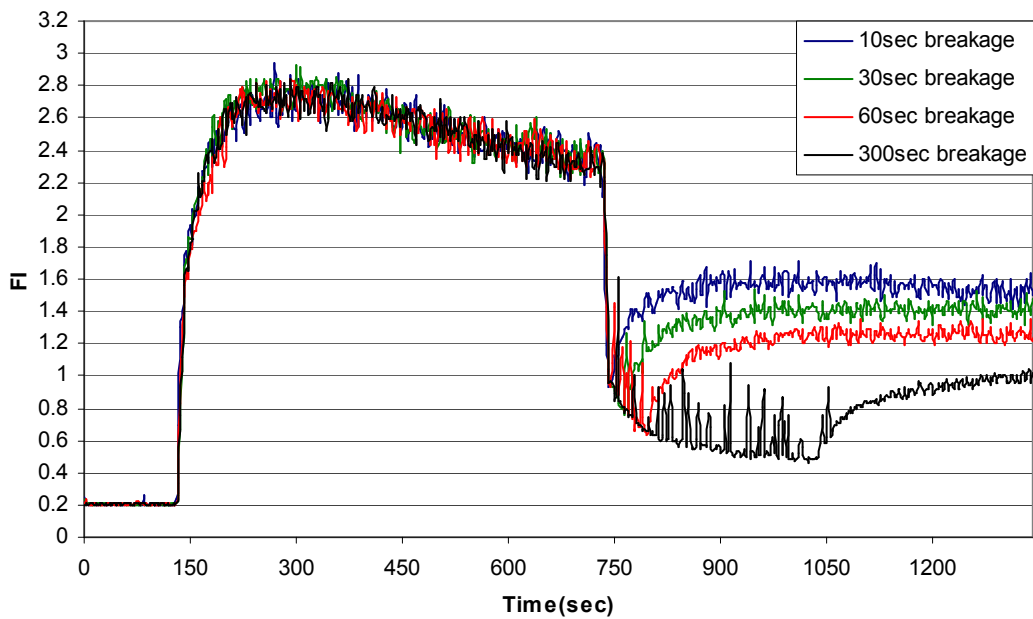


Figure-IV.13: Breakage and re-formation of flocs with PACl at 400 rpm for different durations and at 40 rpm for 10 min, respectively.

The dynamic monitoring of floc formation experiments with PACl gives very similar FI curves, yielding the result that the size of re-formed flocs decreases as the duration of breakage increases. In the cases of 10 s and 30 s breakage, there is a similar degree of recovery after the stirring speed is reduced to 40 rpm, with a decreasing trend as the breakage duration increases, which is the same for floc strength (Figure-IV.14). Flocs regrow to smaller sizes as the time for which they are exposed to high shear rates gets longer. Again, the FI value shows a smaller decrease with only 10 s at 400 rpm, presumably because there is insufficient time to complete the initial rapid breakage. With 5 min at 400 rpm there is evidence of a much more gradual decrease in FI with a more limited recovery at 40 rpm.

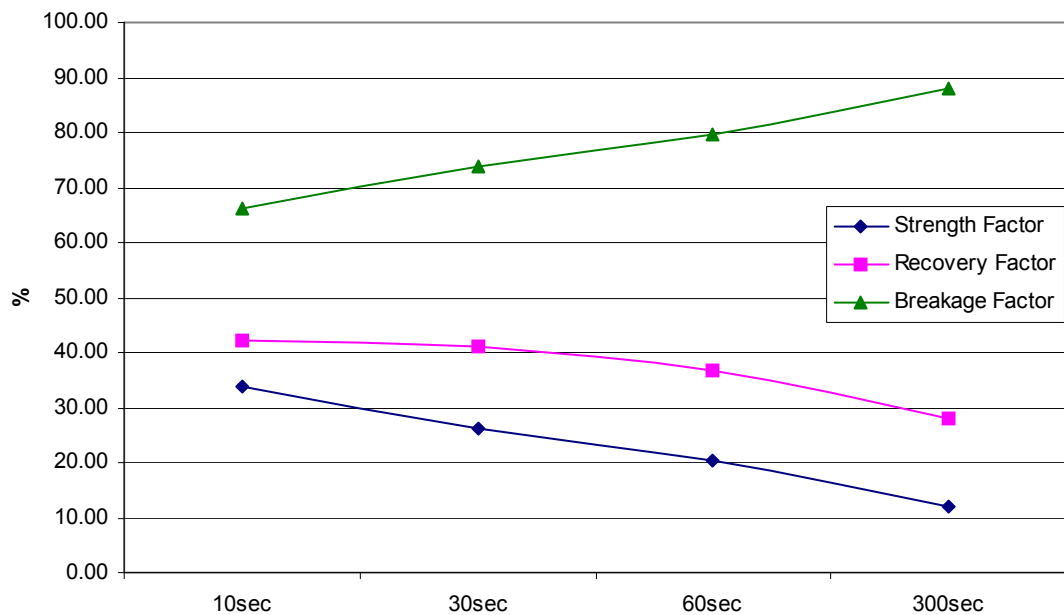


Figure-IV.14: Strength, Recovery and Breakage Factors; investigation of the effect of breakage time with PACl.

As the floc size decreases, it is seen in Figure-IV.15 and Figure-IV.16 that the residual turbidity increases; for longer breakage durations the rise in residual turbidity significantly higher. This is more obviously seen for 300 s breakage period in Figure-IV.16.

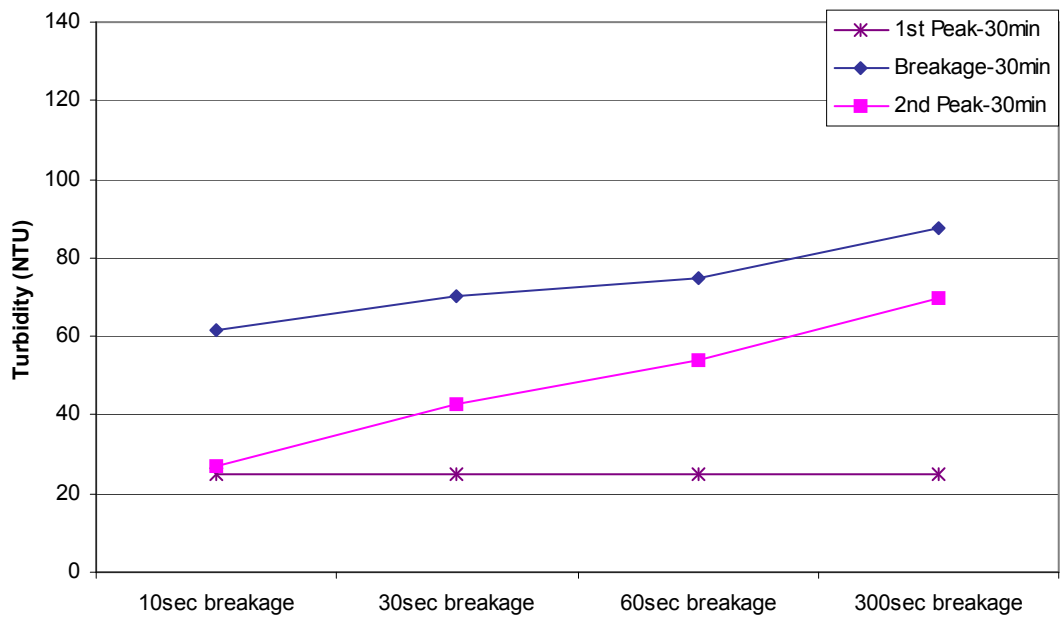


Figure-IV.15: Residual turbidity for different durations of breakage after 30 min settling with PACI.

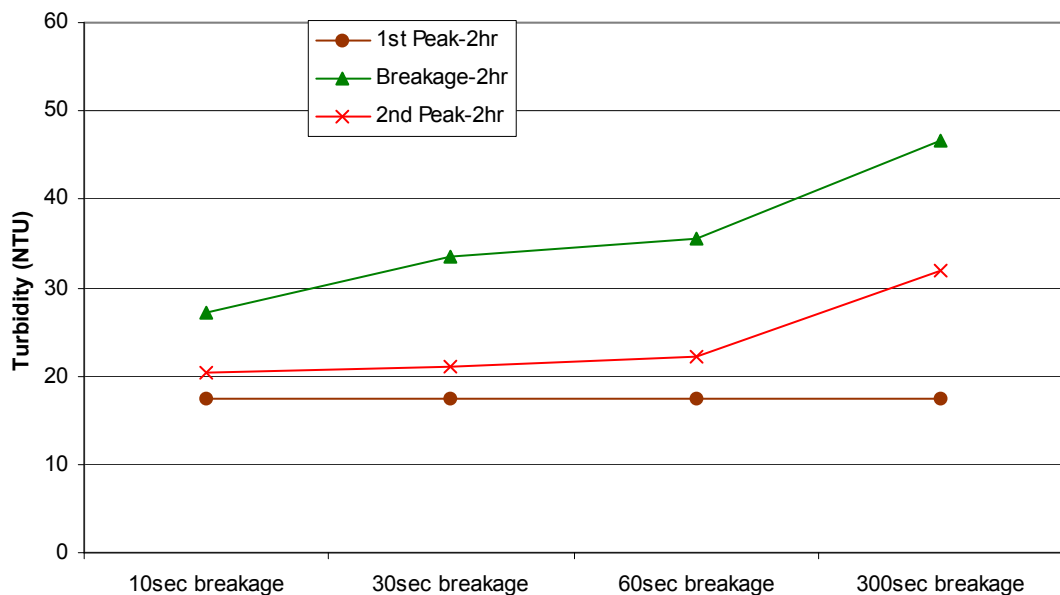


Figure-IV.16: Residual turbidity for different durations of breakage after 2 hr settling with PACI.

When the CST test results in Figure-IV.17 are examined CST values makes a maximum after 30-s breakage and then gradually decreases. Another thing observed in this figure is that CST of broken and regrown flocs get closer to each other as breakage duration increases. Similar to case with alum, in each breakage condition individually, sludges of 2nd peak flocs show highest CST values which is probably due to the highest intrafloc water.

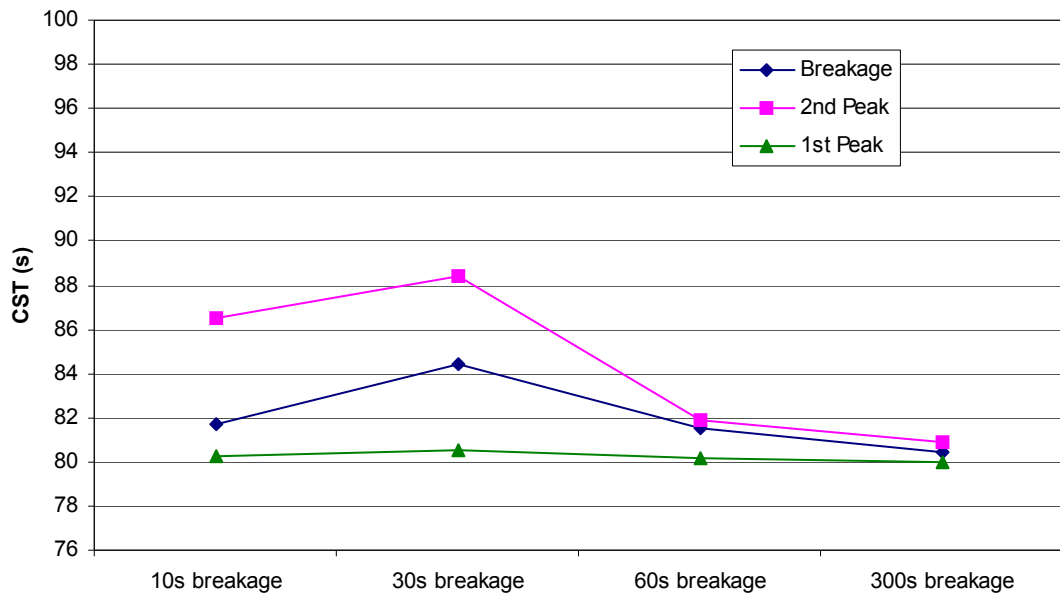


Figure-IV.17: CST test results for different durations of breakage after 30 min and 2 hr settling with PACl.

By examining the sludge volumes for different durations of breakage after 30 min and 2 hr settling with PACl in Figure-IV.18, a very similar trend is observed as with alum. Only the curve of breakage for 30 min shows a slightly different behaviour; volume of sludges consisting of ruptured flocs is less than volume of sludges consisting of unruptured flocs. Obviously, this is due to the fact that 30 min is not sufficient for broken flocs to complete full settling. The interpretation on page 59 for the volumes of alum sludges is also valid for the volumes of PACl sludges. Additionally, a gradual increase in sludge volumes after 2 hr settling with increasing breakage time is obviously seen. As breakage duration increases more bulky sludge is collected, which correlates with the decreasing solids content data in Figure-IV.19.

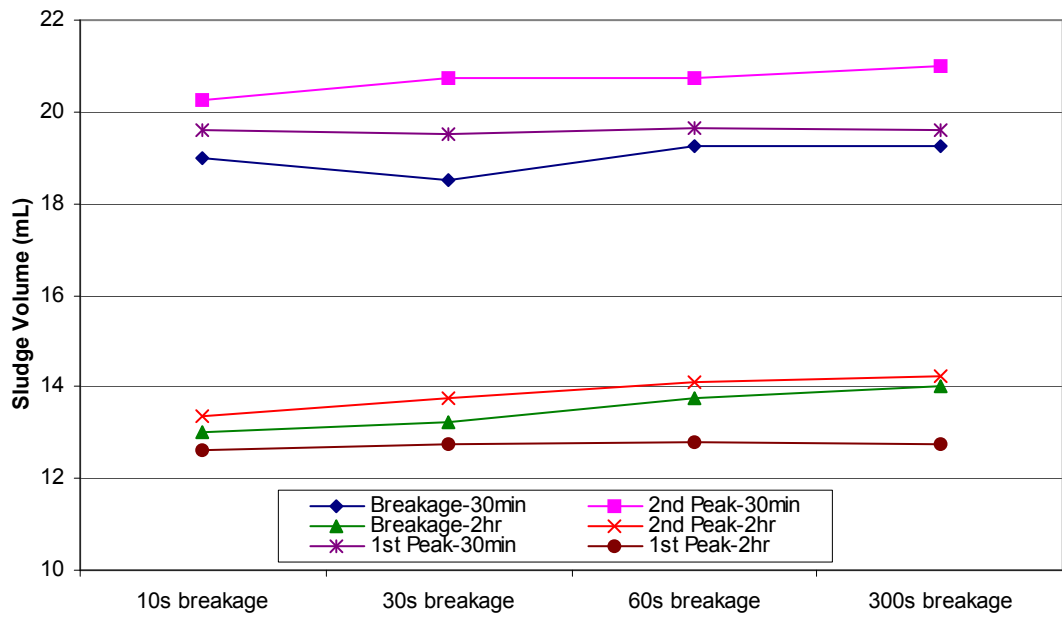


Figure-IV.18: Sludge volume for different durations of breakage after 30 min and 2 hr settling with PACl.

As seen in Figure-IV.19, sludge solids content is closely related to the sludge volumes after 2-hr settling given in Figure-IV.18. Sludge volume, together with the fact that settlability decreases and settled sludge gets more bulky with increased breakage duration, yields the general decreasing trend in Figure-IV.19.

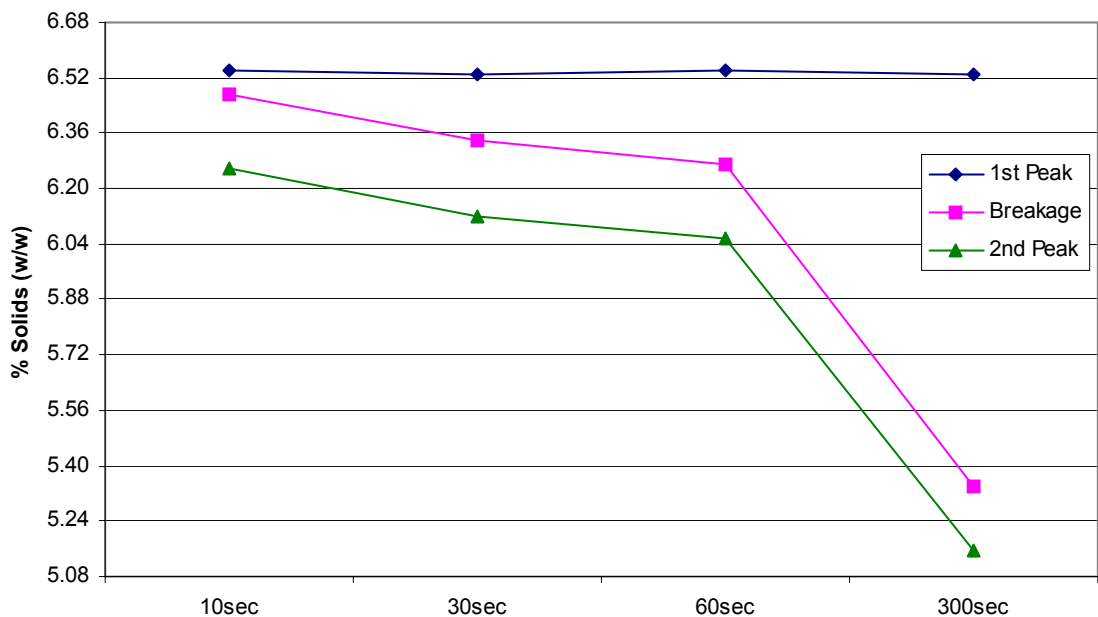


Figure-IV.19: PACl sludge content; % solids (w/w).

There is a correlation between sludge analysis with alum and PACl. In both cases, it is seen that sludge solids content is closely related to settled sludge volume, as the sludge volume increases, sludge solids content decreases and vice versa. Also, in both cases, sludges of 2nd peak flocs give the highest CST values. This is thought to be due to the intrafloc water of these flocs, they have the highest water amount in their floc structures thus it is more hard to release these water. One could think that sludges of 1st peak flocs should have the highest intrafloc water amount. However, since these sludges consolidate and their flocs are compressed into a more compact structure during settling for 2 hours, some intrafloc water may be released out from the floc package. Plots of solids content vs breakage duration for both alum and PACl proves that: sludges of 1st peak flocs have the highest solids content. Because of this, sludges of 1st peak flocs give the lowest CST values.

In all cases PACl gives less residual turbidities than alum. Also, dewaterability of sludges produced with PACl is better than those with alum. Alum produces less volume of sludges in all cases which is the contrary to that given in literature (Gregory and Duan, 2003) and by the PACl manufacturer. This should be due to the high solids concentration of the model suspension; PACl gives much better turbidity removal and much more compact flocs form at high particle concentrations so that less sludge compaction is observed resulting in less sludge volumes.

IV.4. EFFECT OF RAPID MIXING DURATION

To investigate the effect of rapid mixing time on floc formation, nine different breakage durations (0, 5, 10, 30, 60, 120, 180, 240 and 300 s) were applied to the model suspension at the beginning of flocculation tests. The procedure is as follows:

After allowing 2 minutes for steady-state readings to be established, the optimum coagulant dose (6.75 mg/L as Al) was added while mixing at 400 rpm. After different rapid mixing durations, the stirring speed was reduced to 40 rpm for 10 min, and then increased to 400 rpm for 10 s. At the end of breakage period the stirring speed was decreased to 40 rpm for 10 min to allow regrowth of flocs. The results of these four flocculation experiments are presented in Figure-IV.20.

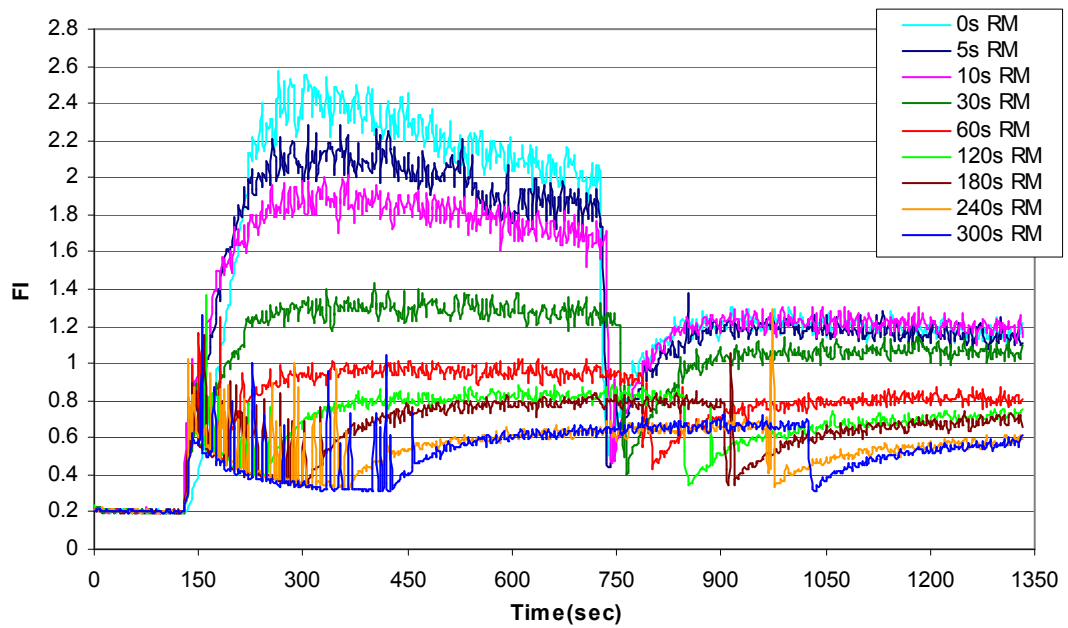


Figure-IV.20: Floc formation, breakage and re-formation for different rapid mixing durations with alum.

From Figure-IV.20 it is seen that the largest flocs are formed with ‘no rapid mixing case’. Flocs formed after 5 s rapid mixing are larger than flocs formed after 10 s rapid mixing, however, the largest flocs regrown after breakage were observed with 10 s rapid mixing. Floc size gradually decreases with increasing rapid mixing duration; the longest rapid mixing duration, 5 min, always gives the smallest floc size. Floc strength gradually increases until 60 s rapid mixing and recovery factor gradually increases until 30 s rapid mixing, then no significant change is observed for both (Figure-IV.21). The relative flocs sizes are consistent with the residual turbidity measurement results, as presented in Figure-IV.22 and 23.

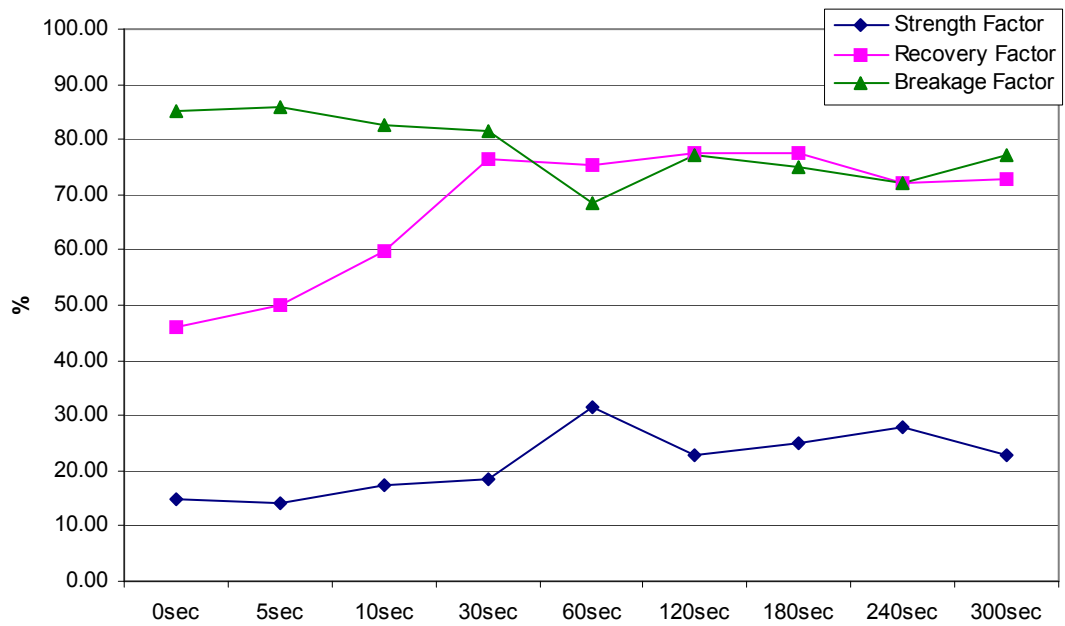


Figure-IV.21: Strength, Recovery and Breakage Factors; investigation of the effect of breakage time with alum.

As expected, broken flocs has the worst settlability and give the highest residual turbidity whereas unruptured flocs give the lowest residual turbidity value in each case. Especially after 10 s, residual turbidity continuously increases as the rapid mixing time increases. A very interesting point is that the lowest residual turbidities are obtained with ‘no rapid mixing condition’ at formation, breakage and re-formation for all cases. This is more obviously seen in Figure-IV.22. This phenomenon is likely related to the solids concentration in the suspension; e.g. the suspension is very concentrated that contact between particles and coagulant species readily occurs, so rapid mixing may seem unnecessary (here we should recall that the purpose of rapid mixing is to provide good dispersion of coagulant and contact

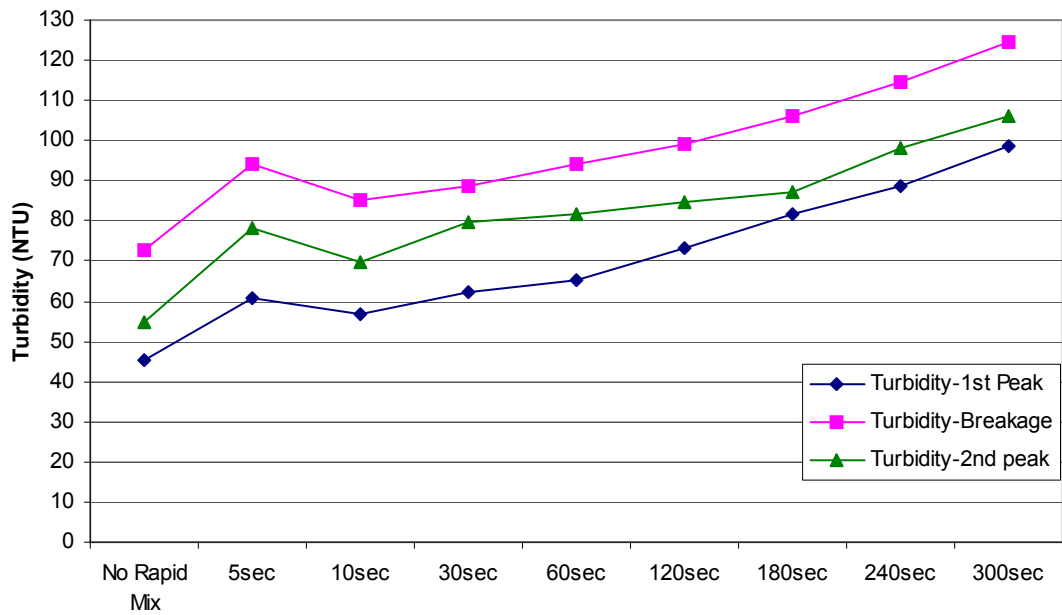


Figure-IV.22: Residual turbidity at formation, breakage and re-formation after 30min settling with alum.

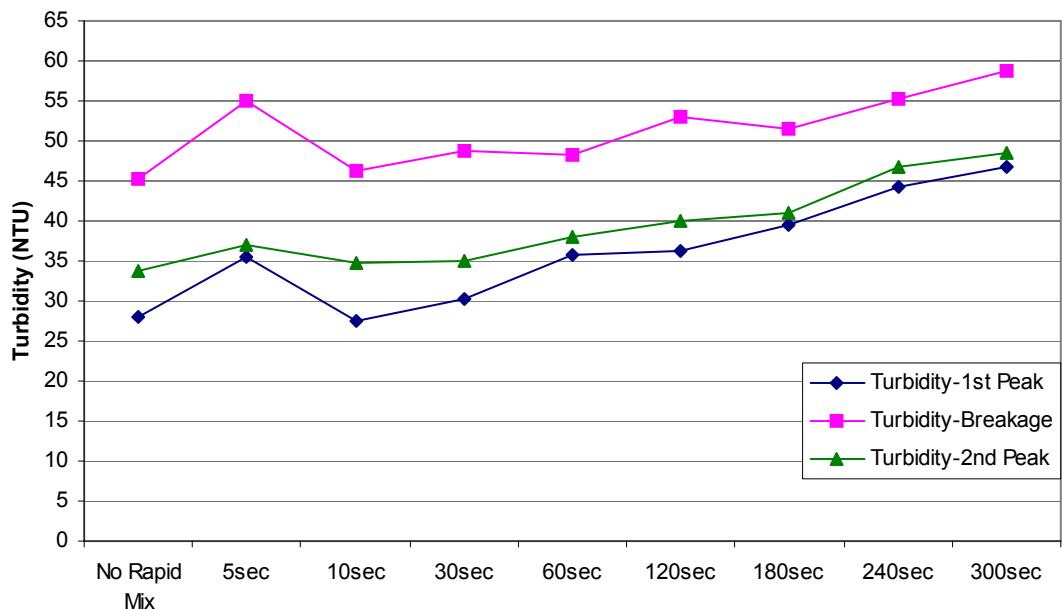


Figure-IV.23: Residual turbidity at formation, breakage and re-formation after 2hr settling with alum.

with as many particles in order to neutralise particle surface charge before metal hydroxides form – metal hydroxides are known to be formed very rapidly, approximately in 1 s). A similar behaviour of two optimum rapid mixing durations were observed by Rossini et al. (1998) in their study with highly turbid suspensions flocculated with alum and ferric chloride. However, from Figure-IV.20 a delay to reach the maximum floc size can be seen with ‘no rapid mixing case’. This delay is

probably the time for contact between particles and coagulant species. Also, this may not be observed with more dilute suspensions. Although flocs formed without rapid mixing are larger than flocs formed with 10 s rapid mixing, the former are not thought to be denser than the latter but looser in structure because it is known that lower agitation intensity causes larger and looser flocs and size effects overcome density effects (Gregory, 1997). An increase in residual turbidity is observed with 5 s rapid mixing, then a decrease with 10 s rapid mixing though the latter generally gives greater residual turbidity than ‘no rapid mixing case’. Although 5 s rapid mixing gives larger flocs than 10 s, the latter gives the lower residual turbidities than the former. This shows that 10 s rapid mixing is the optimum; shorter durations (5 s) give poor mixing, longer durations seem to result in poorly settleable flocs and worsened turbidity removal.

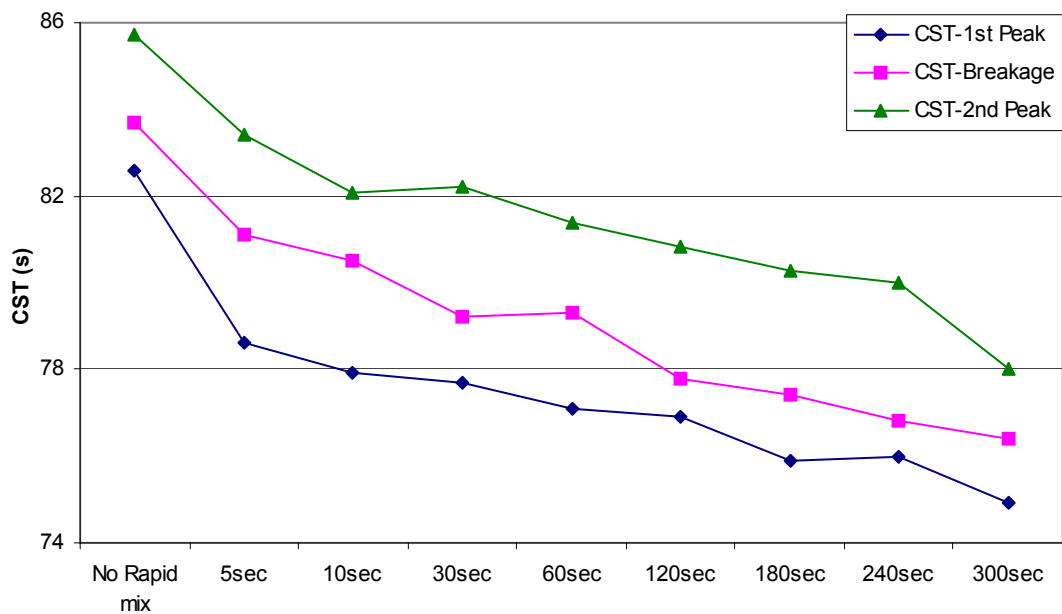


Figure-IV.24: CST at formation, breakage and re-formation after 2 hr settling with alum.

From Figure-IV.24, a decreasing trend in CST with increasing rapid mixing duration is seen. This is more obvious for broken flocs. Fully grown and regrown flocs show similar characteristics which is probably due to the fact that as the time of rapid mixing increases the size difference between these two decreases. Also, from the results it can be said that generally CST decreases as floc size decreases for each individual rapid mixing duration. Turchiuli and Fargues (2004) reported decreasing CST with decreasing floc size.

When Figure-IV.25 is examined a decrease in sludge volume after 30 min settling with increasing rapid mixing time is seen. Obviously, settling efficiency decreases with decreasing floc size (consistent with residual turbidity measurements) and 30 min is not long enough for complete settling of especially flocs formed with prolonged rapid mixing.

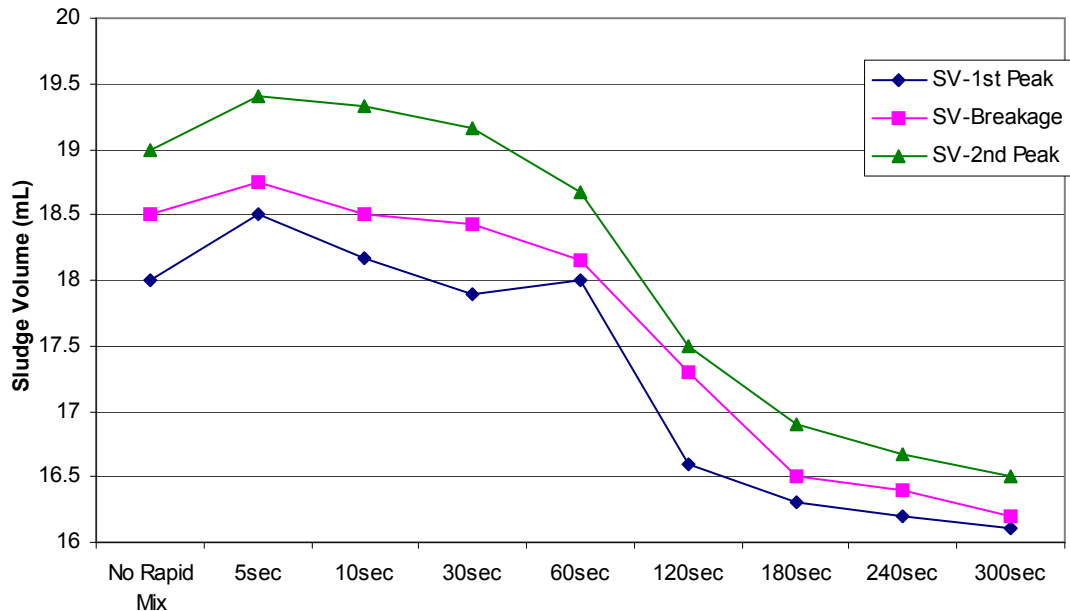


Figure-IV.25: Sludge volume for different durations of rapid mixing after 30 min settling with alum.

In Figure-IV.26 it can be said that sludge volume gradually increases until 60-s rapid mixing, then a slight decrease is observed. Broken flocs have the worst settling, thus they form least amount of sludge. 1st peak flocs have the best settlability, thus the highest sludge volume may be expected with these flocs. However, they may be compressed and compacted and the sludge consolidates to give the lower volume than that expected (generally, the highest sludge volume reduction between 30 min and 2 hr settling is observed with these flocs). The 2nd peak flocs show slightly lower settlability than 1st peak flocs so the amount flocculated and settled particles for them are closer to those for 1st peak flocs. But since these 2nd peak flocs are smaller and not as loose as 1st peak flocs, they show less compaction. Thus the sludge volume of 2nd peak flocs is more than that of 1st peak flocs. Also, sludge volume of 2nd peak flocs does not change significantly with longer rapid mixing durations than 60 s, which is thought to be related to floc size; as rapid mixing time is increased, the size of reformed flocs get closer to each other.

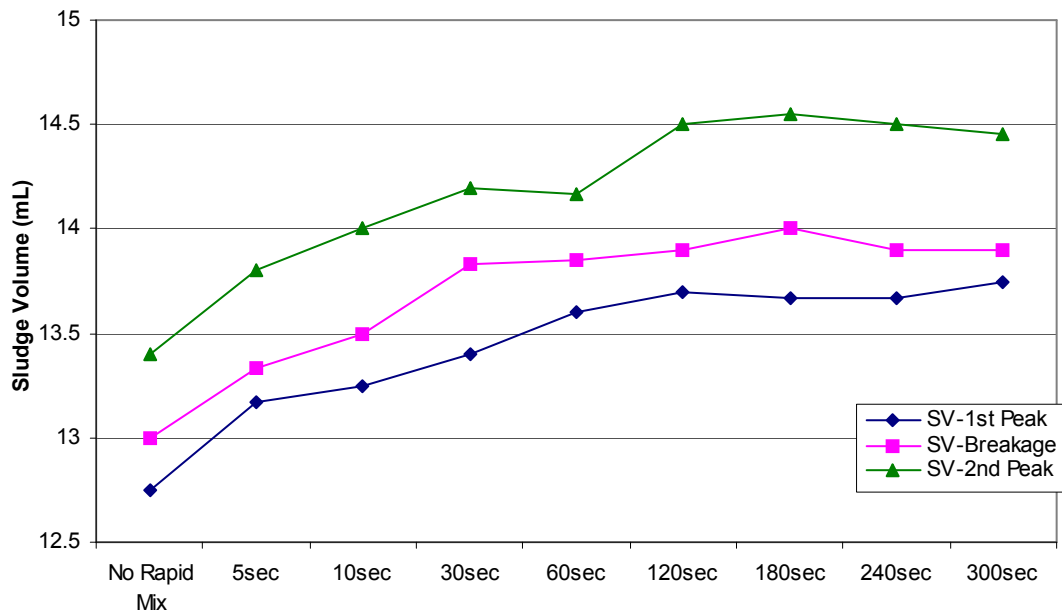


Figure-IV.26: Sludge volume for different durations of rapid mixing after 2 hr settling with alum.

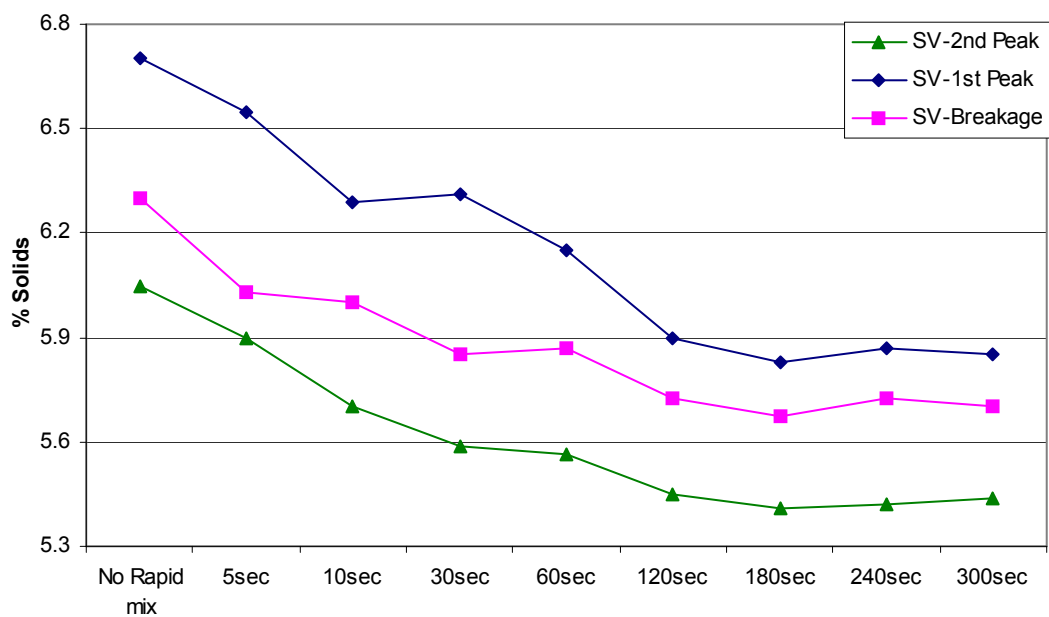


Figure-IV.27: Alum sludge content; % solids (w/w).

Figure-IV.27 should be examined together with Figure-IV.26. For prolonged rapid mixing durations sludge volume increases and percentage of solid particles in sludge decreases as a result of poorer settlability due to decreased floc size.

The same experiments were carried out with PACl. The results of formation, breakage and re-formation tests under different rapid mixing conditions are presented in Figure-IV.28.

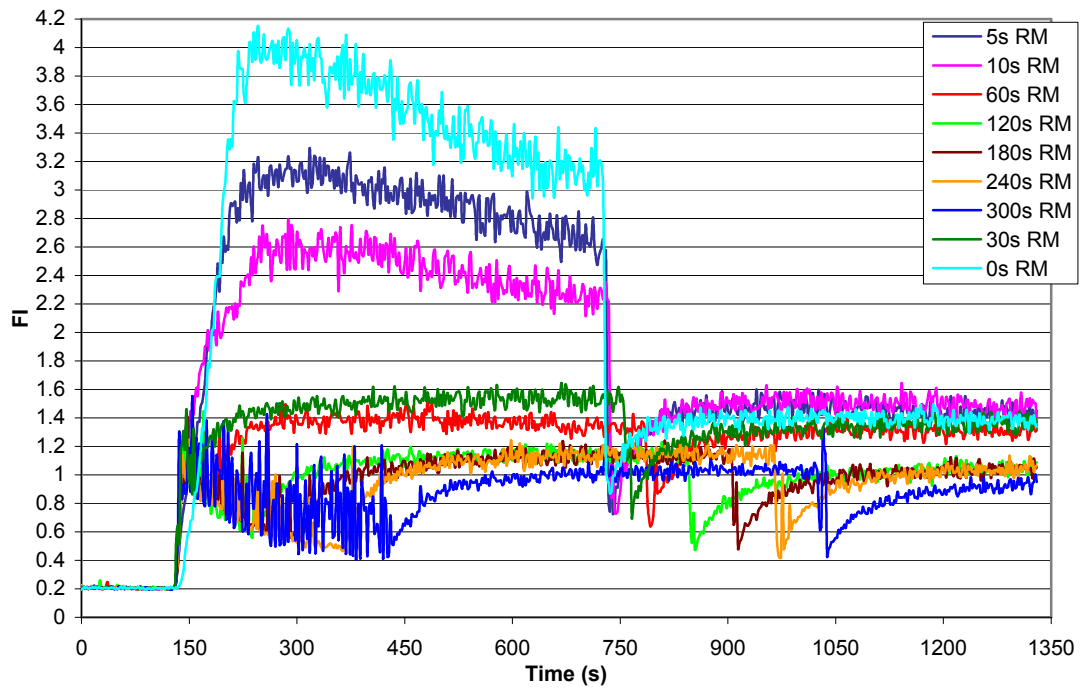


Figure-IV.28: Floc formation, breakage and re-formation for different rapid mixing durations with PACI.

From Figure-IV.28 it is seen that the largest flocs are formed with ‘no rapid mixing case’. Flocs formed after 5 s rapid mixing are larger than flocs formed after 10 s rapid mixing, however, the largest flocs regrown after breakage were observed with 10 s rapid mixing. Floc size gradually decreases with increasing rapid mixing duration; the longest rapid mixing duration, 5 min, always gives the smallest floc size. Floc strength gradually increases until 60 s rapid mixing, then a decrease is observed. Recovery factor gradually increases until 60 s rapid mixing, then no significant change is observed (Figure-IV.29). The relative flocs sizes are consistent with the residual turbidity measurement results, as presented in Figure-IV.30 and 31.

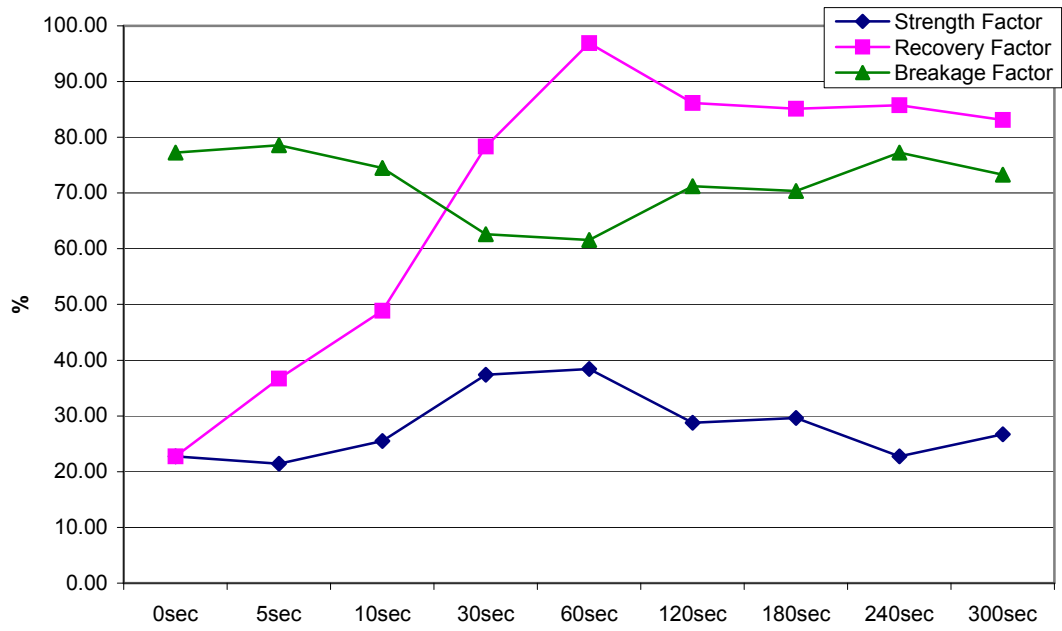


Figure-IV.29: Strength, Recovery and Breakage Factors; investigation of the effect of breakage time with PACl.

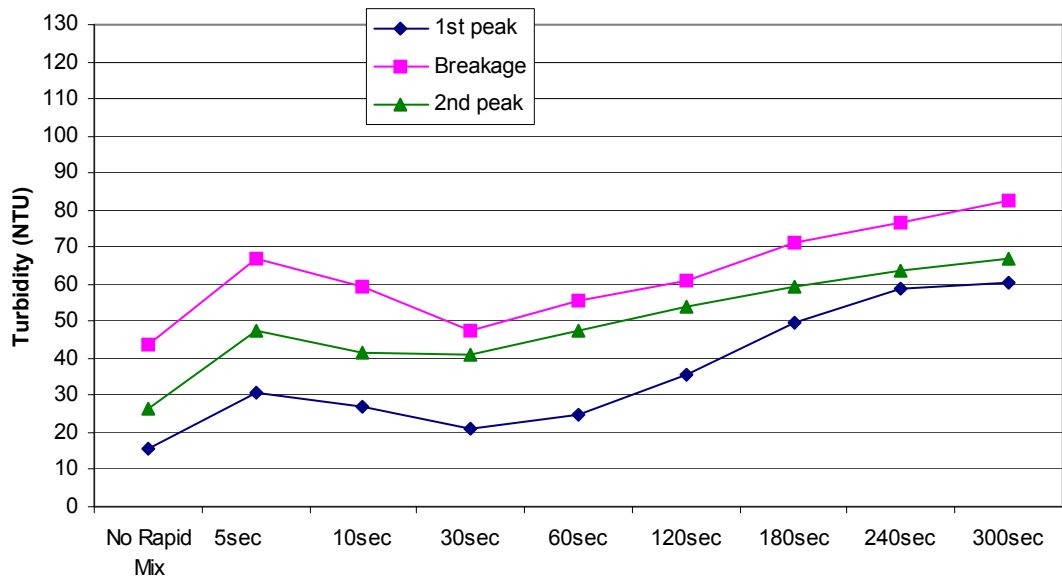


Figure-IV.30: Residual turbidity at formation, breakage and re-formation after 30min settling with PACl.

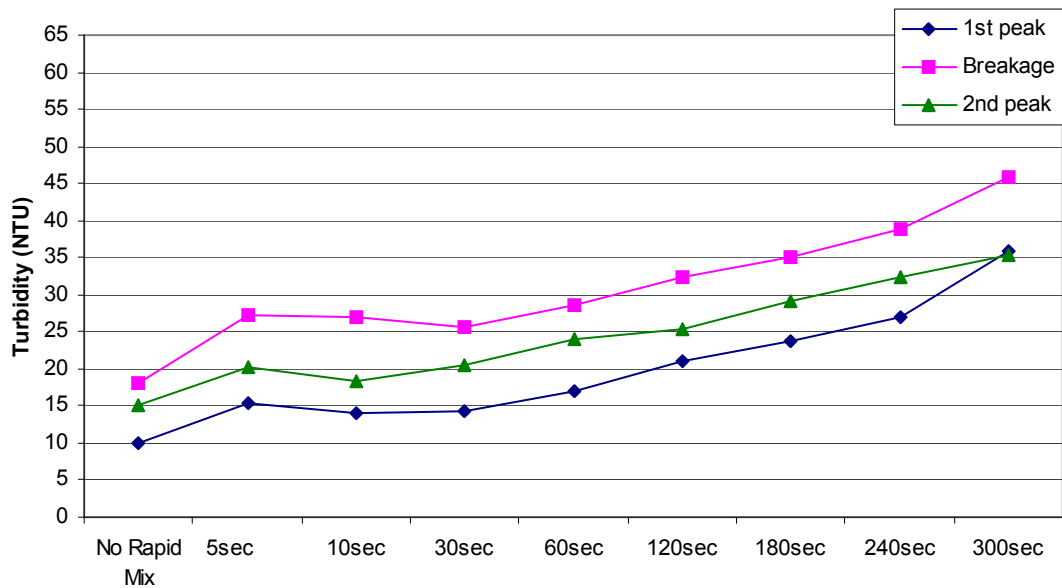


Figure-IV.31: Residual turbidity at formation, breakage and re-formation after 2hr settling with PACl.

As expected, broken flocs has the worst settlability and give the highest residual turbidity whereas unruptured flocs give the lowest residual turbidity value in each case. Especially after 30 s, residual turbidity continuously increases as the rapid mixing time increases. A very interesting point is that the lowest residual turbidities are obtained with ‘no rapid mixing case’ all at formation, breakage and re-formation. This phenomenon is likely related to the solids concentration in the suspension; e.g. the suspension is very concentrated that contact between particles and coagulant species readily occurs, so rapid mixing may seem unnecessary (here we should recall that the purpose of rapid mixing is to provide good dispersion of coagulant and contact with as many particles in order to neutralise particle surface charge before metal hydroxides form – metal hydroxides are known to be formed very rapidly, approximately in 1 s). A similar behaviour of two optimum rapid mixing durations were observed by Rossini et al. (1998) in their study with turbidity suspensions flocculated with alum and ferric chloride. However, from Figure-IV.28 a delay to reach the maximum floc size can be seen with ‘no rapid mixing case’. This delay is probably the time for contact between particles and coagulant species. Also, this may not be observed with more dilute suspensions. Although flocs formed without rapid mixing are larger than flocs formed with 30 s rapid mixing, the former are not thought to be denser than the latter but looser in structure because it is known that lower agitation intensity causes larger and looser flocs and size effects overcome density effects (Gregory, 1997). An increase in residual turbidity is

observed with 5 s rapid mixing, then a decrease with 10 s to 30 s rapid mixing though the latter generally gives greater residual turbidity than ‘no rapid mixing case’. Although 10 s rapid mixing gives larger floc sizes to fully grown flocs than 30 s, the latter generally gives the lower residual turbidities than the former. This shows that 30 s rapid mixing is the optimum; shorter durations (5 s and 10 s) give poor mixing, longer durations seem to result in poorly settleable flocs and worsened turbidity removal.

From Figure-IV.32 a decreasing trend in CST with increasing rapid mixing duration is seen. This is more obvious for fully grown and broken flocs. Also, from the results it can be said that generally CST decreases as floc size decreases for each individual rapid mixing duration. Turchiuli and Fargues (2004) reported decreasing CST with decreasing floc size.

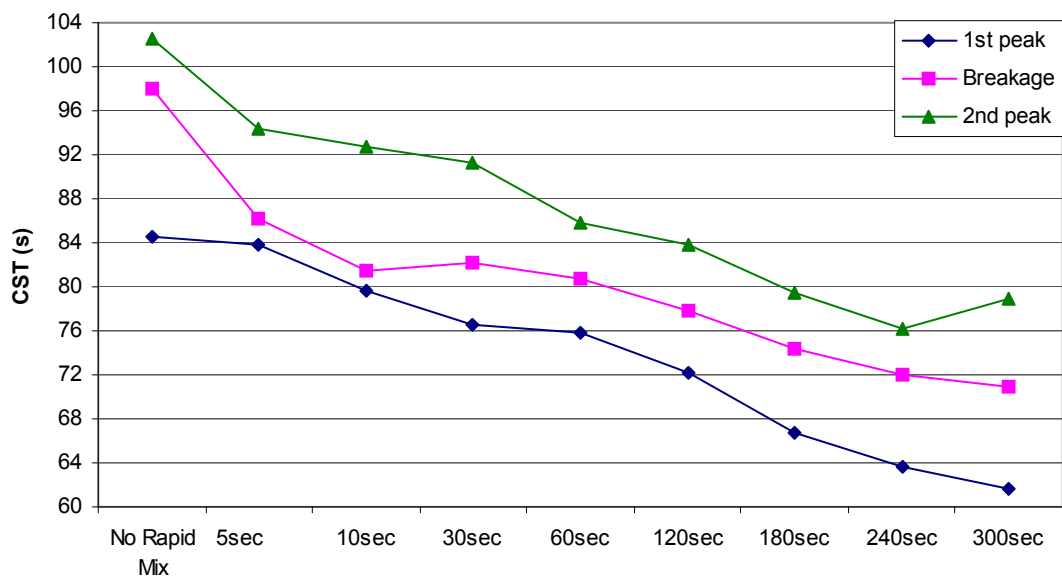


Figure-IV.32: CST at formation, breakage and re-formation after 2 hr settling with PACI.

When Figure-IV.33 is examined an increase in sludge volume after 30 min settling with increasing rapid mixing time is seen until a rapid mixing duration of 60 s. Further rapid mixing does not significantly change 30-min settled sludge volume.

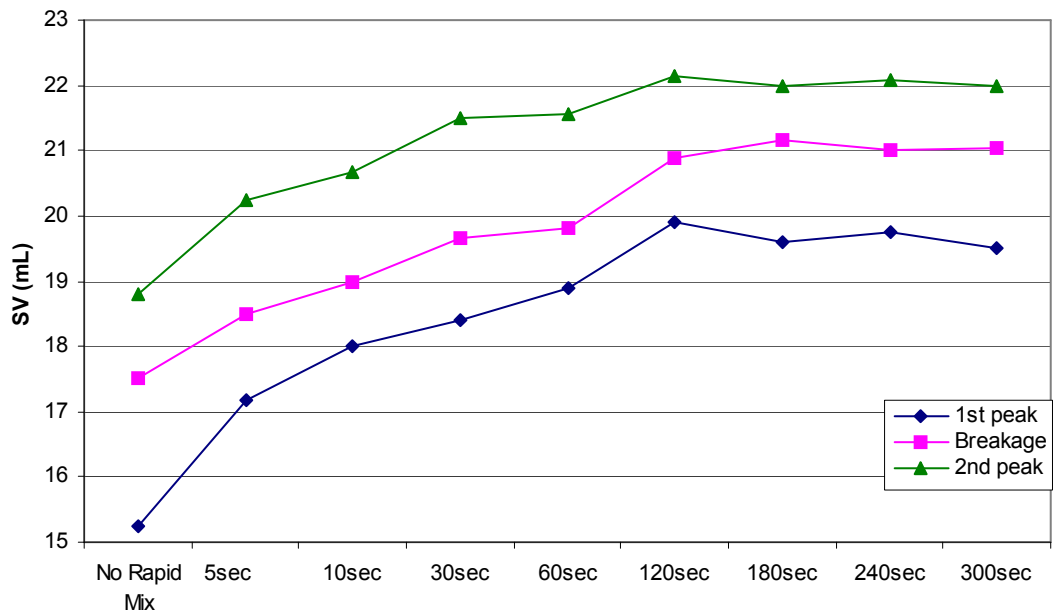


Figure-IV.33: Sludge volume for different durations of rapid mixing after 30 min settling with PACl.

The increasing trend in sludge volume with increasing rapid mixing time is more obvious. Since residual turbidity and sludge volume after 2 hr settling increase with increasing rapid mixing duration it can be interpreted that settlability decreases with increasing rapid mixing time. As a result, a gradual decrease in sludge solids content should be expected, which is obviously seen in Figure-IV.35.

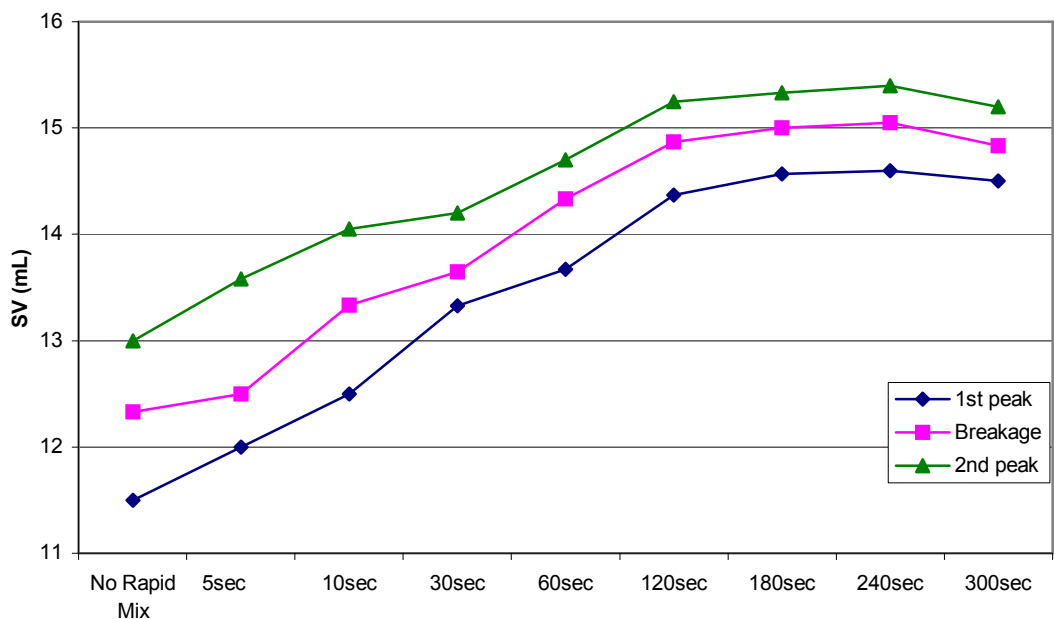


Figure-IV.34: Sludge volume for different durations of rapid mixing after 2 hr settling with PACl.

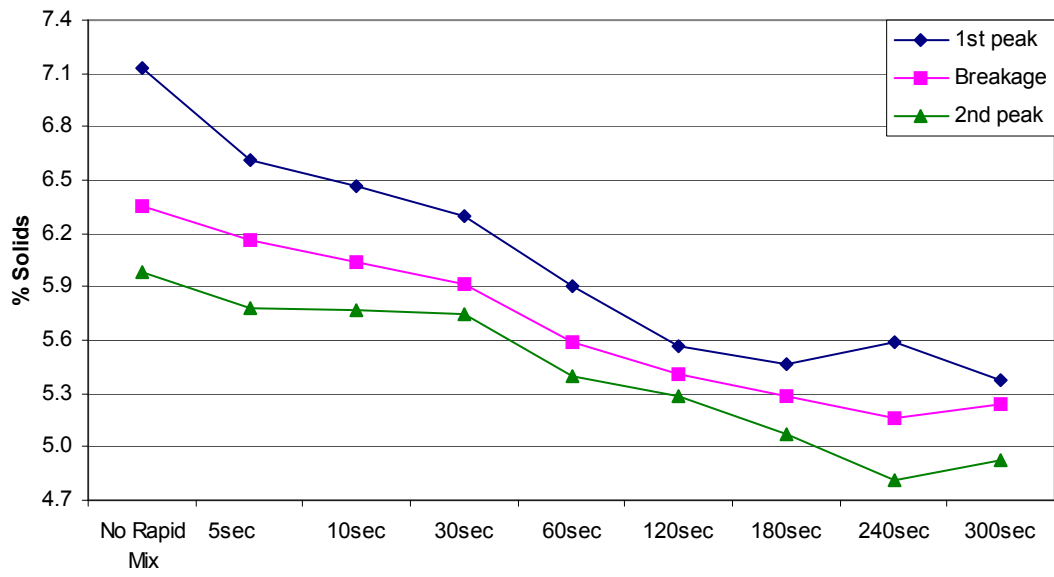


Figure-IV.35: PACl sludge content; % solids (w/w).

CHAPTER V

CONCLUSION

Different breakage and rapid mixing durations were applied to model kaolin suspension flocs. Flocs formed with alum and a PACl (PAX 216) were subjected to higher shear rate (400 rpm) for rupture. When the stirring speed is increased to 400 rpm, floc breakage occurs immediately and is nearly complete within a short period. The 30 and 60 second breakage periods giving nearly the same decrease in FI. Also, in these cases, there is a similar degree of recovery after the stirring speed is reduced to 40 rpm. With only 10 seconds at 400 rpm the FI value shows a slightly smaller decrease, presumably because there is insufficient time to complete the initial breakage, and there is rather more recovery at 40 rpm. With 300 seconds at 400 rpm there is evidence of a much more gradual decrease in FI with a more limited recovery at 40 rpm. The new plateau was always lower than the first value and was reached rather more slowly indicating that the breakage of alum flocs under the stated conditions is not reversible. The floc formation/breakage/re-formation cycle can be repeated several times, giving a steadily decreasing size of the re-formed flocs (Yukselen and Gregory 2002). Although the PACl coagulant gives larger flocs at 40 rpm than alum, there is about the same observed size recovery and floc strength. Increased breakage durations caused increased residual turbidities.

Although there have been previous reports of the irreversible nature of floc breakage with hydrolysing coagulants, the reasons remain unclear. Irreversible breakage is thought to be due to chemical bonds that are broken. When particle interaction is of a physical nature (such as van der Waals or electrostatic attraction) there is no obvious reason why aggregates should not re-form after breakage

(Yukselen and Gregory (2004a) have shown proof for reversible floc breakage with polymers).

It was found that prolonged rapid mixing causes smaller floc formation and worsened settling efficiency, which is resulting to increasing residual turbidity with increasing rapid mixing duration.

A general trend of decreasing CST values with decreasing floc size (due to increased breakage and rapid mixing durations) was observed, which is at the opposite of one could have expected considering surface drag losses: the capillary suction time is lower when flocs are smaller. Similar results were presented by Turchiuli and Fargues, 2004.

REFERENCES

1. Amirtharajah, A. and Mills, K. M., (1982). Rapid-mix design for mechanisms of alum coagulation. *J. AWWA*, 74, 4, p. 210.
2. Amirtharajah, A. and Tambo, N., (1991). Mixing in water treatment. In Amirtharajah, A., Clark, C. C. and Rhodes T. R. eds., *Mixing in Coagulation and Flocculation*, AWWA (Research Foundation), Denver, CO, p. 3-34.
3. Bache, D.H., Johnson, C., Papavasiliopoulos, E., Rasool, E., and McGillian, F.J., (1999). Sweep coagulation: structures, mechanisms and practice. *J. Water Supply: Res. Technol.*, AQUA Vol. 48, No. 5, p. 201-210.
4. Bache, D.H. and Papavasiliopoulos, E.N., (2003). Dewatering of aluminohumic sludge: impacts of hydroxide. *Water Research*, 37, p.3289-3298.
5. Brakalov, L.B., (1987). A connection between orthokinetic coagulation capture efficiency of aggregates and their maximum size. *Chemical Engineering Science*, 42, p. 2373-2383.
6. Flynn, C.M., (1984). *Chem. Rev.*, 84, p. 31.
7. Clark, M.M. and Flora, J.R., (1991). Floc restructuring in varied turbulent mixing. *Journal of Colloid and Interface Science*, 147, p. 407-421.
8. De Hek, H., Stol, R.J. and De Bruyn, P.L., (1978). *J. of Colloid Interface Sci.*, 64, p. 72.
9. Deng, Y., (1997). *Water Research.*, 31, p. 1347.
10. Dentel, S.K., (1991). *Crit. Rev. Environ. Control.*, 21, p. 41.
11. Duan, J., (1997). Influence of Dissolved Silica on Flocculation of Clay Suspensions with Hydrolysing Metal Salts. PhD Thesis, University of London.
12. Duan J. and Gregory J., (2003). Coagulation by hydrolysing metal salts. *Adv. in Colloid Interface Sci.*, 100-102, p. 475-502.
13. Elimelech, M., Gregory, J., Jia, X. and Williams, R.A., (1995). Particle Deposition and Aggregation. Measurement, Modelling and Simulation, Chapter 6, Butterworth-Heinemann, Oxford.

14. Francois, R.J. and Van Haute, A.A., (1984). Floc strength measurements giving experimental support for a four level hydroxide floc structure. *Studies in Environmental Science*, 23, p. 221-234.
15. Francois, R.J., (1987) Strength of aluminium hydroxide flocs. *Water Research*, 21, p. 1023-1030.
16. Francois, R.J., (1988) Growth kinetics of hydroxide flocs. *J. AWWA*, 80, 6, p. 92-96.
17. Gorczyca, B. and Ganczarczyk, J., (1999). Structure and porosity of alum coagulation flocs. *Water Qual. Res. J. Can.*, 34, p. 653.
18. Gregory, J., (1989). Fundamentals of flocculation. In: *CRC Critical Reviews in Environmental Control*, 19, (Part 3), p. 185-230.
19. Gregory, J. and Nelson, D.W., (1986). Monitoring of aggregates in flowing suspensions. *Colloids Surf.*, 18, p. 175-188.
20. Gregory, J., (1996). Polymer adsorption and flocculation. In: Finch, C.A. (Ed.), *Industrial Water Soluble Polymers*. Royal Society of Chemistry, Cambridge, UK, pp. 62-75.
21. Gregory, J., (1997). The density of particle aggregates. *Water Science and Technology*, 36 (4), p. 1-13.
22. Gregory, J. and Rossi, L., (2001). Dynamic testing of water treatment coagulants. *Water Science and Technology: Water Supply*, 1(4), p. 65-72.
23. Gregory, J. and Dupont, V., (2001). *Water Sci. Technol.*, 44, p. 231.
24. Gregory, J., Rossi, L. and Bonechi, L., (2000). Monitoring flocs produced by water treatment coagulants. In H. Hahn, E. Hoffmann, and H. Odegaard, Eds. *Chemical Water and Wastewater Treatment VI*. Berlin: Springer, p. 56.
25. Hayden, P.L. and Rubin, A.J., (1974). *Aqueous-Environmental Chemistry of Metals*, Ann Arbor Science Publishers, Ann Arbor, p. 180.
26. James, R.O. and Healy, T.W., (1972). *J. Colloid Interface Sci.*, 40, p. 53.
27. Jarvis P., Jefferson J., Gregory J. and Parsons S.A., (2005). A review of floc strength. *Water Research*, Vol. 39, No. 14, p. 3121-3137.
28. Jiang, J.Q. and Graham, N.J.D., (1998). *Water Research*, 32, p. 930.
29. Kan, C., Huang, C. and Pan, J. R., (2002). Time requirement for rapid-mixing in coagulation. *Colloids and Surfaces A: Physicochemical and Engineering Aspects*, 203, p. 1-9.
30. Knocke, W. R., Dishman, C. M. and Miller, G. F., (1993). Measurement of chemical sludge floc density and implications related to sludge dewatering. *Water Environ. Res.*, 65, p. 735.

31. Lee, C.H. and Liu, J.C., (2000). Enhanced sludge dewatering by dual polyelectrolytes conditioning. *Water Research*, Vol. 34, No. 18, p. 4430-4436.
32. Lee, C.H. and Liu, J.C., (2001). Sludge dewaterability and floc structure in dual polymer conditioning. *Advances in Environmental Research*, 5, p. 129-136.
33. Letterman, R.D., Vanderbrook, S.G. and Sricharoenchaikit, P., (1982). *J. Am. Water Works Assoc.*, 74, p. 44.
34. Letterman, R.D., Amirtharjah, A. and O'Melia, C.R., (1999). Chapter 6, "Coagulation and Flocculation" in *Water Quality and Treatment*, 5th edition, McGraw-Hill Inc., NY.
35. Martin, R.B., (1991). *J. Inorg. Biochem.*, 44, p 141.
36. Matijevic, E., Mathai, K.G., Ottewill, R.H. and Kerker, M., (1961), *J. Phys. Chem.*, 65, p. 826.
37. Matijevic, E., (1973). *J. Colloid Interface Sci.*, 43, p. 217.
38. Matsuo, T. and Unno, H., (1981). Forces acting on floc and strength of floc. *Journal of Environmental Engineering, ASCE* 107, p. 527-545.
39. Meakin P., (1988). Fractal aggregates. *Adv. in Colloid Interface Sci.*, Vol. 28, No. 4, p. 249-331.
40. Mejia, A.C. and Cisneros, B.J., (2000). Particle size distribution (PSD) obtained in effluents from an advanced primary treatment process using different coagulants. In H. Hahn, E. Hoffmann, and H. Odegaard, Eds. *Chemical Water and Wastewater Treatment VI*. Berlin: Springer, p. 257-268.
41. Mühle, K., (1993). Floc stability in laminar and turbulent flow. In B. Dobias, Ed. *Coagulation and Flocculation*. New York: Dekker, p. 355-390.
42. Ohman, L.-O. and Wagberg, L., (1997). *J. of Pulp Pap. Sci.*, 23, p. J475.
43. Pan, J.R., Huang, C., Cherng, M., Li, K.C. and Lin, C.F., (2003). Correlation between dewatering index and dewatering performance of three mechanical dewatering devices. *Advances in Environmental Research*, 7, p. 599-602.
44. Rossini M., Garcia Garrido J. and Galluzzo M., (1998). Optimization of the coagulation-flocculation treatment: Influence of rapid mix parameters. *Water Research*, Vol. 33, No. 8, p. 1817-1826.
45. Serra, T., Colomer, J. and Casamitjana, X., (1997). Aggregation and breakup of particles in a shear flow. *Journal of Colloid and Interface Science*, 187, p. 466-473.
46. Smith, R.W., (1971). *ACS Adv. Chem. Ser.*, 106, p. 250.

47. Spicer, P.T., Pratsinis, S.E., Raper, J., Amal, R., Bushell, G. and Meesters, G., (1998). Effect of shear schedule on particle size, density, and structure during flocculation in stirred tanks. *Powder Technology*, 97, p. 26-34.
48. Tambo, N. and Hozumi, H., (1979). Physical characteristics of flocs. II. Strength of floc. *Water Research*, 13, p. 421.
49. Turchiuli C., Fargues C., (2004). Influence of structural properties of alum and ferric flocs on sludge dewaterability. *Chemical Engineering Journal*, 103, p. 123–131.
50. Van Benschoten, J.E. and Edzwald, J.K., (1990). *Water Research*. 24, p. 1519.
51. Vesilind A. and Örmeci B., (2000). A modified capillary suction time apparatus for measuring the filterability of super-flocculated sludges. *Water Science and Technology*. Vol. 42, No. 9, p. 135-139.
52. Waite, T.D., (1999). Measurement and implication of floc structure in water and wastewater treatment. *Colloids and Surfaces A*, 151, p. 27–41.
53. Wang, D.S., Tang, H.X. and Gregory, J., (2002). *Environ. Sci. Technol.*, 36, p. 1815.
54. Wesolowski, D.J. and Palmer, D.A., (1994). *Geochim. Cosmochim. Acta*, 58, p. 2947.
55. Wu, C.C., Wu, J.J. and Huang, R.Y., (2003). Effect of floc strength on sludge dewatering by vacuum filtration. *Colloids and Surfaces A: Physicochem. Eng. Aspects*, p. 1-7.
56. Wu, C.C., Wu, J.J. and Huang, R.Y., (2003). Floc strength and dewatering efficiency of alum sludge. *Advances in Environmental Research*, Vol.7, No. 3, p. 617-621.
57. Yukselen, M.A. and Gregory, J., (2002a). Breakage and reformation of alum flocs. *Environmental Engineering Science*, 19, p. 229–236.
58. Yukselen, M.A. and Gregory, J., (2002b). Properties of flocs formed using different coagulants. *Water Science and Technology: Water Supply*, 2, p. 95-101.
59. Yukselen, M.A. and Gregory, J., (2004a). The reversibility of floc breakage. *International Journal of Mineral Processing*, 73, p. 251–259.
60. Yukselen, M.A. and Gregory, J., (2004b). The effect of rapid mixing on the break-up and re-formation of flocs. *Journal of Chemical Technology and Biotechnology*, 79, p. 782-788.
61. Zhao, Y.Q., (2003). Correlations between floc physical properties and optimum polymer dosage in alum sludge conditioning and dewatering. *Chemical Engineering Journal*, 92, p. 227-235.

APPENDIX A

Microphotographs of alum and PACl flocs for different breakage duration conditions.

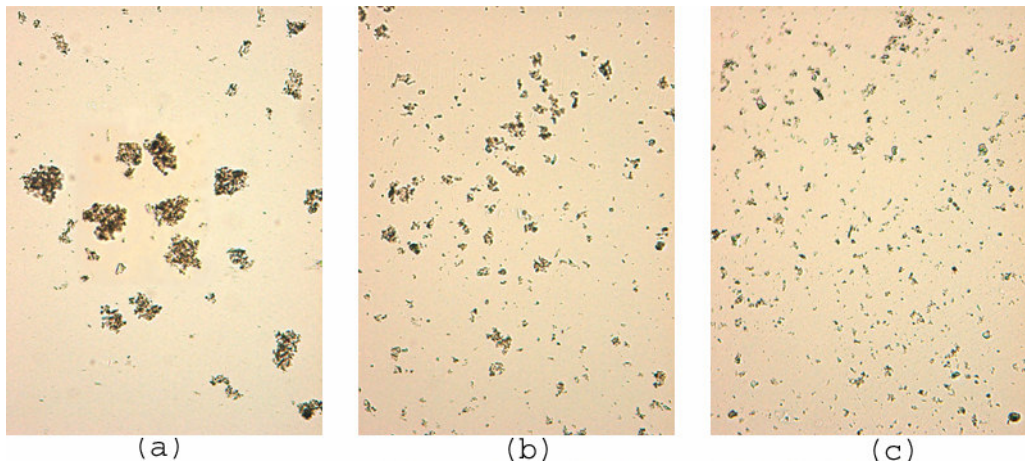


Figure-A.1: Microphotographs of (a) full grown, (b) re-formed and (c) broken flocs with alum for 10 s breakage condition.

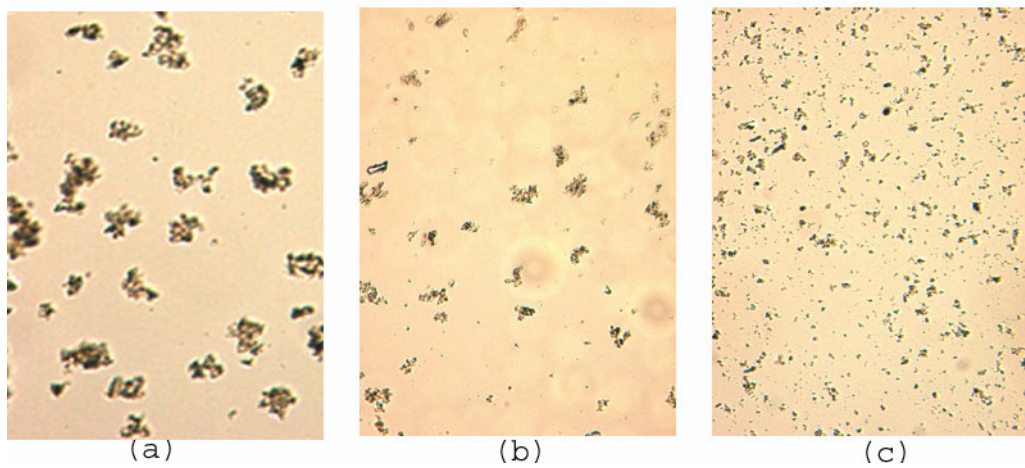


Figure-A.2: Microphotographs of (a) full grown, (b) re-formed and (c) broken flocs with alum for 30 s breakage condition.

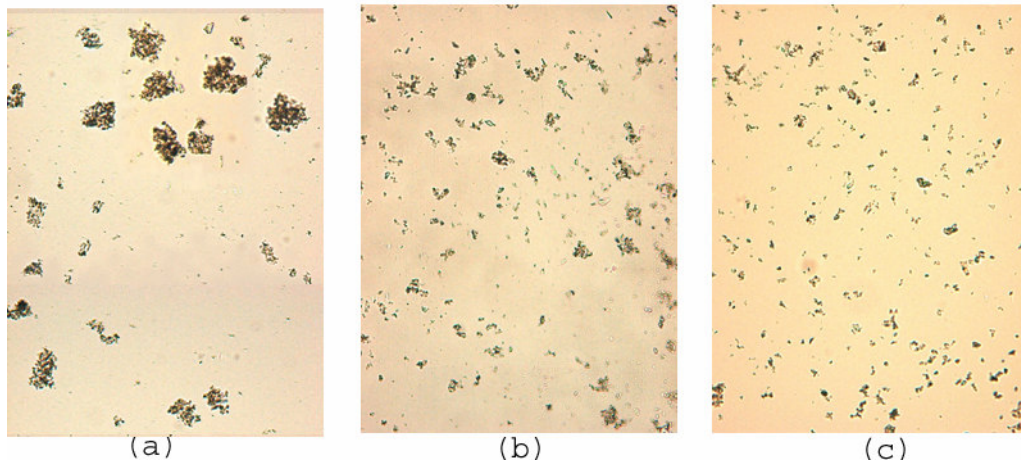


Figure-A.3: Microphotographs of (a) full grown, (b) re-formed and (c) broken flocs with alum for 60 s breakage condition.

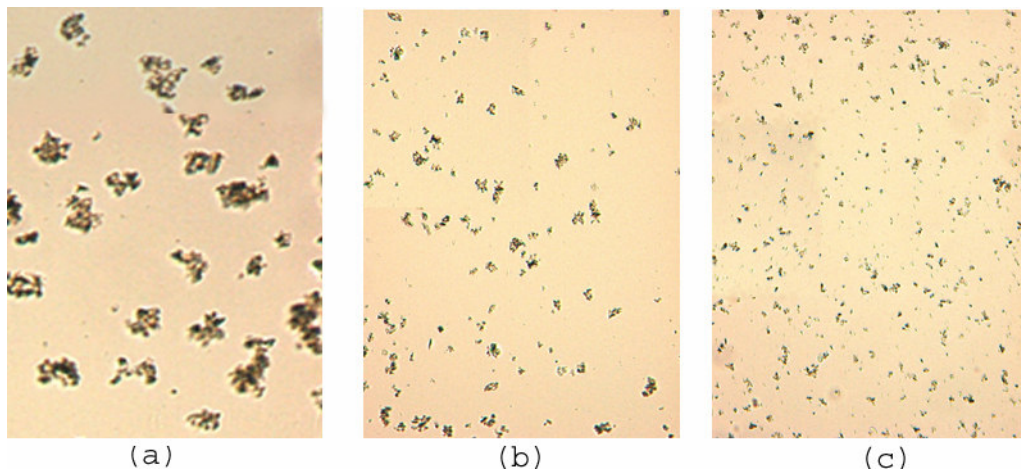


Figure-A.4: Microphotographs of (a) full grown, (b) re-formed and (c) broken flocs with alum for 300 s breakage condition.

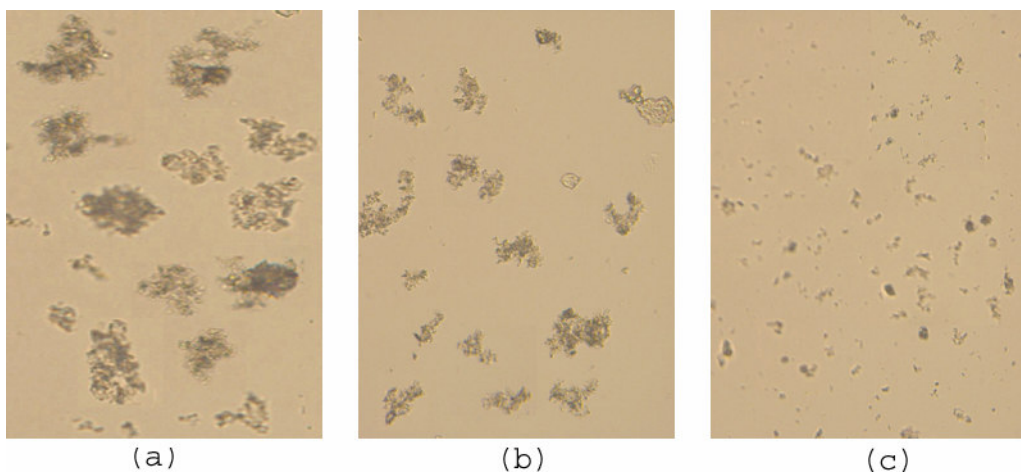


Figure-A.5: Microphotographs of (a) full grown, (b) re-formed and (c) broken flocs with PACl for 10 s breakage condition.

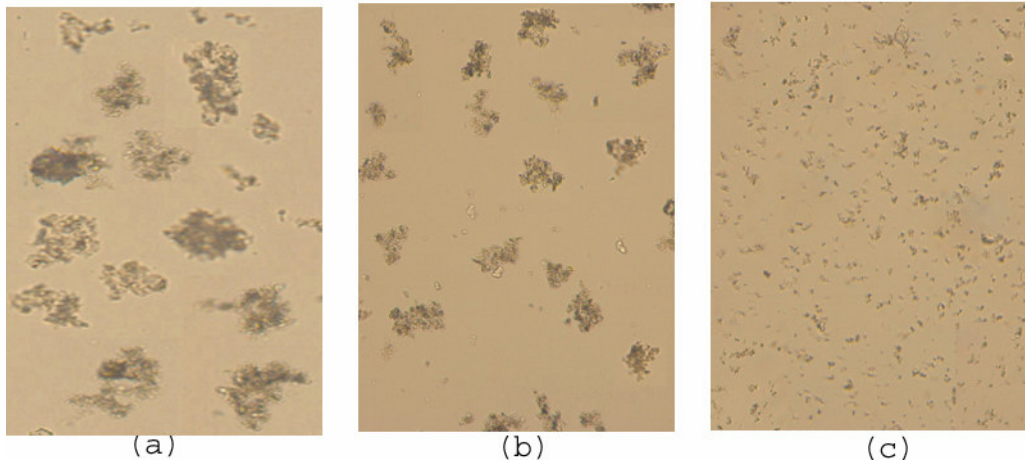


Figure-A.6: Microphotographs of (a) full grown, (b) re-formed and (c) broken flocs with PACl for 30 s breakage condition.

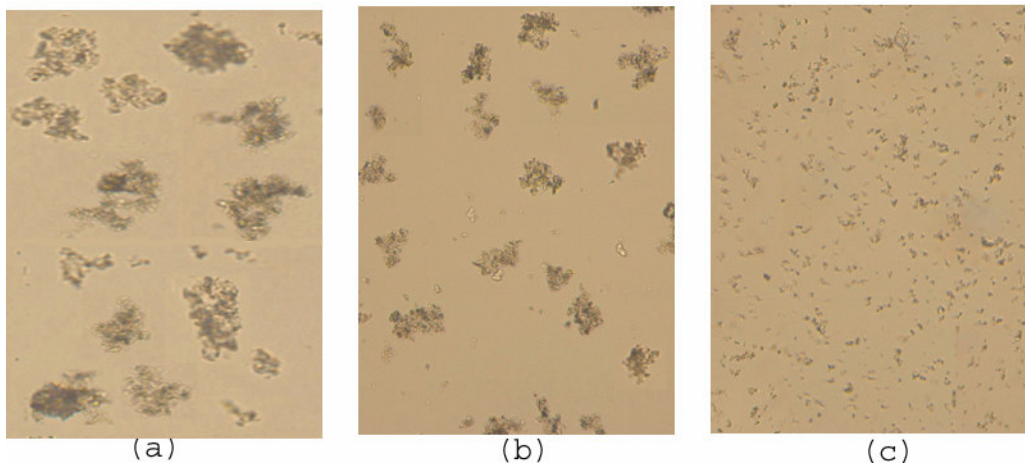


Figure-A.7: Microphotographs of (a) full grown, (b) re-formed and (c) broken flocs with PACl for 60 s breakage condition.

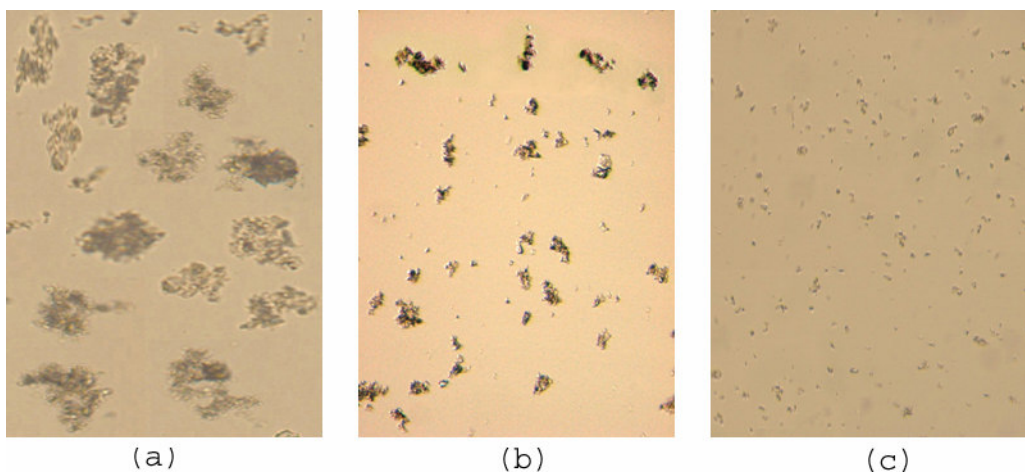


Figure-A.8: Microphotographs of (a) full grown, (b) re-formed and (c) broken flocs with PACl for 300 s breakage condition.

APPENDIX B

Microphotographs of alum and PACl flocs for different rapid mixing duration conditions.

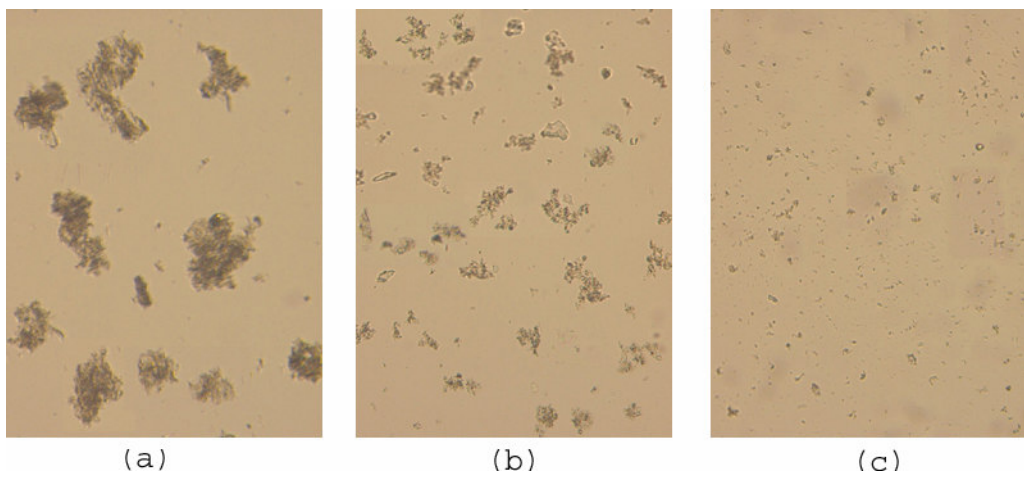


Figure-B.1: Microphotographs of (a) full grown, (b) re-formed and (c) broken flocs with alum for “no rapid mixing” condition.

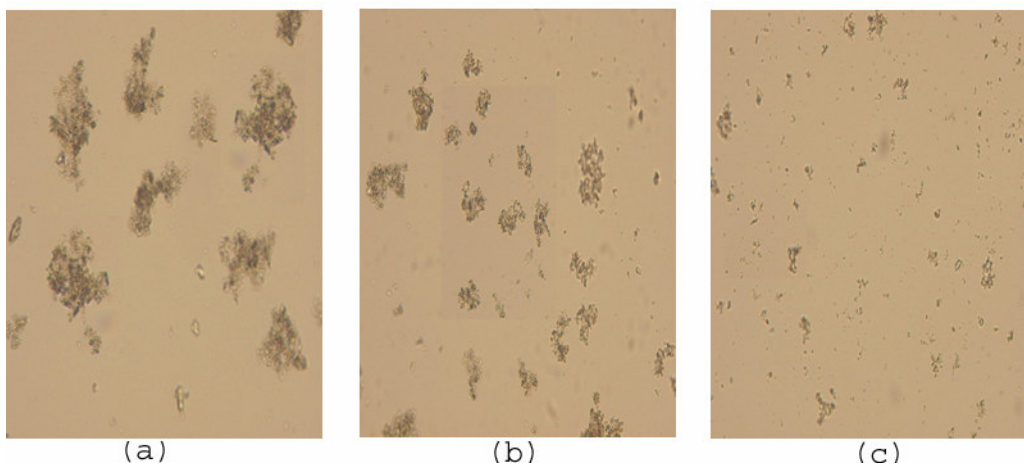


Figure-B.2: Microphotographs of (a) full grown, (b) re-formed and (c) broken flocs with alum for 5 s rapid mixing condition.

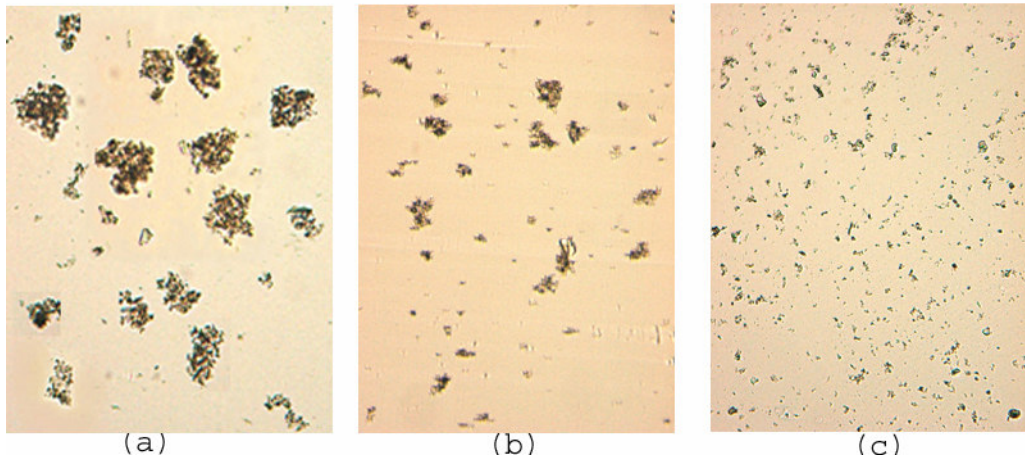


Figure-B.3: Microphotographs of (a) full grown, (b) re-formed and (c) broken flocs with alum for 10 s rapid mixing condition.

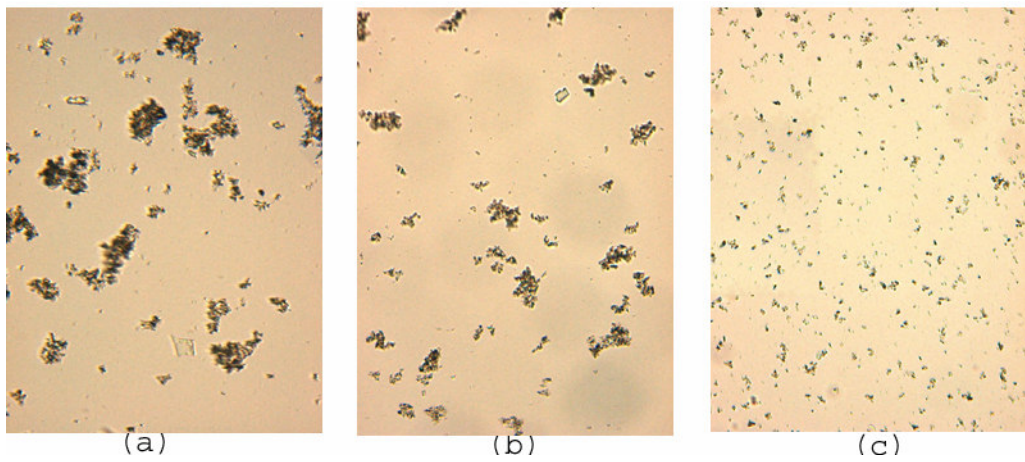


Figure-B.4: Microphotographs of (a) full grown, (b) re-formed and (c) broken flocs with alum for 30 s rapid mixing condition.

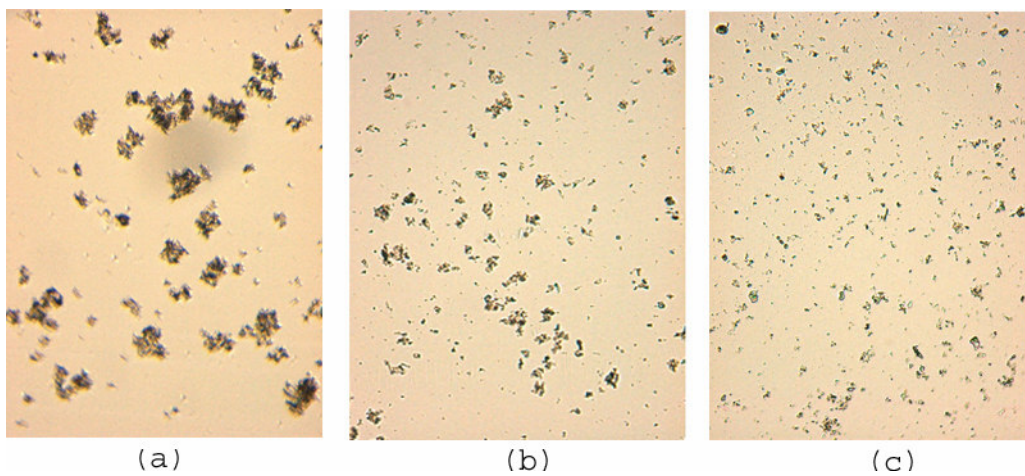


Figure-B.5: Microphotographs of (a) full grown, (b) re-formed and (c) broken flocs with alum for 60 s rapid mixing condition.

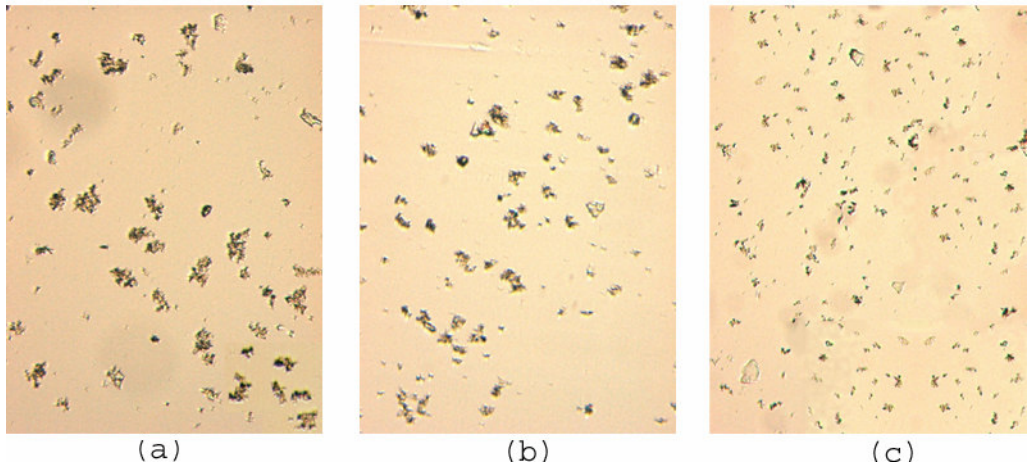


Figure-B.6: Microphotographs of (a) full grown, (b) re-formed and (c) broken flocs with alum for 120 s rapid mixing condition.

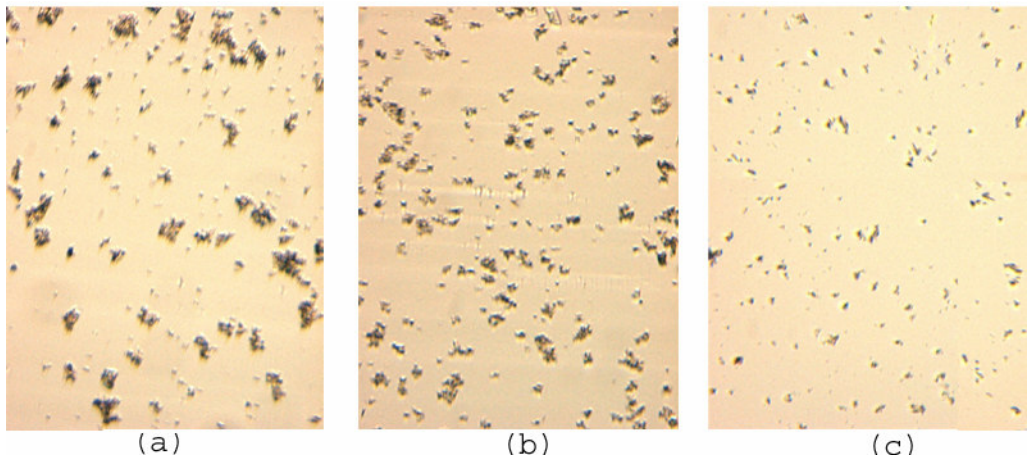


Figure-B.7: Microphotographs of (a) full grown, (b) re-formed and (c) broken flocs with alum for 180 s rapid mixing condition.

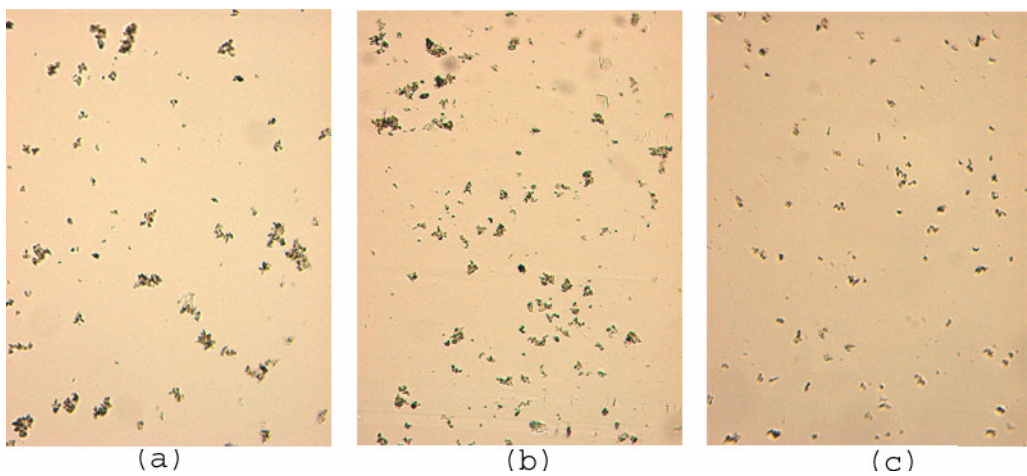


Figure-B.8: Microphotographs of (a) full grown, (b) re-formed and (c) broken flocs with alum for 240 s rapid mixing condition.

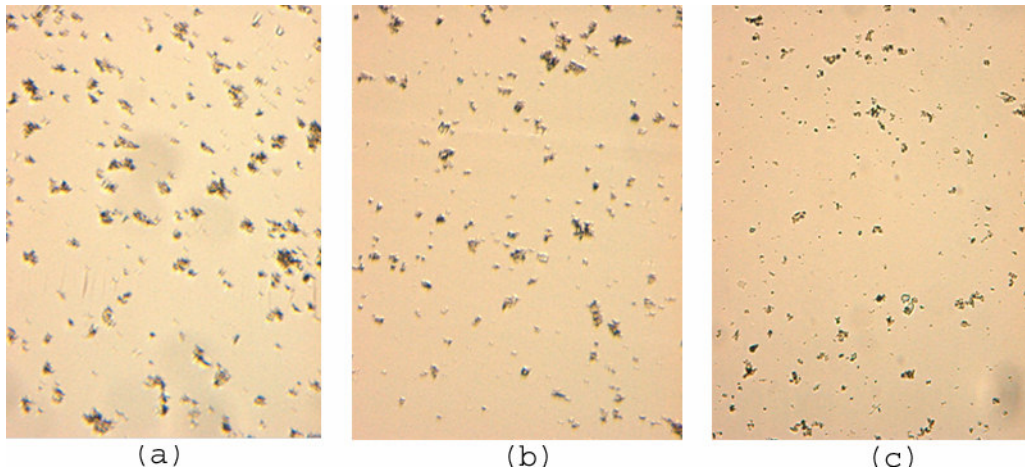


Figure-B.9: Microphotographs of (a) full grown, (b) re-formed and (c) broken flocs with alum for 300 s rapid mixing condition.

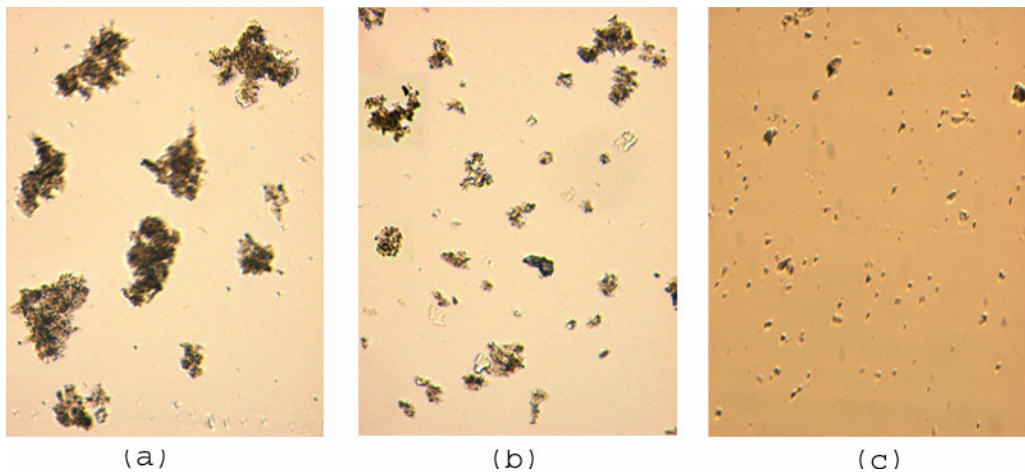


Figure-B.10: Microphotographs of (a) full grown, (b) re-formed and (c) broken flocs with PACl for “no rapid mixing” condition.

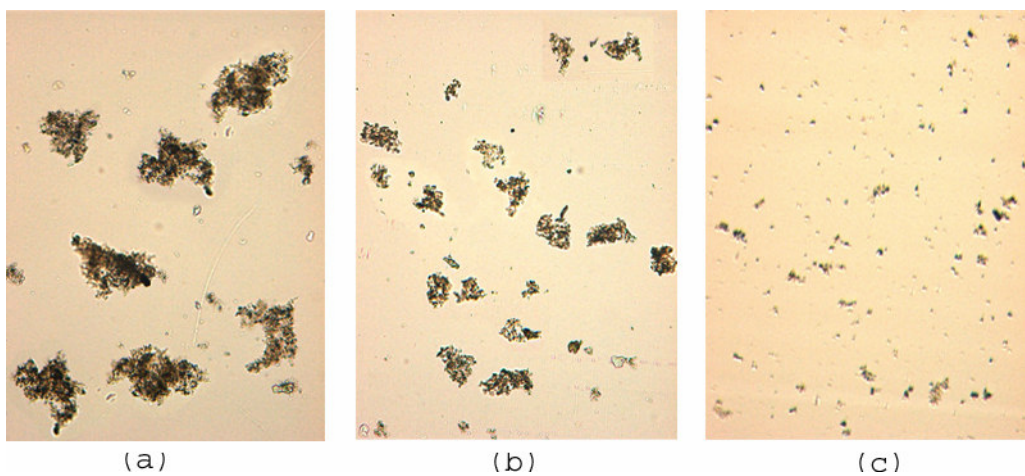


Figure-B.11: Microphotographs of (a) full grown, (b) re-formed and (c) broken flocs with PACl for 5 s rapid mixing condition.

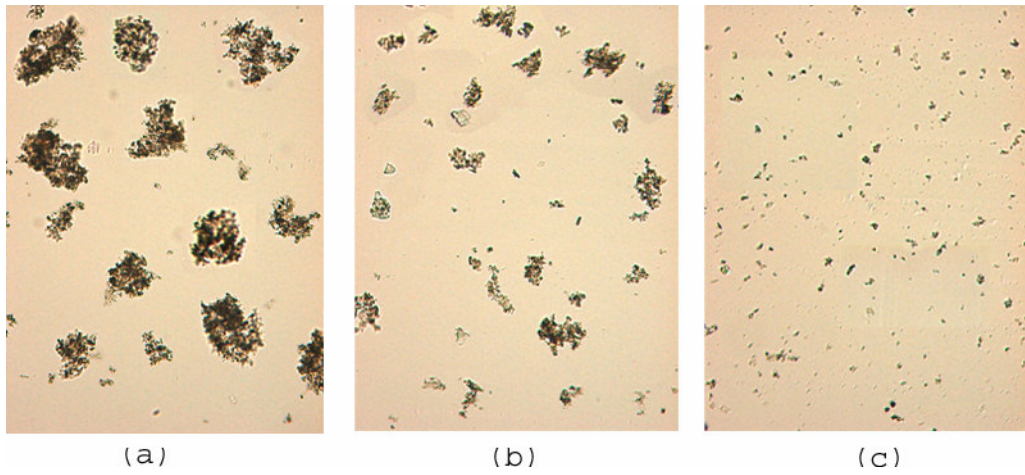


Figure-B.12: Microphotographs of (a) full grown, (b) re-formed and (c) broken flocs with PACI for 10 s rapid mixing condition.

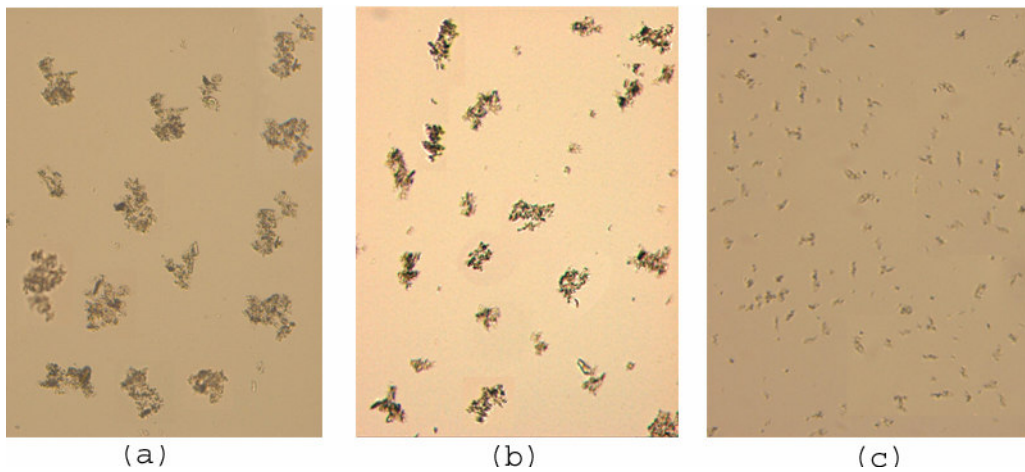


Figure-B.13: Microphotographs of (a) full grown, (b) re-formed and (c) broken flocs with PACI for 30 s rapid mixing condition.

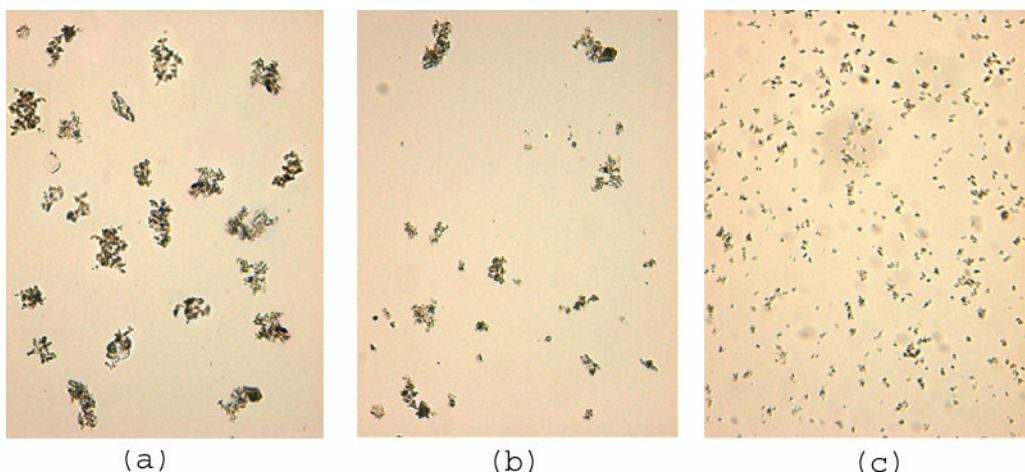


Figure-B.14: Microphotographs of (a) full grown, (b) re-formed and (c) broken flocs with PACI for 60 s rapid mixing condition.

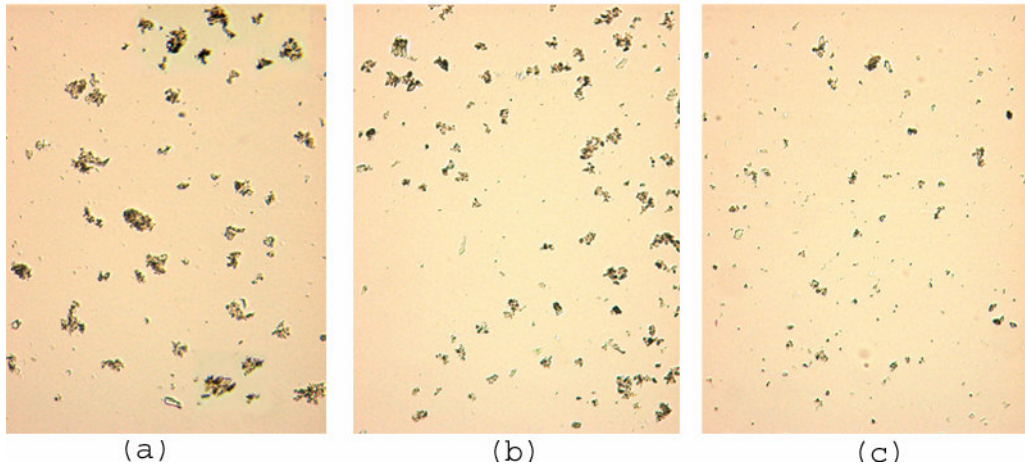


Figure-B.15: Microphotographs of (a) full grown, (b) re-formed and (c) broken flocs with PACI for 120 s rapid mixing condition.

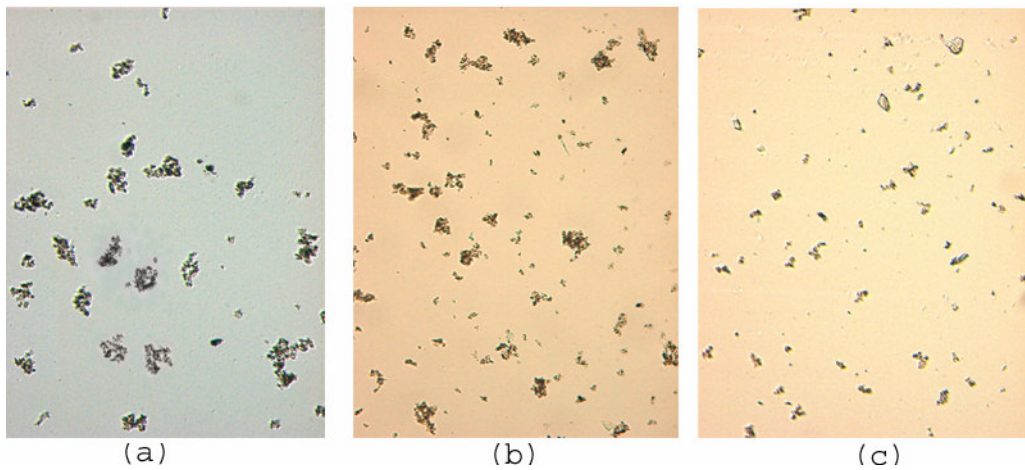


Figure-B.16: Microphotographs of (a) full grown, (b) re-formed and (c) broken flocs with PACI for 180 s rapid mixing condition.

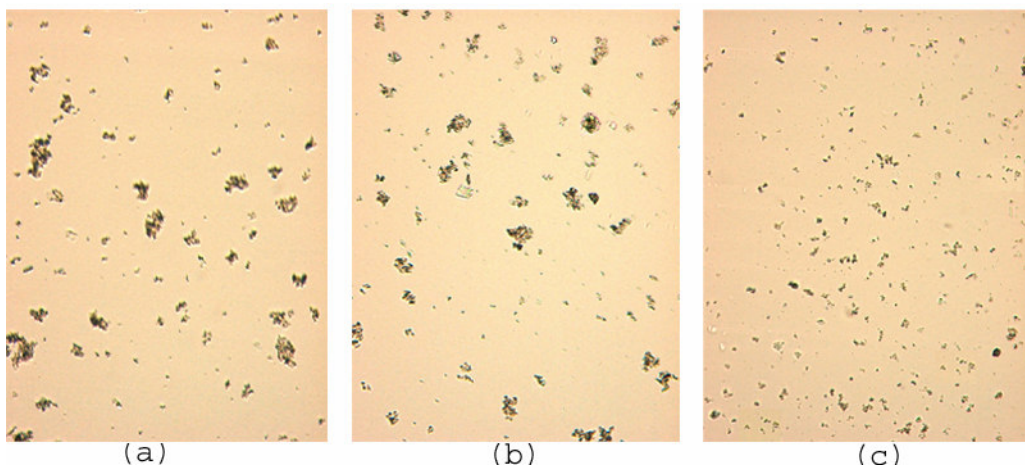


Figure-B.17: Microphotographs of (a) full grown, (b) re-formed and (c) broken flocs with PACI for 240 s rapid mixing condition.

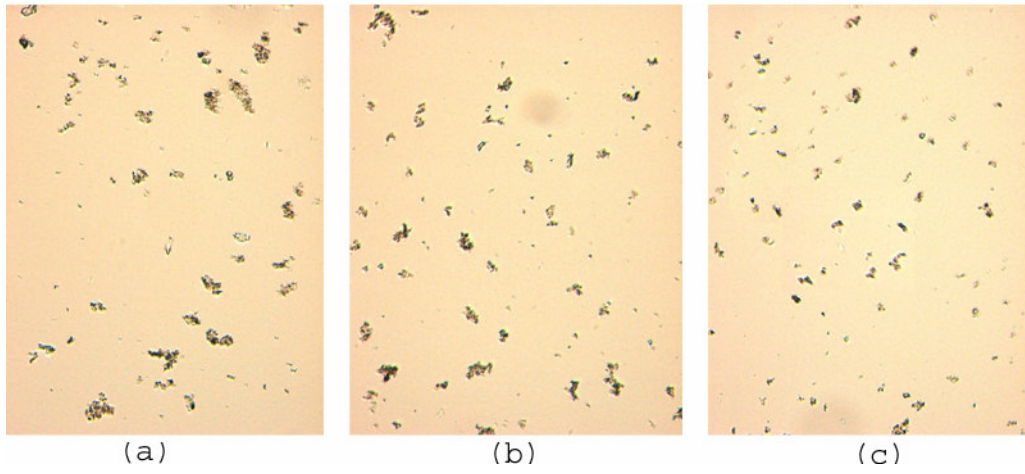


Figure-B.18: Microphotographs of (a) full grown, (b) re-formed and (c) broken flocs with PACl for 300 s rapid mixing condition.

CURRICULUM VITAE

SERDAR ŞAM

Address: Üsküdar/ISTANBUL

e-mail: ssam@eng.marmara.edu.tr

1 Personal Information

-Place; Date of Birth: Bornova; 16th October, 1979

2 Educational Background

1986 – 1991 Turgutlu İnkılap Primary School, Manisa

1991 – 1995 Turgutlu Anatolian High School, Manisa

1995 – 1998 Izmir Yamanlar Collage, Izmir

1998 – 2003 Environmental Engineering Department, Marmara University,
Istanbul

3 Personal Skills

-Foreign Language: English

-Computer Skills: Windows and MS Office applications, Autocad, Visual Basic, Fortran, Macromedia Flash – Dreamweaver, Jasc Paint Shop Pro – Animation Shop, Adobe Photoshop, SPSS